Electronic Thesis and Dissertation Repository

5-2-2011 12:00 AM

Glutamatergic Metabolites and Gray Matter Losses in Schizophrenia: A Longitudinal Study Using In Vivo Proton Magnetic Resonance Spectroscopy

Naoko Aoyama, *The University of Western Ontario*

Supervisor: Dr. Peter C. Williamson, *The University of Western Ontario*
Joint Supervisor: Dr. Terry Thompson, *The University of Western Ontario*
A thesis submitted in partial fulfillment of the requirements for the Doctor of Philosophy degree in Medical Biophysics
© Naoko Aoyama 2011

Glutamatergic Metabolites and Gray Matter Losses in Schizophrenia: A Longitudinal Study Using In Vivo Proton Magnetic Resonance Spectroscopy

(Spine title: Schizophrenia and Proton Magnetic Resonance Spectroscopy)

(Thesis format: Integrated Article)

by

Naoko Aoyama

Graduate Program in Medical Biophysics

A thesis submitted in partial fulfillment
of the requirements for the degree of
Doctor of Philosophy

The School of Graduate and Postdoctoral Studies
The University of Western Ontario
London, Ontario, Canada

THE UNIVERSITY OF WESTERN ONTARIO
School of Graduate and Postdoctoral Studies

CERTIFICATE OF EXAMINATION

<u>Supervisor</u>   <u>Examiners</u>

_____   _____
Dr. Peter C. Williamson   Dr. Neil Gelman

_____   _____
Dr. R. Terry Thompson   Dr. Greg Marsh

<u>Supervisory Committee</u>   _____
                                                   Dr. Ian Cameron

_____
Dr. Robert Bartha   _____
                                                   Dr. Seyed Mirsattari

_____
Dr. Gerald R. Moran

The thesis by

Naoko <u>Aoyama</u>

entitled:

**Glutamatergic Metabolites and Gray Matter Losses in
Schizophrenia: A Longitudinal Study Using In Vivo Proton
Magnetic Resonance Spectroscopy**

is accepted in partial fulfillment of the
requirements for the degree of
Doctor of Philosophy

_____   _____
          Date   Chair of the Thesis Examination Board

Abstract

Approximately one in a hundred people suffer from schizophrenia. Symptoms are partially improved by medication but most symptoms are lifelong. There is no cure. The causes and mechanisms are still unknown. Glutamate, an excitatory neurotransmitter, is a possible cause of the schizophrenia symptoms. Excessive glutamate levels eventually lead to the neurodegeneration. Longitudinal studies are necessary to observe the neurodegenerative process.

Seventeen first episode schizophrenia patients and 17 comparable healthy volunteers underwent a longitudinal study using proton magnetic resonance imaging and spectroscopy to measure structural and neurochemical changes *in vivo*. Metabolite levels were measured from a 1.5cm^3 voxel in the left anterior cingulate and the left thalamus using the stimulated echo acquisition mode sequence (STEAM). Gray matter in the entire brain was examined with a voxel-based morphometry using the Statistical Parametric Mapping.

Total glutamatergic metabolite levels (tGL), N-acetylaspartate (NAA) levels, and gray matter were significantly decreased in schizophrenia over 80 months. Reduced tGL and NAA levels were significantly correlated with gray matter loss in areas related to schizophrenic symptoms. Loss of tGL levels was negatively correlated with social functioning measure. Significantly decreased tGL levels were possibly associated with gray matter loss in the voxel of interest. The metabolite signal-to-noise ratio decreased as a function of MR system age, but that did not significantly affect the findings presented in this thesis.

These findings demonstrate the feasibility of long-term MRS studies of neurological disorders and have a number of implications for the understanding of the pathophysiology of schizophrenia. Changes in glutamatergic metabolites and gray matter losses were consistent with neurodegeneration. The effects of an early neurodevelopmental lesion leading to glutamatergic abnormalities at the onset of illness or the effects of chronic medication could not be ruled out.

Structural and metabolite changes in these patients over the early years of illness have implicated glutamate as a possible target of therapeutic intervention in this disorder. Current

treatments do not prevent deterioration of their social skills. The association between the loss of glutamatergic metabolites and social functioning in this study suggests that it might be possible to arrest this process with pharmaceuticals that target glutamate.

Keywords

Co-Authorship Statement

This thesis is composed of one manuscript accepted with revisions by British Journal of Psychiatry (Chapter 2) and two manuscripts prepared for submission (Chapter 3 and 4).

I acquired the data for the follow-up study at 80 months in schizophrenia patients and the second follow-up study for the controls. I re-analyzed the baseline and 1st follow up scans for the patients and analyzed the final scans of the patients and controls. I performed all the fitting of the spectra and performed the required statistical analyses. As primary author of three of the chapters (manuscripts) I wrote the initial draft of the manuscripts, incorporated all the suggestions for the co-authors and made the changes requested during the external review process.

Dr. Peter C. Williamson supervised the entire work described in this thesis, designed the studies, developed the hypotheses, and reviewed all manuscripts (Chapter 2-4). He also diagnosed all the patients with Structural Clinical Interview for DSM-IV (SCID) and conducted the Scales for the Assessment of Positive/Negative Symptoms (SAPS/SANS).

Dr. Dick J. Drost supervised the first study (Chapter 2), taught MR physics and edited the manuscript.

Dr. R. Terry Thompson supervised the second and third studies (Chapter 3 and 4), taught MR physics, and reviewed those two manuscripts.

Dr. Jean Théberge acquired the data for the never-treated and 10 months assessment in schizophrenia, the initial scan in controls) and reviewed all manuscripts (Chapter 2-4).

Dr. Gerald R. Moran provided consultation and reviewed two manuscripts (Chapter 3 and 4).

Dr. Richard WJ Neufeld consulted on the statistical designs and analyses in the entire work in this thesis (Chapter 2-4).

Dr. Robert C. Gardner consulted on and instructed the statistical analysis (Chapter 3).

Dr. Ravi S. Menon consulted on the spectroscopy protocol used on the 4 Tesla MR system (Chapter 2).

Maria Densmore performed volumetric analyses of all data sets, did the voxel-based morphometry, and performed the brain tissue segmentation for spectroscopy voxels (Chapter 2-4).

Betsy Schaefer conducted interviews with all subjects in order to measure the clinical scales, scheduled the scanning time, and recruited the healthy volunteers (Chapter 2-4).

Drs. Rahul Manchanda and Sandra Northcott referred the schizophrenia patients (Chapter 2).

Dr. Naglingam Rajakumar suggested the regions of interest based on physiological perspectives and instructed the localization of the spectroscopy voxel (Chapter 2).

Dr. William F. Pavlosky reviewed MRI scans to rule out brain abnormalities as required.

All of the co-authors read and approved the final manuscripts.

Acknowledgments

This thesis would have never been completed without help from a number of people in the University of Western Ontario. I especially thank to the following people.

I would like to acknowledge my supervisors Drs Peter C. Williamson and R. Terry Thompson. Dr. Williamson supervised my entire work in the University of Western Ontario. He taught me the basics of psychiatry, neuroanatomy, neuropathology, and how to write the thesis. Dr. Thompson supervised me the last 2 years after my former supervisor had retired. He taught me MR physics, answered my questions, and supported my thesis writing. Dr. Dick J. Drost is my previous supervisor. Dr. Drost taught me the principle of MR physics as well as English, educated how to accomplish PhD, and took care of my social life. These three supervisors showed me enormous enthusiasm for research.

Many thanks to Dr. Jean Théberge, who taught me MR physics and reviewed manuscripts. Since I took over his project, he instructed and educated how to use the 4 Tesla MR system, how to develop a pulse sequence, and how to run the program for the spectral analysis.

Many thanks to Dr. Richard WJ Neufeld, who consulted on all statistical design and analyses in this work. He also educated me on statistics because I did not have enough statistical knowledge.

Thanks to Drs Rob Bartha and Gerald R. Moran, advisory committee member. Dr. Bartha consulted on the problems with sequence development at 4 Tesla MR system. Dr. Moran gave me a number of thoughts and inputs in my thesis. He helped me analyze the data and write the thesis.

Thanks to Wendy Hough, a secretary of Medical Biophysics. Although I often asked her help in the last minutes, she was always available and gave me helpful advice with her smile.

I would like to thank Dr. Francis PH Chan, Darla McNeil, Pamela Bere in Schulich School of Medicine & Dentistry. Many thanks to Drs Peter Brown and David Sutton, psychological counselors, and Nancy, a counseling secretary, at Student Health Services. These six people supported me since I felt a difficulty in continuing in the PhD program.

Table of Contents

List of Tables

List of Figures

List of Appendices

List of Abbreviations

1H	Proton
31P	Phosphorus
ANCOVA	Analysis of covariance
ANOVA	Analysis of variance
B_0	static magnetic field, main field
B_1	rotating magnetic field
BA	Brodmann Area
CHESS	CHEmical Shift Selective
Cho	Choline
Cr	Creatine
CRLB	Cramér–Rao Lower Bound
CSF	Cerebral Spinal Fluid
CSI	Chemical Shift Imaging
CT	Computed Tomography
CV	Coefficient of Variation
dB	decibel
d.f.	degrees of freedom
DSM IV	Diagnostic and Statistical Manual of Mental Disorders, fourth edition
FDR	False Discovery Rate
FID	Free Induction Decay
FLASH	Fast Low Angle SHot
FOV	Field Of View
FWHM	Full Width at Half Maximum
γ	gyromagnetic ratio
GABA	γ-aminobutyric acid
G_y	B_0 gradient along y-axis
Gln	Glutamine
Glu	Glutamate
HLSVD	Hankel-Lanczos Singular Value Decomposition
LCModel	Linear Combination Model

LSPRS	Life Skills Profile Rating Scale
MANOVA	Multivariate Analysis Of VAriance
M	Magnetization vector (M_x, M_y, M_z)
M_0	net magnetization
MRI	Magnetic Resonance Imaging
MRS	Magnetic Resonance Spectroscopy
MRSI	Magnetic Resonance Spectroscopic Imaging
Myo	Myo-inositol
ms	millisecond
NAA	N-acetylaspartate
NMDA	N-methyl D-aspartate
NMR	Nuclear Magnetic Resonance
ppm	parts per million
PRESS	Point-RESolved Spectroscopy
QUALITY	Quantification Improvement by converting Line Shapes to the Lorentzian Type
RF	Radiofrequency
SANS	Scale for the Assessment of Negative Symptoms
SAPS	Scale for the Assessment of Positive Symptoms
SCID	Structured Clinical Interview for DSM-IV
Syl	Scyllo-inositol
SNR	Signal-to-Noise Ratio
SPF	Split-Plot Factorial
STEAM	STimulated Echo Acquisition Mode
SVD	Singular Value Decomposition
t	time, variable delay time
T	Tesla
T1	Spin-lattice relaxation time constant.
T2	Spin-spin relaxation time constant.
Tau	Taurine
tCr	Total Creatine (Cr + Phosphocreatine)
TE	Echo Time

tGL	Total glutamatergic metabolites (Glu + Gln)
TM	Mixing Time
TR	Repetition Time
μs	micro second
ω_0	Larmor frequency

Chapter 1

1 Introduction

1.1 Schizophrenia

Schizophrenia is a severe mental disorder, which was first referred to as dementia praecox by Emil Kraepelin in 1896.[1] He noticed that some psychotic patients had a deteriorating course similar to patients with dementia while the others recovered. The latter group was referred to as manic depressive patients. Later, Eugen Bleuler introduced the term schizophrenia,[2] highlighting the disturbed "sense of self" noticeably present in the disorder. Major symptoms of schizophrenia described in the DSM IV criteria[3] are classified as positive symptoms (e.g. hallucination and delusions), negative symptoms (e.g. social withdrawal and flat emotion) and cognitive symptoms (e.g. poor attention and executive functioning). Positive symptoms are usually suppressed with the antipsychotic drugs while negative symptoms are not improved as much with these medications. Thus far, there is no cure for schizophrenia and its causative mechanism is unclear.

There have been many epidemiological and genetic studies of schizophrenic patients. Research has shown that a family member of schizophrenic patients is more likely to develop the disease than the general population. In the case of monozygotic twins, the chance of developing schizophrenia increases to 50 percent when the other suffers from schizophrenia.[4] If someone is a first degree relative, the risk is about 10 percent compared to about 1 percent in the general population. A few groups reported that the number of schizophrenia patients born during a flu epidemic in 1957 was significantly higher than the general population.[5] Other studies have found increased risk of schizophrenia associated with obstetrical complications[6] such as bleeding in pregnancy. Thus, schizophrenia is a complex disorder with both genetic and environmental factors contributing.

1.1.1   Pathological evidence

From post mortem studies, abnormalities in nerve cells in schizophrenia were found such as pyramidal cell disarray in the hippocampus, associated with long-term memory.[7] Pakkernberg[8] found decreased total neuronal number in the mediodorsal thalamus, a central sensory processing region in the human brain. Selemon et al.[9] showed higher neuronal density in the prefrontal cortex in schizophrenia compared to the normal human brain, suggesting a potential malfunction in higher order processing. In other studies, significantly decreased GABAergic interneurons were seen in schizophrenia.[10] GABA (gamma aminobutryric acid) is an inhibitory neurotransmitter, which mediates the glutamatergic signals in the brain.[11,12] Significantly decreased glutamic acid decarboxylase (GAD)67 expression was seen in the brain tissues of schizophrenia subjects. GAD67 protein is produced when GABA is synthesized from glutamate, an excitatory neurotransmitter in the brain. Significant GAD67 reduction has been reported in the prefrontal cortex in this patient population.[13] Akbarian et al. found that cell migration in the prefrontal cortex and hippocampus occurred in deeper area in schizophrenia compared to controls.[14,15] These postmortem findings and Falkai et al.[16] suggest an abnormality in the brain developmental process affecting cortical structure. However, postmortem studies have a number of limitations such as the confounding effects of medication, aging and other medical illnesses.

1.1.2   Brain imaging (CT, MRI)

Recent developments in neuroimaging have facilitated the *in vivo* examination of patients and controls. The most consistent finding has been the larger size of the lateral ventricles in chronic schizophrenic patients. This abnormality was found in studies using computed tomography (CT)[17] and magnetic resonance imaging (MRI).[18] In terms of the anatomical structure, a reduction in size in schizophrenia compared to controls has been reported in several regions including the dorsolateral prefrontal cortex, hippocampus, thalamus, anterior cingulate and superior temporal gyrus.[19]

Gray matter losses in schizophrenia, compared to normal subjects, were observed in several regions in the brain such as the frontal cortex, dorsolateral prefrontal regions, hippocampus, and superior temporal gyrus.[19] However, findings in gray matter loss have not been consistent in terms of the brain region. Thompson et al.[20] examined gray matter loss in schizophrenia subjects and healthy controls over five years. They showed a significant reduction in cortical gray matter in schizophrenia subjects compared with controls. This study and several similar longitudinal studies[21,22] imply that neuroanatomical abnormalities in schizophrenia may be progressive.[17]

1.1.3   Functional connectivity

Besides the structural abnormalities in schizophrenia, there has also been research to examine the functional connectivity in the brain. Diffusion tensor imaging (DTI) techniques provide a view of the connectivity in the brain regions, inferring the directional connectivity through the measurement of the apparent diffusion coefficient (ADC).[23] Many studies have shown the increased myelin density in the white matter, suggesting a complex functional connectivity in schizophrenia.[24] Functional MRI (fMRI) has shown a functional disconnectivity in schizophrenia such as in default network studies.[25] A default network is considered to be the basic functional connectivity in the resting state of the normal brain. A few studies of the default network showed that some of the functional connections are abnormal in schizophrenia.[26] Bluhm et al.[27] reported that functional connectivity from the posterior cingulate is significantly weaker or unidentified in the first episode schizophrenia patient when compared to healthy volunteers.

Thus, there are a number of structural and functional abnormalities found in many brain regions in schizophrenia patients. The heterogeneity of these findings points to a number of genetic and environmental factors, all of which may affect final common pathways leading to the symptoms of schizophrenia. Among possible final common pathways, limbic basal ganglia thalamocortial circuits have been the most studied.[28]

1.1.4   Candidate circuit: Basal ganglia-thalamocortical circuit

The central nervous system is composed of billions of nerve cells (neurons). The signals, such as sensory information, are transmitted as electric stimuli with neurotransmitters, which are biochemical compounds, pooled in the axon terminals.
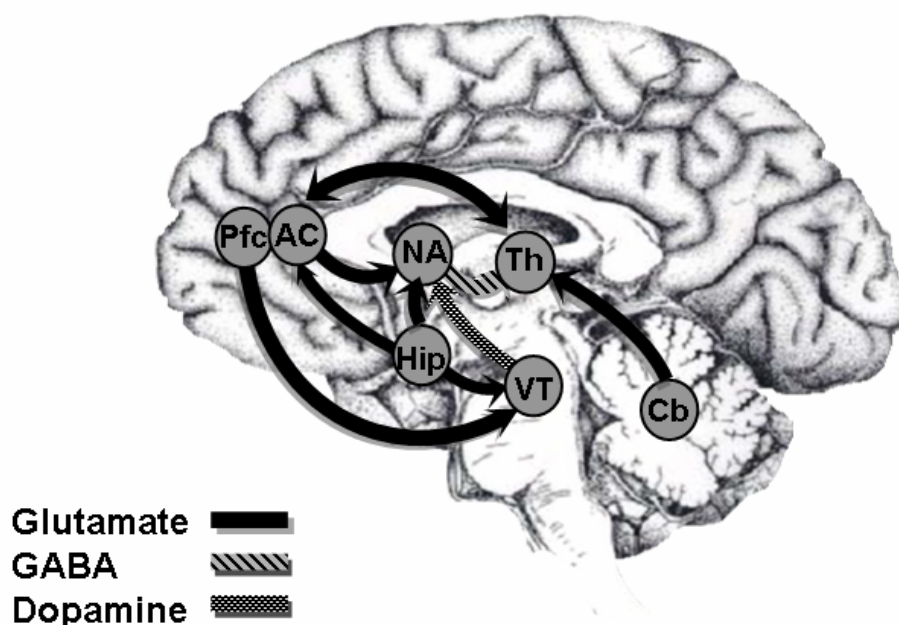
Figure 1-1: Limbic basal ganglia thalamocortical circuit

AC, anterior cingulate; Cb, cerebellum; Hip, hippocampus; NA, nucleus accumbens; Pfc, prefrontal cortex; Th, thalamus; VT, ventral tegmentum. (This illustration is adapted from Figure 2-2 in [29])

Figure 1-1 represents one potential candidate neuronal circuit implicated in schizophrenic anomalies, called the limbic basal ganglia thalamocortical (BGTC) circuit. This BGTC circuit, one of the basic neuronal pathways in the normal human brain, is considered to be a possible candidate circuit for schizophrenia because this circuit is responsible for the connections between the brain regions related to schizophrenic symptoms. The anterior cingulate is associated with attention and emotional processing.[30] The thalamus is

considered to be a gateway to the brain since all neuronal signals except olfactory information pass through this region. Most of the connections are glutamatergic. Glutamate is an amino acid found in many areas of the body, but is abundant in the nervous system where it is a major excitatory neurotransmitter. The understanding from this candidate circuit in local abnormalities will be extended to the entire brain encompassed by the neuronal pathways. For instance, if significantly higher or lower glutamate is observed in the thalamus, it may result in malfunction of the entire candidate circuit, composed of glutamatergic connections.

Another important excitatory neurotransmitter associated with the BGTC is dopamine. In this BGTC, dopaminergic neurons project from the ventral tegmentum to the nucleus accumbus which is an important node in this pathway. Currently, most medication for schizophrenia targets the dopamine neurotransmission.[31] Since schizophrenic positive symptoms are improved with these medications, dopamine is thought to be a key neurotransmitter implicated in this disorder.[32]

1.1.5   Etiological theories of schizophrenia

As indicated above, the glutamate and dopamine theories are good candidates for investigations to elucidate possible mechanisms of schizophrenia. From a pathophysiological point of view, these two hypotheses of schizophrenia will be discussed below. The Dopamine Hypothesis is suggested through the effect of antipsychotic medication that suppresses psychosis by blocking the dopamine receptor.[32] The Glutamate Hypothesis is suggested by the results of drugs that cause glutamate receptor hypofunction. In normal and schizophrenic subjects these drugs induce both psychotic symptoms (e.g. hallucinations) and negative symptoms (e.g. flat affect and lack of motivation). While the Glutamate Hypothesis has some advantages, there is not a large amount of direct evidence suggesting that glutamate is the major cause of schizophrenia. It is also possible that both dopamine and glutamate may be involved in the pathophysiology of schizophrenia.

1.1.5.1   Dopamine hypothesis

The abuse of drugs that stimulate dopamine often causes hallucinations and delusions that resemble the positive symptoms of schizophrenia.[33] Dopamine is one of the major excitatory neurotransmitters, associated with several functions such as motor activity, attention and reward.[34] Positron emission tomography studies have shown an increased dopamine re-uptake, compared to a control group, in the D2 receptor at the ventral tegmentum in schizophrenic subjects as well as psychotic patients.[35] Most antipsychotic medications block the D2 receptor to prevent binding of the dopamine, resulting in significant improvement in psychotic symptoms, but showing less improvement in the negative symptoms. Thus, dopamine is most likely involved in schizophrenic symptoms, but is not likely the main etiological factor.

1.1.5.2   Glutamate hypothesis

This thesis has focused on another excitatory neurotransmitter; glutamate. Although glutamate is an essential excitatory neurotransmitter in vertebrates, it may be involved in the symptoms of schizophrenia. In an animal study, Olney and Farber[36] reported that phencyclidine, a drug that inhibits the glutamate neurotransmission by blocking the N-methyl D-aspartate (NMDA) glutamate receptor, could induce schizophrenic-like changes. The rats that received phencyclidine demonstrated progressive loss of gray matter in regions found to have similar changes in schizophrenia. Curiously patients who ingest drugs that block NMDA receptors develop both positive and negative symptoms.[37] Blockage of the NMDA receptor leads to impaired GABAergic activity, which inhibits the glutamatergic neurotransmission.   However when GABA activity is impaired there is another pathway that is activated that leads to excessive glutamate neurotransmission when the NMDA receptor is blocked.

This excessive glutamate neurotransmission can be toxic to neurons (excitotoxicity), and may affect the glutamate pathways in the entire BGTC circuit. This toxic process

eventually leads to the neuronal dysfunction, loss of synapses or neuronal death (neurodegeneration). Thus we hypothesized that glutamatergic anomalies in schizophrenia may lead to limited neurodegeneration associated with a loss of neuropil and functional deficits. This theory could explain why schizophrenia symptoms such as social withdrawal improved little and often persist throughout the lifetime of the patients.

1.1.6   Neurodevelopment versus Neurodegeneration

It is unclear at what time point schizophrenia is pathologically evident. Schizophrenic symptoms typically appear around adolescence when a family member notices unusual behavior or psychotic symptoms. This could coincide with cortical pruning, which may uncover an early neurodevelopmental lesion. However, there is a debate over whether schizophrenia is a neurodevelopmental or a neurodegenerative disorder. The former theory indicates that there are abnormalities before-birth but that these are hidden or hardly visible. These problems during gestation lead to a dealignment of the cortical layers or abnormal cell migration as indicated above. This neurodevelopmental hypothesis suggests that these anomalies do not progress after their manifestation during adolescence.[38] On the other hand, the neurodegenerative hypothesis suggests that there is some sort of degenerating process after the development of psychiatric symptoms in schizophrenia subjects.[39] This theory has not been widely adopted due to a lack of evidence of cell death in schizophrenia.[40] For instance, a significant decrease in brain cell number is found in several regions in Alzheimer's disease patients, one of the neurodegenerative disorders. Instead of evidence of cell death, loss of neuropil and smaller neuronal size in schizophrenia are often reported. However, limited forms of excitotoxicity not associated with cell death have been reported.[41] Since deteriorating social function is one of the clinical criteria in schizophrenia, we hypothesized that schizophrenia may be a neurodegenerative disorder as well as a neurodevelopmental disorder. To examine this hypothesis, we focused on the neurotransmitter glutamate, which possibly leads to neuronal dysfunction. We have selected proton magnetic resonance spectroscopy (MRS) to track the glutamatergic metabolites in schizophrenic subjects *in vivo*.

1.2 The Investigative Technique: Magnetic resonance spectroscopy

Magnetic resonance imaging and spectroscopy are excellent techniques to measure structural and neurochemical changes/differences *in vivo* as there is no ionizing radiation. Thus, serial investigations are possible in both patients and healthy controls.

1.2.1 Principles of magnetic resonance imaging and spectroscopy

The research groups of Purcell[42] and Bloch[43] independently introduced the principle of nuclear magnetic resonance (NMR) in 1946. They discovered that nucleus in strong magnetic field, precess with a certain frequency (Larmor frequency). These precessing nuclei could be made to interact with specific radio frequency energies and a nuclear signal could be measured. The Nobel Prize in Physics 1952 was awarded jointly to Felix Bloch and Edward Mills Purcell "for their development of new methods for nuclear magnetic precision measurements and discoveries in connection therewith."

Building independently on this phenomenon the groups of Lauterbur[44] and Mansfield[45] are credited with the discovery of Magnetic Resonance Imaging (independent publications in1973). The Nobel Prize in Physiology or Medicine 2003 was awarded jointly to Paul C. Lauterbur and Sir Peter Mansfield "for their discoveries concerning magnetic resonance imaging."

1.2.1.1 Net magnetization

Nuclear spins precess at the Larmor frequency (ω_0), in a static magnetic field (B_0). We can write the 'Larmor equation' as; $\omega_0 = \gamma B_0$, where γ is the gyromagnetic ratio ($2\pi \times 42.575$ MHz/T for protons). Quantum mechanically, the only allowed orientation of these

spins is either parallel or anti-parallel to the field, with the preferred direction being parallel. In thermal equilibrium, a Boltzmann distribution can describe the ratio of parallel to anti-parallel spins. For example at 1.5T and 37 Celsius, there is an excess of only 1 in 100,000 spins that are parallel to the field. It is this spin excess that produces the net magnetization (M_0) parallel to B_0 and ultimately contributes to nuclear signal which is used to create an image. This net magnetization vector for most practical applications can be treated in a semiclassical formalism, where the motion of the vector in the general magnetic field is determined by the phenomenological Bloch equation:[43]

$$\frac{d\mathbf{M}}{dt} = \gamma \mathbf{M} \times \mathbf{B} + \frac{(M_0 - M_z)}{T1} - \frac{M_{xy}}{T2} \qquad (1\text{-}1)$$

,

where M_z is the longitudinal magnetization, M_{xy} is the transverse component of the magnetization, and T1 and T2 are the spin-lattice and spin-spin relaxation times respectively. Bold font (e.g. $\mathbf{M}$, $\mathbf{B}$) refers to vectors.

1.2.1.2 M_0 rotation along B_1 and FID

Thus far, only a static magnetic field has been considered in the z direction. It is only when the net magnetization vector is perturbed into the transverse (xy) plane that a signal is detected in the receive coil, which is oriented in the xy plane. In order to direct the net magnetization toward the x-y plane, a rotating magnetic field (B_1) is often applied in the x direction. This induces a precession of the net magnetization around the B_1 vector, and eventually into the x-y plane. To rotate in this manner, the frequency of B_1 must be tuned to the Larmor frequency. As the Larmor frequency is typically in the radio frequency (RF) band, the B_1 pulse is often referred to as an RF pulse. The rotation speed around B_1 is slower with respect to the Larmor frequency because the B_1 magnetic field (e.g. 10 μT) is much smaller than the B_0 field (e.g. 1.5T). When the RF pulse is turned off, the net magnetization vector returns to thermal equilibrium (M_0) oriented along the longitudinal direction.

1.2.1.3   FID, and T1 & T2 relaxation

The transverse component of this magnetization decreases as the spins lose their phase coherence. This decrease in the net transverse component with precession at the Larmor frequency is called free induction decay (FID). A FID is always generated when an RF pulse is applied. While the longitudinal magnetization gradually recovers with time, the transverse components of the spins gradually lose their phase coherence and the net transverse magnetization decreases over time. These processes are due to T1 relaxation and T2 relaxation, respectively. The re-growth process involves the energy exchange between spins and the main kinetic energy of the nuclei through the dipole-dipole interaction. A T1 process requires a magnetic field fluctuating near the Larmor frequency. This oscillating magnetic field is generated by another proton or electron in the same molecule or different molecule tumbling or moving with a frequency near the Larmor frequency. T1 is the time that the longitudinal magnetization recovers from zero to 63% of its equilibrium value after the end of the 90 degree RF pulse.

T2 is the decay time associated with the magnetization dephasing process in the transverse plane. Phase coherence decreases quickly when the magnetic field fluctuation induced by molecular motion or tumbling is much slower than the Larmor frequency. To have an effect on the magnetization in the x-y plane these fluctuations must be along the z axis. T2 is the time that the transverse component decreases to 37% after the RF pulse. If the molecule tumbling rate or movement is much faster than the Larmor frequency, T2 in this environment becomes longer and eventually approaches T1. In this case, the static dephasing originating in the local magnetic fields experienced by the spins is removed, because the local magnetic fields are averaged due to "motional averaging."

1.2.1.4   Selective excitation (slice selection), gradients

In order to rotate the net magnetization vector into the x-y plane, the magnetic field B_1 must be maintained for a time, t, such that $\gamma B_1 t = \pi/2$. This would tilt spins throughout the entire volume through $\pi/2$, and is referred to as a 90 degree pulse. In order to rotate the magnetization through 180 degrees, this same RF pulse could be applied, but

maintained for a duration 2t. In order to excite a particular slice however, a linear magnetic field gradient is required. This gradient creates a linear variation in the magnetic field with respect to position, for example along the z-direction. With such a linear gradient, the resonant frequency of the hydrogen nuclei varies depending upon their physical location along the z-direction. While these gradients are active, the physical slice of interest corresponds to a bandwidth of frequencies. In order to excite only those spins corresponding to the physical slice, the RF pulse is typically shaped with a sinc waveform such that a pulse with a particular frequency bandwidth can be generated. As mentioned earlier, it is only when the net magnetization is directed into the x-y plane that the FID is detected by the hardware. It is these signals that must be collected to form an image.

The proton signals are received by a coil, the cross-sectional area of which is set perpendicular to the transverse plane. This RF coil is often the equivalent of a coil of wire tuned to the resonant frequency (the Larmor frequency). Often so called birdcage resonators or birdcage coils are used in MRI, primarily for transmission of signal. A complete description of these coils is beyond the scope of this thesis. However these coils have good uniformity, and are cylindrical coils, placed in parallel with the main magnetic field, and hence the bore of the MRI. These coils are a great advantage in MRI because they can generate transverse magnetic fields while allowing a body to placed along the cylindrical axis. For simplicity however, the signal detection will be considered to be strictly from a simple solenoid.

Once the magnetic field is directed toward the transverse plane, it begins to precess around the static field B_0. Following a 90 degree pulse, the precessing magnetization vector represents a rotating magnetic field that induces an oscillating signal in the RF coil. This signal is the free induction decay. The decay of the magnetization is characterized using the relaxation time T2*, which is composed of T2 and the magnetic field inhomogeneity, which is determined by the magnetic field stability, quality of shimming, and so on. T2* is often written as:

$$\frac{1}{T2^*} = \frac{1}{T2} + \frac{1}{T2'}$$

(1-2)

,

where T2' is the contribution to the decay due to magnet inhomogeneities, and other susceptibility issues such as air-tissue interfaces, iron concentration, etc.

1.2.1.5 Fourier transform (time $\leftrightarrow$ frequency)

Time and frequency, and similarly object space and spatial frequency are intimately related through the Fourier Transform. The Fourier Transform, $F(\omega)$ of a function, $f(t)$, is given by:

$$F(\omega) = \int_{-\infty}^{+\infty} f(t) \exp(-i\omega t)\, dt$$

(1-3)

,

and a similar relationship can be defined between a function in image space, $f(x)$, and its Fourier Transform in spatial frequency (or "Fourier") space, $F(k_x)$. It turns out that the MRI signal is related to the magnetization intensity through a Fourier transform. To illustrate this relationship, it is instructive to first consider the process of phase and frequency encoding in a simple spin echo MRI experiment.

1.2.1.6 Frequency-encoding & phase-encoding (MRI)

A simple spin echo (SE) experiment is illustrated in Figure 1-2. The Readout gradient, or x-gradient, applied at the time of signal readout causes the resonant frequency ($\omega(x)$) to vary with x-position according to:

$$\omega(x) = \omega_0 + \gamma\, G_x\, x$$

(1-4)

,

where ω_0 is the Larmor frequency, γ is the gyromagnetic ratio, and G_x is the x- (readout) gradient.
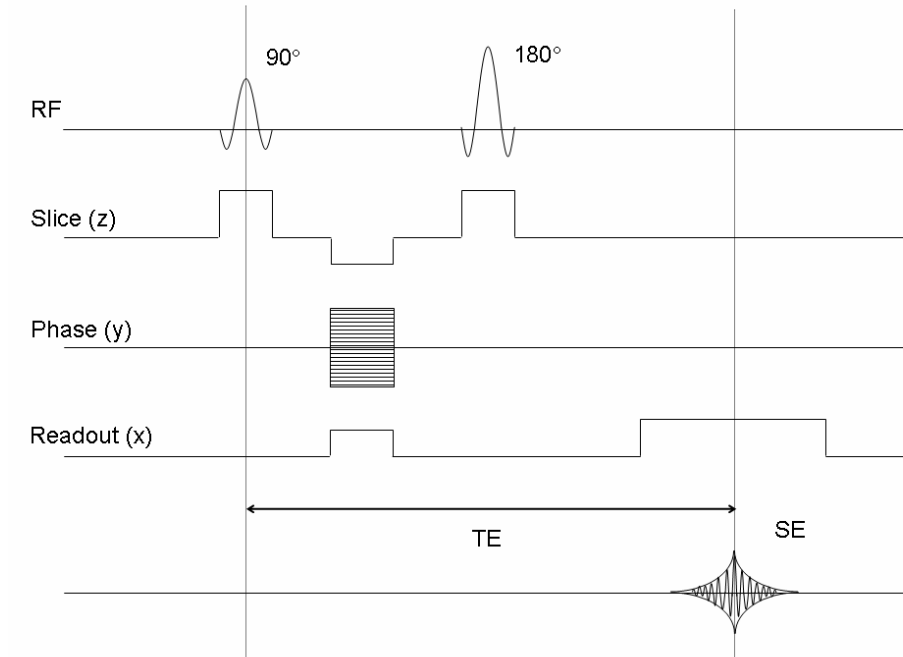
Figure 1-2: MRI Sequence Diagram of a simple Spin-Echo

(Adapted from [46])

This gradient is often referred to as the frequency encoding gradient. According to Figure 1-2, a phase, or y-gradient (G_y), is applied shortly after the initial 90 degree pulse; however it is applied in a different manner than the x-gradient. G_y is applied for a fixed time, t_y, and the entire sequence is repeated a number of times, each with a different gradient magnitude. During the time t_y, the spins are given a different phase ωt_y, depending upon their y position:

$$\omega(y)\, t_y = \omega_0\, t_y + \gamma\, G_y\, y\, t_y$$

<div align="right">(1-5)</div>

.

Each time the sequence is repeated with a different G_y, the spins are given a different amount of phase encoding. This sequence is repeated N times, and an echo is recorded with M points, generating a matrix (N × M) of echo's that differ by the amount of phase encoding. When this block of data is 2D Inverse Fourier Transformed, the image information is recovered. Rather than strictly imaging, MR spectroscopy isolates a signal from a particular region in the volume. When this time varying proton signal is Fourier

transformed, it now turns out to be a spectrum in the frequency domain. The full width at half maximum of the spectrum is determined by $(\pi T2^*)^{-1}$.

1.2.1.7   Sampling rate, image resolution

Spatial frequency is the inverse (Fourier) space with respect to object space. The spatial frequencies are defined in terms of the readout gradient amplitude, G_x, and the phase encoding step, G_y, as:

$$k_x = \frac{\gamma}{2\pi} G_x t$$

(1-6)

,

$$k_y = \frac{\gamma}{2\pi} G_y t_y$$

(1-7)

.

Note that in order to sample the spatial frequencies, time, t, is varied to sample k_x, however the gradient amplitude, G_y, is varied to sample k_y (t_y is a constant). The simplest definition of resolution is to divide the Field Of View (FOV) into N_x or N_y segments, so that the resolution, δ_x and δ_y are given by:

$$\delta_x = \frac{FOV_x}{N_x} \quad ; \quad \delta_y = \frac{FOV_y}{N_y}$$

(1-8)

.

Because position and spatial frequency form a Fourier pair, the width in object space (FOV) is inversely related to the resolution in the frequency space (Δk):

$$FOV_x = \frac{1}{\Delta k_x} \quad ; \quad FOV_y = \frac{1}{\Delta k_y}$$

(1-9)

.

By the same argument however, the extent or width in the frequency domain (Wk_x and Wk_y) should be related to the inverse of the resolution in the spatial domain. With the assumption that the widths in the frequency domain are:

$$Wk_x = N_x \Delta k_x \quad ; \quad Wk_y = N_y \Delta k_y$$

(1-10)

.

Equations (1-8) through (1-10) show that $\delta_x = 1/Wk_x$ and $\delta_y = 1/Wk_y$ as expected. Using equations (1-6) and (1-7), expressions can be easily derived for Δk_x and Δk_y, the sampling period:

$$\Delta k_x = \frac{\gamma}{2\pi} G_x \Delta t \tag{1-11}$$

$$\Delta k_y = \frac{\gamma}{2\pi} \Delta G_y t_y \tag{1-12}$$

where it is now explicit that increments in k_x are related to increments in the digitizer resolution (Δt), and increments in k_y are related to increments in the phase encode gradient (ΔG_y). These expressions can then be used for a given pulse sequence to derive a relationship between the pulse parameters and the FOV, resolution, and sampling rate.

1.2.1.8   Introduction of MRS physics, chemical shift

While MRI is composed primarily of the signals from the hydrogen nuclei of the water molecules, magnetic resonance spectroscopy is closely related to the signals from the hydrogen groups in the chemical structure of the sample or region. Frequencies of these hydrogen groups are off-resonance from the Larmor frequency of water protons. One of the primary contributors to this off-resonance is the chemical shielding, or chemical shift. Because electrons on molecules can also become polarized in a magnetic field, the actual field, and therefore the resonant frequency at the nucleus (ω_{eff}) will be less due to this chemical shielding (σ):

$$\omega_{eff} = \omega_0 (1 - \sigma) \tag{1-13}$$

where σ is the isotropic chemical shielding. In a full quantum mechanical treatment, σ is a tensor quantity. For a simple molecule that can be either parallel (σ_a) or antiparallel (σ_b) to the field, the chemical shielding can be written in terms of an isotropic and an anisotropic term:

$$\sigma = \frac{1}{3} \, (\sigma_b + 2\,\sigma_a) + \frac{1}{3} \, (3\,(\cos\theta)^2 - 1)\,(\sigma_b - \sigma_a) \qquad (1\text{-}14)$$

$$\text{(isotropic)} \qquad\qquad \text{(anisotropic)}$$

.

However in a liquid, the molecules will sample all orientations, and will average to zero the anisotropic chemical shielding. The chemical shift, δ, in parts per million (ppm) is defined as the shielding with respect to a reference, or equivalently, the shift in frequency with respect to a reference:

$$\delta = \sigma\,(\text{ref}) - \sigma\,(\text{sample}) \quad [\text{in ppm}]$$

or $\qquad\qquad\qquad\qquad\qquad\qquad\qquad\qquad\qquad\qquad$ (1-15)

$$\delta = \frac{\omega\,(\text{sample}) - \omega\,(\text{ref})}{\omega\,(\text{ref})} \times 10^6$$

,

where in brain proton MRS, the reference is usually chosen such that NAA = 2.01 ppm.

A phenomenon that generates a fine structure in the NMR spectrum is J-coupling. J-coupling or indirect dipole-dipole coupling is an electronic nuclear interaction between the electrons in a molecule and the hydrogen nucleus, which generates off-resonance perturbations from the proton Larmor frequency. The degree of off-resonance effects depends upon the chemical structure, and the organization of hydrogen nuclei in the molecule. In addition, the spectral shape is no longer a single peak – this interaction introduces a fine structure to the spectrum. The number of peak splittings is determined by the hydrogen groups in the molecular neighborhood.

Because protons have a nuclear spin ½, they are restricted to either the spin up or the spin down state. If a neighboring proton spin is exposed to this local field, then the spins of the hydrogen nuclei will precess either faster or slower than the resonant frequency, depending upon whether this proton neighbor is spin up or spin down. As a result, the spectrum for this single proton is split into a pair of peaks called a doublet. Peaks can also be split by multiple protons in a side group, and peaks can be split into doublets, triplets, etc. This phenomenon is called J-coupling and the distance of the splitting is called the J-coupling constant expressed in Hertz. It is mainly because of the chemical shift, and J-

coupling, that the various metabolites can be identified based upon their unique spectral signature.

1.2.2   Magnetic resonance spectroscopy

In general, there are two types of spectroscopy sequences, single and multiple voxel. A single voxel sequence is composed of three RF pulses, each coincident with their own slice selective gradient applied in each of the Cartesian axes. This process selects three perpendicular slices, with the selected volume corresponding to the intersection of these slices. The most common single voxel spectroscopy sequences are stimulated echo acquisition mode (STEAM) and point-resolved spectroscopy (PRESS). Chemical shift imaging (CSI) and magnetic resonance spectroscopic imaging (MRSI) are common multi-voxel type sequences. While the data are collected from much larger regions compared to single voxel spectroscopy, each volume tends to be bigger and the total data acquisition time is much longer.

1.2.2.1   STEAM vs. PRESS sequences

Both STEAM and PRESS sequences are composed of three RF pulses. Each RF pulse results in a free induction decay, each combination of two RF pulses produces a spin-echo and three RF pulses create a stimulated echo as well as a double spin-echo. While a stimulated echo is the primary signal to be detected in STEAM sequences, a double spin-echo is the primary signal to be detected in PRESS sequences.

The STEAM sequence, depicted in Figure 1-3, is composed of three 90 degree RF pulses, preceded by a CHEmical Shift Selective (CHESS) pulse. The RF pulses create one stimulated echo (STE), three FIDs, three single spin-echoes, and one double spin-echo. Because the stimulated echo is the only signal used, the other FIDs and spin-echoes are spoiled using crushing gradients, dephasing their transverse magnetizations, so that they do not contribute to the overall signal.
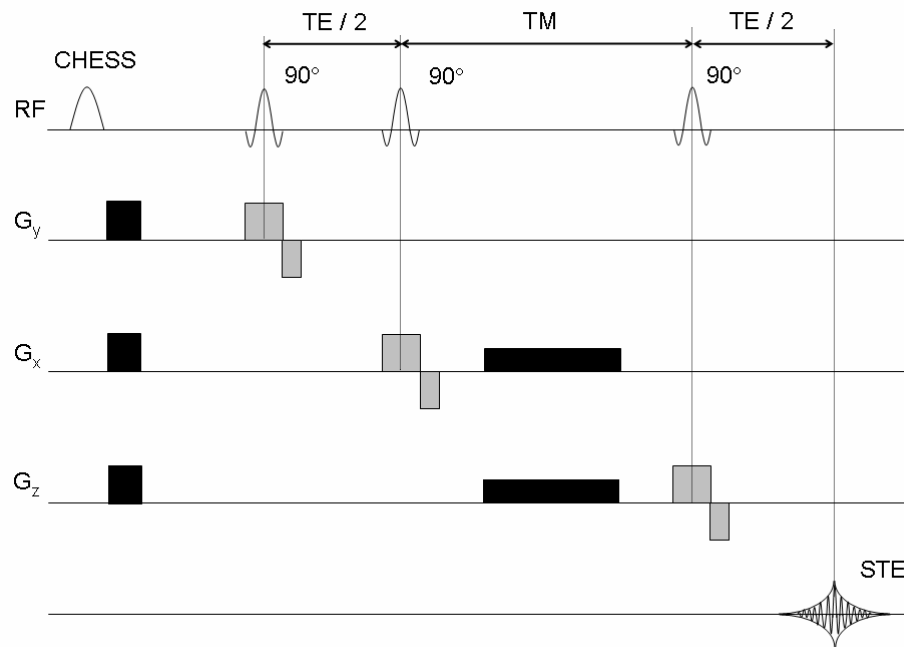
Figure 1-3: STEAM Sequence Diagram

The black rectangles represent spoiling gradients. The gray rectangles represent slice selective gradient with refocusing gradient. (Adapted from [47])

In theory, the signal completely recovers to the original amplitude in a PRESS sequence while only half of the original signal is detected in the STEAM sequence. After the first 90 degree RF pulse in the STEAM sequence, the spins in the transverse plane (x-y plane) dephase during the TE/2 period. For illustration, it can be assumed that the magnetization is composed of 4 spins, their directions 90 degrees apart from each other on the transverse plane after these spins dephase in the rotating frame of reference. The second 90 degree pulse flips these dephased spins to the y-z plane perpendicular to the transverse plane. The two components on the y-axis dephase due to the crushing gradient during the mixing time (TM) period. The third RF pulse rotates the spins along the longitudinal axis onto the transverse x-y plane again. The MR signal is maximized at TE/2 after the last RF pulse. However, the amplitude of this signal is a half of the original signals because the other two transverse spins were dephased during the TM period.

The PRESS sequence in Figure 1-4, on the other hand is composed of one 90 degree and two 180 degree RF pulses. Unlike the STEAM sequence, the double spin-echo (DSE) is the primary signal in the PRESS sequence.
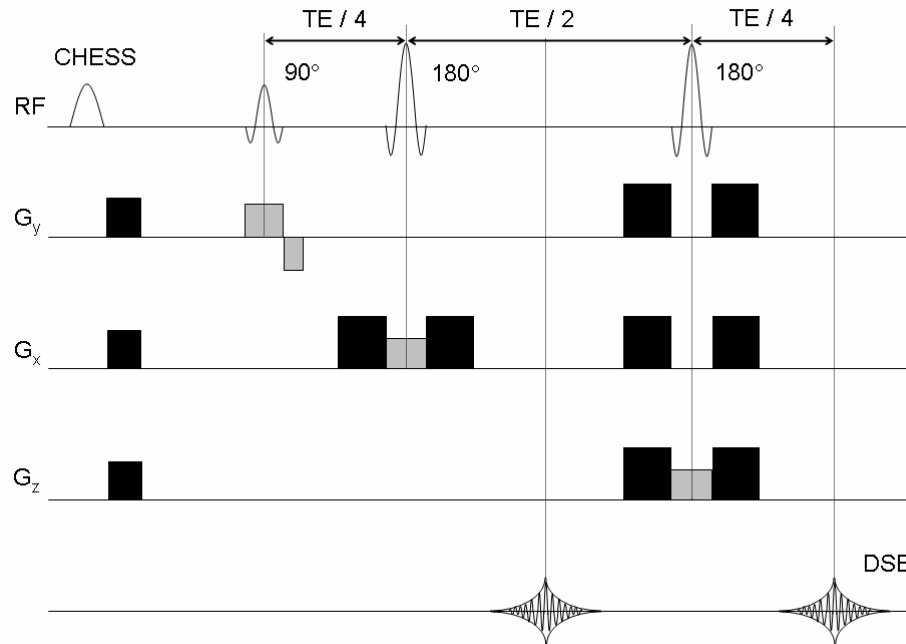
Figure 1-4: PRESS Sequence Diagram

The black rectangles represent spoiling gradients. The gray rectangles represent slice selective gradients. (Adapted from [47])

With a PRESS sequence, the dephasing spins are rephased at every TE/4 following a 180 degree pulse. Balanced gradients are implemented before and after the RF pulse. In practice, the signal does not fully recover due to an imperfect slice profile, which is the Fourier Transform of the RF pulse. A perfect slice profile is a rectangular shape, in which all spins within the range are excited with the desired flip angle. The Fourier Transform of a sinc function of infinite extent is a rectangular function. However, since the RF pulse is implemented in a finite time, the slice profile is not a perfect rectangular shape, with ringing artifacts at the edges of the slice profile.

Optimizing the slice profile of a 180 degree pulse is more difficult than designing the slice profile of 90 degree pulses. In the worst case scenario, only a small portion of the spins around the center of the slice profile rotate through 180 degrees but the others rotate with different flip angles. Another disadvantage of the PRESS sequence is that metabolite signals are sensitive to J-coupling, particularly at longer echo times. 180 degree RF pulses induce spin flips in the neighboring protons and change the metabolite peak shapes, a process called J-evolution.[48] For example, the coupling constant between the methyl protons and methine proton of lactate is approximately 6.9Hz. The doublet peak representing the methyl group at 1.3ppm appears negative at 1/J (~144ms) and positive at 2/J (~288ms) using the PRESS sequence.

1.2.2.2   Quantification Methods

Spectral fitting is performed either in the time domain or in the frequency domain. Time domain fitting, such as Singular Value Decomposition (SVD)[49] or Hankel-Lanczos SVD (HLSVD),[50,51] is often used to subtract the remnant water resonances. Although these methods are user-independent, they only seek the best mathematical combination of the resonances, which does not take any biological meanings into account. Thus, SVD and HLSVD are powerful techniques to subtract unnecessary resonances but these methods are insufficient to perform an *in vivo* spectral fitting.

The linear combination model (LCModel) is the most common spectral fitting technique in *in vivo* MRS.[52] LCModel seeks the best compromise for the sum of these components in the frequency domain using a model, composed of the metabolite peaks and their concentration levels obtained from *in vitro* experiment. This type of model is referred to as an "a priori knowledge" model. The detected MR signal is a summation of the sinusoids with an exponential decay. With setting a range of the parameters, such as the amplitude and phase of the damped sinusoids, a priori knowledge maintains a realistic metabolite levels and their biological combination in the metabolite quantification. Although LCModel is used in the frequency domain, the metabolite components in the a priori knowledge are the Fourier Transformed time domain signals.

Spectral fitting with a prior knowledge is also available in the time domain. The algorithm seeks the minimum difference between the raw data and the model (i.e. the a prior knowledge) in the time domain by adjusting the unconstrained parameters such as the amplitude of the components. As described in "Spectral fitting" in the next section, we have chosen to do the time domain fitting with the Levenberg-Marquardt algorithm.

1.2.2.3   Research Methodology

Since all relevant data were collected and processed in the same manner, the detailed methodologies including data collection, pre-processing, spectral fitting and quantification methods are described in this section.

1.2.2.3.1   Equipment, MRI and MRS sequences

All MR data were collected with a 4.0 Tesla Varian (Palo Alto, California, USA)/Siemens (Erlangen, Germany) whole body scanner with a Varian Unity Inova console and Siemens Sonata gradients, located at the Centre for Functional and Metabolic Mapping of the Robarts Research Institute, London, Ontario, Canada. A transmit and receive, circularly polarized birdcage head coil (XLR Imaging Inc., London, Ontario Canada) was used throughout our studies. The volunteer's head was placed inside of the head coil and set at the center of the head coil aligned with the subject's eyebrows. Global shimming was manually performed with the first and second order shims to reduce the magnetic field inhomogeneity.

A sagittal scout image was taken to plan the center of the transverse slices which cover the entire head. The center slice passed through the genu of the corpus callosum and the dorsal end of the splenium of the corpus callosum. Then, T1 weighted transverse images were collected with a 3D MP-RAGE sequence which is a three-dimensional magnetization prepared fast low angle shot (FLASH) sequence, flip angle $= 30$ degrees, $TR = 11.4$ ms, $TE = 6.2$ ms, inversion time (TI) $= 500$ ms, matrix size $= 256 \times 256$, field of

view $= 20 \times 20\,\text{cm}^2$, resolution $= 0.78 \times 0.78\,\text{mm}^2$, 64 contiguous slices of thickness $= 2.75\,\text{mm}$.

Using those T1-weighted images, the $10 \times 15 \times 10\,\text{mm}^3$ (right-left, anterior-posterior, inferior-superior direction) spectroscopy voxels were positioned in the left anterior cingulate (Brodmann Area (BA) 32 & 24) and the left thalamus. MR spectroscopy data were acquired with a single voxel STEAM sequence (TE $= 20$ ms, mixing time (TM) $= 30$ ms, TR $= 2000$ ms, dwell time $= 500\,\mu\text{s}$, 8 step phase-cycling) with a chemical shift selective pulse (CHESS) for water suppression. After the voxel localization, 90 degree RF pulse powers were optimized and local shimming was manually performed with a water unsuppressed spectrum. The CHESS pulse, which was composed of three Gaussian RF pulses, was turned on to optimize the RF power and pulse length. Metabolite data were acquired with water suppression (256 averages), followed by the water unsuppressed data (16 averages). This MRS procedure was conducted in the left anterior cingulate and the left thalamus.

1.2.2.3.2   Pre-processing

Water suppressed data were corrected for eddy current and the spectrum line shape with the QUality and Eddy Current Correction (QUECC) technique,[53] which is a combination of the "QUAntification improvement by converting LIneshapes to the Lorentzian TYpe" QUALITY[54] and "Eddy Current Corrections" (ECC), using the water reference spectrum. QUALITY deconvolution was performed on the first 400 complex points (100ms) in the time domain and ECC was performed on the rest of the complex points. Residual water resonances (4.2 - 6.2 ppm) were subtracted using the HLSVD algorithm.[51,55,56]

1.2.2.3.3   Spectral fitting

Pre-processed data were fit using in-house software called Fitman[56,57] (Lawson Health Research Institute) to the first 1024 complex points (512ms) in the time domain. The

fitting procedure was based on the Levenberg-Marquardt methods to minimize the differences between raw data and the prior knowledge. Our model was created with the twelve metabolites from *in vitro* measurement and eleven macromolecules from literature values. [58,59] Each metabolite spectrum was composed of single Lorentzian peaks while macromolecule spectra were Gaussian. Our template is composed of 247 single peaks with six parameters; chemical shift, amplitude (signal intensity at $t = 0$), Lorentzian linewidth, phase, delay time, and Gaussian linewidth. To reduce the time to find the global minimum, all parameters except amplitude are constrained in our model.

1.2.2.3.4 Metabolite quantification and volumetric analyses

Metabolite concentration levels are quantified using the internal water reference. Corresponding signal amplitudes are summed for each metabolite to express the peak area. Metabolite concentration levels were calculated using the following formulae[60]:

$$\frac{\dfrac{\dfrac{Area_{\text{metabolite}}}{Averages_{\text{metabolite}}}}{10^{(\text{Gain\_metabolite [dB] / 20})} \bullet scaling\ factor_{\text{metabolite}}}}{\dfrac{\dfrac{Area_{\text{water}}}{Averages_{\text{water}}}}{10^{(\text{Gain\_water [dB] / 20})} \bullet scaling\ factor_{\text{water}}}} \bullet \frac{\#\ of\ {}^1H_{\text{water}}}{\#\ of\ {}^1H_{\text{metabolite}}} \bullet Water\ percent \bullet 55.5556 \bullet 1000\ [\text{mM / l}] \ ,$$

(1-16)

$$Water\ percent = \frac{0.81 \times f_{\text{GM}} + 0.71 \times f_{\text{WM}}}{1 - f_{\text{CSF}}} \bullet \frac{\dfrac{Water_{\text{density 38C}}\ [\text{g / cm}^3]}{Water_{\text{molecular weight 38C}}\ [\text{g / Mol}]} \bullet 1000\ [\text{cm}^3 / l]}{55.5556\ [\text{Mol / l}]} \ ,$$

(1-17)

where *Area* is the peak area of spectrum, Averages is the number of transients, Gain represents the receiver gain, # of ${}^1H$ is the number of proton nuclei in the molecule (i.e. # of ${}^1H_{\text{water}}$ is 2), *scaling factor* is the scaling (e.g. 10^{-4}) of the raw data, *Water*${}_{\text{density 38C}}$ is the density of water at human body temperature, and *Water*${}_{\text{molecular weight 38C}}$ is the

molecular weight of water at human body temperature. Metabolite peak area is divided by the water peak area since water is set as the internal reference with the concentration level 55.5556 [Mol / l]. Water percentage is adjusted by the brain tissue fraction in the spectroscopy voxel because of different water percentage in each brain tissue: 81% in the gray matter (GM), 71% in the white matter (WM), and 100% in the cerebral spinal fluid (CSF).[61] There is an assumption that no metabolite exists in the CSF. The denominator $(1 - f_{CSF})$ is required to correct the water signal from the CSF. This adjustment is limited for the small CSF fraction in the spectroscopy voxel.

The fraction of the brain tissue is calculated from each spectroscopy voxel ($1.5 \, cm^3$) with ANALYZE and in-house software called Xstatpack, developed by J Davis. The detailed segmentation analysis is described in the Methods section in Chapter 3.

Volumetric changes in gray matter were measured with voxel-based morphometry (VBM)[62,63] on the T1-weighted anatomical images using Statistical Parametric Mapping (SPM) (Wellcome Department of Imaging Neuroscience, University College London, UK). Normalization was performed on all images with the T1-weighted template developed by the Montreal Neurological Institute. Images were segmented into gray, white and CSF compartments. Segmented images were then modulated using the Jacobian determinants, created in the normalization step. Lastly, images were smoothed with an isotropic Gaussian filter of 12mm full width at half maximum. A general linear model with t-statistics was applied for the statistical comparisons.

1.2.3   Techniques and Disease: MRS findings in schizophrenia

Abnormal glutamatergic metabolite levels have been found in cross-sectional schizophrenia studies using 1H MRS. Significantly elevated glutamine levels in the anterior cingulate were found in never-treated schizophrenia patients[64] and in patients at high risk to develop psychosis.[65] Tibbo et al.[66] reported a higher glutamate/glutamine ratio in the right medial frontal lobe in patients at high generic risk compared to those at low risk for schizophrenia. In the thalamus, Théberge et al.[62] found an increased

glutamine level in schizophrenia while Stone et al.[65] reported a decreased glutamate level in high-risk mental state patients. In the chronic studies, significantly decreased glutamate and/or glutamine levels were found in the anterior cingulate.[67-70] Théberge et al.[70] also reported a significantly increased glutamine level in the thalamus in chronic schizophrenia patients.

One of the issues with 1H MRS measures of glutamate is that only 15-20% of the glutamate MR signals are involved in the neurotransmission and the rest of the signals come from the pooled glutamate in the vesicle,[71] which does not have the same toxicity as the glutamate released into the synaptic cleft. For this reason, the focus of this thesis has been on measuring glutamine, a precursor of glutamate. Glutamate neurotransmitters in the synaptic gap are taken up by the glial cells, converted to glutamine, synthesized again to glutamate and pooled in the vesicle in the axon terminals. While 80% of the glutamate MR signal comes from the pooled glutamate in the neurons, most of the physiologically active glutamate comes from glutamine produced in glial cells.[71] Therefore, glutamine may be a better indicator of the glutamate neurotransmission although part of the pool of glutamate also arises from glucose via the tricarboxylic acid cycle.[72]

Phosphorous magnetic resonance spectroscopy (31P MRS) allows the investigation of neuronal damage, which may be caused by excitotoxicity. Phosphorous MRS is a useful technique to observe the energy metabolism and cell membrane phospholipid metabolism. Phosphocreatine (PCr) and inorganic phosphorous (iP) indicate the energy metabolism. Phosphomonoesters (PME) and phosphodiesters (PDE) indicate the phospholipid synthesis and membrane breakdown products. While significantly decreased PME and increased PDE were found in the first episode studies,[73,74] the phospholipid membrane metabolism showed an increased, decreased or even normal levels in chronic studies.[75-77]

Both 1H and 31P MRS findings are inconsistent in the chronic studies. This inconsistency may be due to the variability in type and dose of medication used to treat these patients. Longitudinal studies, however, are required to observe the disease process.

Using 1H MRS, Théberge et al.[60] examined seventeen never-treated schizophrenia patients and completed their 30 month follow-up scans. It was reported that at the onset there was an increased glutamine level in the patients compared to the healthy volunteers, however those elevated glutamine levels were decreased in schizophrenia over the 30 month assessments. In a longitudinal 31P MRS study, Miller et al.[78] reported an elevated PME in first episode schizophrenia patients compared to controls, with a significantly decreased PDE in schizophrenia patients at the 30 month assessment when compared with their initial assessment.

These two longitudinal studies suggest a degenerative process in the first few years in schizophrenia. However, several key questions are raised by these studies:

1. First, how long does this process persist in schizophrenia? Chapter 2 of this thesis is an extension of the previous longitudinal study (Théberge et al.[60]) to investigate whether these results persist out to 80 months.

2. Secondly, are metabolite levels such as glutamatergic metabolites and NAA affected by structural changes in the brain? To address this question, the third chapter of this thesis is designed to probe whether or not changes in the gray matter in the spectroscopy voxel could be associated with observed changes in metabolite levels.

3. Lastly, it was noted from our long-term study that due to a hardware modification, there was a change in the noise level of the system. Hardware replacements and/or upgrades are inevitable, particularly as the duration of a study becomes longer. Although our MR technician carefully maintained the MR system, with rigorous quality control, this change in the system noise may have affected the metabolite signal-to-noise ratio in our study. Thus the third and final question is: Did the signal-to-noise ratio change due to this hardware modification, and was the metabolite quantification affected? Chapter 4 represents a series of data manipulations and simulations which were designed to answer this question.

1.3   Hypotheses

1. Significantly higher glutamatergic metabolites during the first episode will decrease in schizophrenia in a time course. Glutamatergic metabolite decreases will correlate with widespread gray matter losses and social functioning at a 7 year follow-up (Chapter 2).

2. Loss of glutamatergic metabolites in first episode patients over time will be related to gray matter loss in the voxel of interest but will not be significantly affected by signal-to-noise changes associated with gray matter loss. NAA levels will be less likely to be affected by gray matter loss in the voxel of interest or signal-to-noise changes (Chapter 3).

3. Significant differences in brain metabolites observed in our long-term study would persist after the data manipulation to simulate a constant signal-to-noise ratio throughout this study. Signal-to-noise ratio may be maintained in a reasonable range during our long-term study (Chapter 4).

1.4   Overview of the thesis

This thesis is composed of two clinical studies (Chapters 2 and 3), and one technical study (Chapter 4). Chapter 2 has been accepted, and the other two chapters (Chapter 3 and 4) will be submitted for publication.

Chapter 2 contains a long term follow-up schizophrenia study using *in vivo* proton magnetic resonance spectroscopy. Eighty month follow-up scans were performed with the same schizophrenia patients as in our 30 months study to see if the deterioration persists in this disease. This manuscript has been accepted by British Journal of Psychiatry.

Chapter 3 contains a study to examine the metabolite levels adjusted by the amount of gray matter in the spectroscopy voxel. Significantly decreased metabolite levels and the amount of gray matter were observed in the long term study, presented in Chapter 2. This

analysis shows whether the loss of gray matter in the spectroscopy voxel is responsible for the changes in the metabolite levels.

Chapter 4 contains a technical study to examine how the MR signal-to-noise ratio affects the metabolite quantification. Metabolite signal-to-noise ratios tended to be higher in the first two years of the 80 months follow-up study (Chapter 2). A possible explanation is related to a hardware replacement, which is one of the potential confounding factors to consider, particularly as the length of a longitudinal study grows. To assess this issue, data manipulation in the corresponding data sets and noise simulation were performed to see the influence of signal-to-noise ratio as well as the precision of the metabolite quantification.

Chapter 5 is a summary chapter to discuss the entire results (Chapter 2 to 4) and future work.

Appendix A contains preliminary work to compare mood disorder and schizophrenia using the same methodology described in Chapter 2. These mental diseases are often misdiagnosed due to an overlap in the clinical symptoms.

Appendix B describes the methodology used in this thesis.

Appendix C presents a sample spectrum.

Appendix D contains the ethics approval.

1.5 References

1. Kraepelin E. *Dementia praecox and paraphrenia* (1919). Barclay RM, translator; Robertson GM, editor. Huntington, New York: Robert E Krieger; 1971.

2. Bleuler EP. *Dementia Praecox or the Group of Schizophrenias (Dementia Praecox oder Gruppe der Schizophrenien)*. New York: International Universities Press; 1950 (original 1911).

3. First MB, Spitzer RL, Gibbon M, Williams JBW. *Structured Clinical Interview for DSM-IV Axis I Disorders (SCID)*. New York: New York State Psychiatric Institute, Biometrics Research; 1997.

4. Cardno AG, Gottesman II. Twin studies of schizophrenia: from bow-and-arrow concordances to star wars Mx and functional genomics. *Am J Med Genet*. 2000;**97**(1):12-7.

5. Mednick SA, Huttunen MO, Machón RA. Prenatal influenza infections and adult schizophrenia. *Schizophr Bull*. 1994;**20**(2):263-7.

6. Cannon M, Jones PB, Murray RM. Obstetric complications and schizophrenia: historical and meta-analytic review. *Am J Psychiatry*. 2002;**159**(7):1080-92.

7. Kovelman JA, Scheibel AB. A neurohistological correlate of schizophrenia. *Biol Psychiatry*. 1984;**19**(12):1601-21.

8. Pakkenberg B. Pronounced reduction of total neuron number in mediodorsal thalamic nucleus and nucleus accumbens in schizophrenics. *Arch Gen Psychiatry*. 1990;**47**(11):1023-8.

9. Selemon LD, Rajkowska G, Goldman-Rakic PS. Abnormally high neuronal density in the schizophrenic cortex. A morphometric analysis of prefrontal area 9 and occipital area 17. *Arch Gen Psychiatry*. 1995;**52**(10):805-18; discussion 819-20.

10. Benes FM, McSparren J, Bird ED, SanGiovanni JP, Vincent SL. Deficits in small interneurons in prefrontal and cingulate cortices of schizophrenic and schizoaffective patients. *Arch Gen Psychiatry*. 1991;**48**(11):996-1001.

11. Akbarian S, Huang HS. Molecular and cellular mechanisms of altered GAD1/GAD67 expression in schizophrenia and related disorders. *Brain Res Rev*. 2006;**52**(2):293-304.

12. Lewis DA, Hashimoto T, Volk DW. Cortical inhibitory neurons and schizophrenia. *Nat Rev Neurosci*. 2005;**6**(4):312-24.

13. Woo TU, Kim AM, Viscidi E. Disease-specific alterations in glutamatergic neurotransmission on inhibitory interneurons in the prefrontal cortex in schizophrenia. *Brain Res*. 2008;**1218**:267-77.

14. Akbarian S, Bunney WE Jr, Potkin SG, Wigal SB, Hagman JO, Sandman CA, Jones EG. Altered distribution of nicotinamide-adenine dinucleotide phosphate-diaphorase cells in frontal lobe of schizophrenics implies disturbances of cortical development. *Arch Gen Psychiatry*. 1993;**50**(3):169-77.

15. Akbarian S, Viñuela A, Kim JJ, Potkin SG, Bunney WE Jr, Jones EG. Distorted distribution of nicotinamide-adenine dinucleotide phosphate-diaphorase neurons in

temporal lobe of schizophrenics implies anomalous cortical development. *Arch Gen Psychiatry.* 1993;**50**(3):178-87.

16. Falkai P, Bogerts B. Cytoarchitectonic and developmental studies in schizophrenia. In: Kerwin R, editor. *Cambridge Medical Reviews: Neurobiology and Psychiatry.* Vol 2. Cambridge, UK: Cambridge University Press; 1993. p. 43-70.

17. Weinberger DR, Torrey EF, Neophytides AN, Wyatt RJ. Lateral cerebral ventricular enlargement in chronic schizophrenia. *Arch Gen Psychiatry*. 1979;**36**(7):735-9.

18. Shenton ME, Dickey CC, Frumin M, McCarley RW. A review of MRI findings in schizophrenia. *Schizophr Res.* 2001;**49**(1-2):1-52.

19. DeLisi LE. The concept of progressive brain change in schizophrenia: implications for understanding schizophrenia. *Schizophr Bull.* 2008;**34**(2):312-21.

20. Thompson PM, Vidal C, Giedd JN, Gochman P, Blumenthal J, Nicolson R, Toga AW, Rapoport JL. Mapping adolescent brain change reveals dynamic wave of accelerated gray matter loss in very early-onset schizophrenia. *Proc Natl Acad Sci U S A*. 2001;**98**(20):11650-5.

21. van Haren NE, Hulshoff Pol HE, Schnack HG, Cahn W, Brans R, Carati I, Rais M, Kahn RS. Progressive brain volume loss in schizophrenia over the course of the illness: evidence of maturational abnormalities in early adulthood. *Biol Psychiatry.* 2008;**63**(1):106-13.

22. Takahashi T, Wood SJ, Yung AR, Soulsby B, McGorry PD, Suzuki M, Kawasaki Y, Phillips LJ, Velakoulis D, Pantelis C. Progressive gray matter reduction of the superior temporal gyrus during transition to psychosis. *Arch Gen Psychiatry.* 2009;**66**(4):366-76.

23. Lim KO, Helpern JA. Neuropsychiatric applications of DTI - a review. *NMR Biomed.* 2002;**15**(7-8):587-93.

24. Davis KL, Stewart DG, Friedman JI, Buchsbaum M, Harvey PD, Hof PR, Buxbaum J, Haroutunian V. White matter changes in schizophrenia: evidence for myelin-related dysfunction. *Arch Gen Psychiatry.* 2003;**60**(5):443-56.

25. Gusnard DA, Raichle ME, Raichle ME. Searching for a baseline: functional imaging and the resting human brain. *Nat Rev Neurosci*. 2001;**2**(10):685-94.

26. Garrity AG, Pearlson GD, McKiernan K, Lloyd D, Kiehl KA, Calhoun VD. Aberrant "default mode" functional connectivity in schizophrenia. *Am J Psychiatry.* 2007;**164**(3):450-7.

27. Bluhm RL, Miller J, Lanius RA, Osuch EA, Boksman K, Neufeld RW, Théberge J, Schaefer B, Williamson P. Spontaneous low-frequency fluctuations in the BOLD

signal in schizophrenic patients: anomalies in the default network. *Schizophr Bull.* 2007;**33**(4):1004-12.

28. Alexander GE, Crutcher MD, DeLong MR. Basal ganglia-thalamocortical circuits: parallel substrates for motor, oculomotor, "prefrontal" and "limbic" functions. *Prog Brain Res.* 1990;**85**:119-46.

29. Williamson P. *Mind, brain, and schizophrenia.* Oxford: Oxford University Press; 2006.

30. Vogt BA, Regions and Subregions of the Cingulate Cortex. In: Vogt BA, editor. *Cingulate Neurobiology and Disease*. Oxford: Oxford University Press; 2009. p. 3-36.

31. Seeman P. Dopamine receptors and the dopamine hypothesis of schizophrenia. *Synapse.* 1987;**1**(2):133-52.

32. O'Donnell P, Grace AA. Dysfunctions in multiple interrelated systems as the neurobiological bases of schizophrenic symptom clusters. *Schizophr Bull.* 1998;**24**(2):267-83.

33. Curran C, Byrappa N, McBride A. Stimulant psychosis: systematic review. *Br J Psychiatry.* 2004;**185**:196-204.

34. Schultz W. Reward signaling by dopamine neurons. *Neuroscientist*. 2001;**7**(4):293-302.

35. McGowan S, Lawrence AD, Sales T, Quested D, Grasby P. Presynaptic dopaminergic dysfunction in schizophrenia: a positron emission tomographic [18F]fluorodopa study. *Arch Gen Psychiatry*. 2004;**61**(2):134-42.

36. Olney JW, Farber NB. Glutamate receptor dysfunction and schizophrenia. *Arch Gen Psychiatry.* 1995;**52**(12):998-1007.

37. Krystal JH, Karper LP, Seibyl JP, Freeman GK, Delaney R, Bremner JD, Heninger GR, Bowers MB Jr, Charney DS. Subanesthetic effects of the noncompetitive NMDA antagonist, ketamine, in humans. Psychotomimetic, perceptual, cognitive, and neuroendocrine responses. *Arch Gen Psychiatry.* 1994;**51**(3):199-214.

38. Weinberger DR. From neuropathology to neurodevelopment. *Lancet.* 1995;**346**(8974):552-7.

39. Lieberman JA. Is schizophrenia a neurodegenerative disorder? A clinical and neurobiological perspective. *Biol Psychiatry*. 1999;**46**(6):729-39.

40. Weinberger DR, McClure RK. Neurotoxicity, neuroplasticity, and magnetic resonance imaging morphometry: what is happening in the schizophrenic brain? *Arch Gen Psychiatry*. 2002;**59**(6):553-8.

41. McEwen BS. Stress and hippocampal plasticity. *Annu Rev Neurosci.* 1999;**22**:105-22.

42. Purcell EM, Torrey HC, Pound RV. Resonance Absorption by Nuclear Magnetic Moments in a *Solid. Phys Rev.* 1946;**69**(1-2):37–8.

43. Bloch F. Nuclear Induction. *Phys Rev.* 1946;**70**(7-8);460–74.

44. Lauterbur PC. Image formation by induced local interactions: examples employing nuclear magnetic resonance. *Nature.* 1973;**242**:190-1.

45. Mansfield P, Grannell PK. NMR 'diffraction' in solids? J *Phys C: Solid State Phys.* 1973;**6**:L422–L427.

46. Brown MA, Semelka RC. *MRI: basic principles and applications*. 3rd ed. Hoboken, N.J. : Wiley-Liss; c2003.

47. Mandal PK. Magnetic Resonance spectroscopy (MRS) and its application in Alzheimer's Disease. *Concepts Magn Reson Part A Bridg Educ Res.* 2007;**30A**(1):40-64.

48. Ernst T, Hennig J. Coupling effects in volume selective 1H spectroscopy of major brain metabolites. *Magn Reson Med.* 1991;**21**(1):82-96.

49. de Beer R, van Ormondt D. Analysis of NMR data using time domain fitting procedures. In: Diehl P, Fluck E, Gunther H, Kosfeld R, Seelig J, editors. *NMR Basic Principles and Progress.* Vol 26. Berlin: Springer-Verlad; 1992. p. 201–248.

50. Barkhuisen H, de Beer R, van Ormondt D. Improved algorithm for noniterative time-domain model fitting to exponentially damped magnetic resonance signals. *J Magn Reson.* 1987;**73**:553-57.

51. van den Boogaart A, Ala-Korpela M, Jokisaari J, Griffiths JR. Time and frequency domain analysis of NMR data compared: an application to 1D 1H spectra of lipoproteins. *Magn Reson Med.* 1994;**31**(4):347-58.

52. Provencher SW. Estimation of metabolite concentrations from localized in vivo proton NMR spectra. *Magn Reson Med.* 1994;**30**;672–9.

53. Bartha R, Drost DJ, Menon RS, Williamson PC. Spectroscopic lineshape correction by QUECC: combined QUALITY deconvolution and eddy current correction. *Magn Reson Med.* 2000;**44**(4):641-5.

54. de Graaf AA, van Dijk JE, Bovée WM. QUALITY: quantification improvement by converting lineshapes to the Lorentzian type. *Magn Reson Med.* 1990;**13**(3):343-57.

55. Vanhamme L, van den Boogaart A, Van Huffel S. Improved method for accurate and efficient quantification of MRS data with use of prior knowledge. *J Magn Reson.* 1997;**129**(1):35-43.

56. Bartha R, Drost DJ, Williamson PC. Factors affecting the quantification of short echo in-vivo 1H MR spectra: prior knowledge, peak elimination, and filtering. *NMR Biomed.* 1999;**12**(4):205-16.

57. Bartha R, Drost DJ, Menon RS, Williamson PC. Comparison of the quantification precision of human short echo time (1)H spectroscopy at 1.5 and 4.0 Tesla. *Magn Reson Med.* 2000; **44** (2):185-92.

58. Kauppinen RA, Kokko H, Williams SR. Detection of mobile proteins by proton nuclear magnetic resonance spectroscopy in the guinea pig brain ex vivo and their partial purification. *J Neurochem.* 1992;**58**(3):967-74.

59. Behar KL, Ogino T. Characterization of macromolecule resonances in the 1H NMR spectrum of rat brain. *Magn Reson Med.* 1993;**30**(1):38-44.

60. Théberge J, Williamson KE, Aoyama N, Drost DJ, Manchanda R, Malla AK, Northcott S, Menon RS, Neufeld RW, Rajakumar N, Pavlosky W, Densmore M, Schaefer B, Williamson PC. Longitudinal grey-matter and glutamatergic losses in first-episode schizophrenia. *Br J Psychiatry.* 2007;**191**:325-34.

61. Stanley JA, Drost DJ, Williamson PC, Thompson RT. The use of a priori knowledge to quantify short echo in vivo 1H MR spectra. *Magn Reson Med.* 1995;**34**(1):17-24.

62. Ashburner J, Friston KJ. Voxel-based morphometry--the methods. *Neuroimage.* 2000; **11** (6 Pt 1): 805-21.

63. Ashburner J, Friston KJ. Why voxel-based morphometry should be used. *Neuroimage.* 2001; **14**: 1238-43.

64. Théberge J, Bartha R, Drost DJ, Menon RS, Malla A, Takhar J et al. Glutamate and glutamine measured with 4.0 T proton MRS in never-treated patients with schizophrenia and healthy volunteers. *Am J Psychiatry.* 2002;**159**:1944-6.

65. Stone JM, Day F, Tsagaraki H, Valli I, McLean MA, Lythgoe DJ, O'Gorman RL, Barker GJ, McGuire PK; OASIS. Glutamate dysfunction in people with prodromal symptoms of psychosis: relationship to gray matter volume. *Biol Psychiatry.* 2009;**66**(6):533-9.

66. Tibbo P, Hanstock C, Valiakalayil A, Allen P. 3-T proton MRS investigation of glutamate and glutamine in adolescents at high genetic risk for schizophrenia. *Am J Psychiatry.* 2004;**161**(6):1116-8.

67. Lutkenhoff ES, van Erp TG, Thomas MA, Therman S, Manninen M, Huttunen MO, Kaprio J, Lönnqvist J, O'Neill J, Cannon TD. Proton MRS in twin pairs discordant for schizophrenia. *Mol Psychiatry*. 2010;**15**(3):308-18.

68. Tayoshi S, Sumitani S, Taniguchi K, Shibuya-Tayoshi S, Numata S, Iga J, Nakataki M, Ueno S, Harada M, Ohmori T. Metabolite changes and gender differences in schizophrenia using 3-Tesla proton magnetic resonance spectroscopy (1H-MRS). *Schizophr Res*. 2009;**108**(1-3):69-77.

69. van Elst LT, Valerius G, Büchert M, Thiel T, Rüsch N, Bubl E, Hennig J, Ebert D, Olbrich HM. Increased prefrontal and hippocampal glutamate concentration in schizophrenia: evidence from a magnetic resonance spectroscopy study. *Biol Psychiatry*. 2005;**58**(9):724-30.

70. Théberge J, Al-Semaan, Williamson PC, Menon RS, Neufeld RWJ, Schaefer B et al. Glutamate and glutamine in the anterior cingulate and thalamus of medicated patients with chronic schizophrenia and healthy comparison subjects measured with 4.0-T proton MRS. *Am J Psychiatry*. 2003;**160**:2231-3.

71. Rothman DL, Behar KL, Hyder F, Shulman RG. In vivo NMR studies of the glutamate neurotransmitter flux and neuroenergetics: implications for brain function. *Annu Rev Physiol*. 2003;**65**:401-27.

72. Rothman DL, Novotny EJ, Shulman GI, Howseman AM, Petroff OA, Mason G, Nixon T, Hanstock CC, Prichard JW, Shulman RG. 1H-[13C] NMR measurements of [4-13C]glutamate turnover in human brain. *Proc Natl Acad Sci U S A*. 1992;**89**(20):9603-6.

73. Pettegrew JW, Keshavan MS, Panchalingam K, Strychor S, Kaplan DB, Tretta MG, Allen M. Alterations in brain high-energy phosphate and membrane phospholipid metabolism in first-episode, drug-naive schizophrenics. A pilot study of the dorsal prefrontal cortex by in vivo phosphorus 31 nuclear magnetic resonance spectroscopy. *Arch Gen Psychiatry*. 1991;**48**(6):563-8.

74. Fukuzako H, Fukuzako T, Hashiguchi T, Kodama S, Takigawa M, Fujimoto T. Changes in levels of phosphorus metabolites in temporal lobes of drug-naive schizophrenic patients. *Am J Psychiatry*. 1999;**156**(8):1205-8.

75. Volz HR, Riehemann S, Maurer I, Smesny S, Sommer M, Rzanny R, Holstein W, Czekalla J, Sauer H. Reduced phosphodiesters and high-energy phosphates in the frontal lobe of schizophrenic patients: a (31)P chemical shift spectroscopic-imaging study. *Biol Psychiatry*. 2000;**47**(11):954-61.

76. Shioiri T, Kato T, Inubushi T, Murashita J, Takahashi S. Correlations of phosphomonoesters measured by phosphorus-31 magnetic resonance spectroscopy in the frontal lobes and negative symptoms in schizophrenia. *Psychiatry Res*. 1994;**55**(4):223-35.

77. Yacubian J, de Castro CC, Ometto M, Barbosa E, de Camargo CP, Tavares H, Cerri GG, Gattaz WF. 31P-spectroscopy of frontal lobe in schizophrenia: alterations in phospholipid and high-energy phosphate metabolism. *Schizophr Res*. 2002;**58**(2-3):117-22.

78. Miller J, Williamson P, Jensen JE, Manchanda R, Menon R, Neufeld R, Rajakumar N, Pavlosky W, Densmore M, Schaefer B, Drost DJ. Longitudinal 4.0 Tesla (31)P magnetic resonance spectroscopy changes in the anterior cingulate and left thalamus in first episode schizophrenia. *Psychiatry Res*. 2009;**173**(2):155-7.

Chapter 2

2 Gray matter and social functioning correlates of glutamatergic metabolite loss in schizophrenia[1]

2.1 Introduction

The majority of structural neuroimaging studies in schizophrenia have found progressive changes such as gray matter loss in subcortical regions.[1] There has been considerable controversy about what causes the progressive changes. Possible explanations include the effects of medication,[2] reduced neuropil[3] and excitotoxicity induced by N-methyl-D-aspartate glutamate receptor dysfunction.[4] One of the proposed methods to investigate the relative contribution of these factors is to combine volumetric analyses with functional and neurochemical studies.[1] Proton magnetic resonance spectroscopy (1H MRS) at high field strengths allows examination of some aspects of excitotoxic processes by the quantification of both glutamate and its precursor glutamine in a small volume of interest. Very few studies have correlated longitudinal volumetric and neurochemical measurements in schizophrenia.

We previously reported elevated glutamine levels in the left anterior cingulate and left thalamus in never-treated first episode schizophrenia[5] and decreased levels of glutamate and glutamine in the left anterior cingulate of chronically-ill patients,[6,7] which supports the possibility of an excitotoxic process. However, these illness phase-related changes may be confounded by age and medication effects. More recently, our group examined longitudinal changes in glutamatergic metabolites and gray matter in first episode schizophrenia over 30 months.[8] Within the patient group, decreased thalamic glutamine was found at 30 months compared to the baseline. Furthermore, a striking loss of gray matter in widespread cortical regions such as dorsolateral prefrontal cortex and temporal regions was found over 30 months in these patients. Gray matter loss in the superior

---

[1] A version of this chapter has been accepted for publication in British Journal of Psychiatry (January, 2011)

temporal gyrus was significantly correlated with the loss of thalamic glutamine. The correlation between gray matter and glutamine loss could indicate a degenerative process but the study was limited by a relatively short follow-up period. If there is a degenerative process in schizophrenia, it likely persists for several years.

The purpose of this study was to extend our glutamatergic and volumetric assessments to seven years in first episode patients studied before treatment and after stabilization with antipsychotics. We hypothesized that if there is a degenerative process in schizophrenia patients, we would see a loss in not only glutamine but also glutamate and N-acetylaspartate (NAA), a marker of neuronal integrity[9] in the anterior cingulate and the thalamus. The glutamate-glutamine cycle accounts for 80-100% of total glutamate trafficking in the brain.[10] Thus glutamine may be an indicator of glutamatergic signalling[11] while loss of glutamate, glutamine, and NAA may suggest loss of synaptic neuropil. We further hypothesized that the changes in these metabolites would correlate with loss of gray matter, particularly in regions which might be expected to be involved in schizophrenia such as the frontal and the temporal regions. If these changes in glutamatergic metabolites reflect meaningful functional brain changes, we hypothesized that we would see a correlation between changes in these metabolites and measurements of social functioning despite treatment with medication.

2.2 Method

2.2.1 Participants

Seventeen patients diagnosed with schizophrenia participated in this study. The diagnosis was established with the Structured Clinical Interview for DSM-IV[12] by a psychiatrist (P.W.). Ten of the patients were classified as paranoid type and seven patients were classified as undifferentiated subtype. Patients were scanned three times: at their first assessment in a never-treated state (NT), at 10 months, and at 80 months after their initial examination. The MRS data at NT and 10 months from fourteen schizophrenia patients have been reported in our previous study.[8] Demographic information on participants is shown in Table 2-1. Education levels, handedness and length of illness were rated as in

our previous study.[8] Symptoms were evaluated with the Scale for the Assessment of the Negative Symptoms (SANS)[13] and the Scale for the Assessment of the Positive Symptoms (SAPS).[14] Social functioning was evaluated with the Life Skills Profile rating scale (LSPRS),[15] composed of 39 items with a four-point response scale. This questionnaire was completed by a family member living with each patient or a caseworker through a phone interview within a few weeks after their latest assessment.

Seventeen matched healthy volunteers were recruited for the original study with an advertisement distributed in London, Ontario. The controls were of comparable age, gender, handedness, education level and parental education level. Healthy volunteers were scanned twice (Con1, Con2); the mean interval between the two assessments was approximately 43 months. Unfortunately, scanner replacement precluded longer follow-up in the control group. Subjects having a history of alcohol abuse and/or drug abuse in the two years before the scan or head injuries were excluded. Nine healthy volunteers participated in our previous study.[8] The demographic data is displayed in Table 2-1. All participants provided written informed consent according to the guidelines of the Review Board for the Health Sciences Research Involving Human Subjects at the University of Western Ontario.

Table 2-1: Participants' demographic information and data availability

	Groups[a]				
	NT (n = 17)	10 months (n = 17)	80 months (n = 17)	Con1 (n = 17)	Con2 (n = 17)
Age, mean (s.d.), years	25(7)	25(8)	32(9)	29(10)	32(10)
Gender[b]	14M/3F	14M/3F	14M/3F	13M/4F	13M/4F
Handedness[c]	12R/3L/2A	12R/3L/2A	12R/3L/2A	13R/4L	13R/4L
Educational level[d], mean (s.d.)					
Participants	2(1)	2(1)	2(1)	3(1)	3(1)
Parents	3(1)	3(1)	3(1)	3(1)	3(1)
Subtype[e]	10P/7U	10P/7U	10P/7U		
LOI, mean (s.d.), months	22(24)	33(27)	106(43)		
Symptom scale, mean (s.d.)					
SANS	44(12)	33(11)	33(12)		
SAPS	35(13)	8(8)	7(9)		
LSPRS, mean (s.d.)			128(18)		
Scan period, mean (s.d.), months		9(4)	84(31)		43(14)
Data availability[f]					
Anterior Cingulate, MRS	15X/2E	14X/1E/2M	16X/1E	17X	17X
Thalamus, MRS	16X/1E	12X/3E/2M	17X	17X	16X/1E
VBM	17X	15X/2M	17X	17X	17X

LOI, length of illness; LSPRS, Life Skills Profile rating scale; MRS, magnetic resonance spectroscopy; SANS, Scale for the assessment of negative symptoms; SAPS, Scale for the Assessment of Positive Symptoms; VBM, voxel-based morphometry.
a. Groups: schizophrenia patients: NT, never-treated; 10 months, on medication for approximately 10 months after their first scan; 80 months, approximately 80 months medication after their initial assessment; controls: Con1, healthy volunteers comparable age, gender and parental educational level with NT patients; Con2, follow-up scan for the healthy volunteers in Con1 group.
b. M, male; F, female.
c. R, right-handed; L, left-handed; A, ambidextrous.
d. 1, grade 10 or below; 2, grade 11-13; 3, college 1-3 years; 4, college 4 years or more.
e. Subtype: P, paranoid; U, undifferentiated.
f. Data availability: X, available; E, excluded; M, missing.

Medication information is shown in Table 2-2. Five of the schizophrenia patients had received antidepressant and/or benzodiazepines 1-10 days prior to their initial assessment but had not taken any antipsychotic medication. Twelve of the patients had not received any medication prior to their initial scan. All except one patient had been treated with atypical antipsychotics at 10 months assessment. At the 80 months scan time, four of the

patients were not taking any medication. Two patients had been treated with typical antipsychotics while the remainder had been treated with atypical antipsychotics. For the patients on antipsychotic treatment, chlorpromazine equivalent doses were calculated in our previous study.[8] In addition to the medication listed in Table 2-2, three patients had been prescribed the following treatment: metformin in one tablet for diabetes, salbutamol for asthma or tylenol for pain relief. None of the healthy volunteers, except one participant who had taken a multivitamin daily, took any medication or supplements 24 hours prior to the date of scan.

Table 2-2: Medication: daily dosage

	NT (n=17)		10 months (n=17)		80 months (n=17)	
	n	Mean dosage, mg (s.d.)	n	Mean dosage, mg (s.d.)	n	Mean dosage, mg (s.d.)
No medication	12		1		4	
Antipsychotics						
Haloperidol			1	1	2	1.3 (0.4)
Zuclopenthixol					1	6.4
Risperidone			5	3.7 (2.1)	3	3.3 (2.1)
Olanzapine			3	7.5 (2.5)	3	26.7 (5.8)
Quetiapine			3	300 (100)	3	317 (275)
Ziprasidone			2	100 (84.9)		
Clozapine					2	300 (141)
Antidepressants						
Paroxetine	1	30[b]				
Citalopram	2	20 (0)[b]				
Sertraline			1	50		
Bupropion					1	100
Benzodiazepines						
Clonazepam	1	4[b]	3	0.8 (0.3)	1	0.5
Lorazepam	3	2 (1.7)[b]			1	0.5
Zopiclone	1	7.5[b]				
Benztropine			1	3	2	1.5 (0.7)
CPZ eq[a], mg/day				196 (146)		282 (285)

NT, never-treated schizophrenia patients.
a. Chlorpromazine equivalent dose.
b. Taken 1-10 days prior to the scan.

2.2.2   Imaging and spectroscopy

Data were acquired with a 4.0 Tesla whole body MR scanner located at the Centre for Functional and Metabolic Mapping of the Robarts Research Institute, London, Ontario, Canada. A circularly polarized transmit/receive head coil was used. The MR system was monitored by an MR technician, who performed weekly quality control with using the phantom and with the echo planner imaging sequence. All data acquisition and quantification procedures were performed as described in our previous study[8]: Imaging, voxel positioning (left anterior cingulate and left thalamus (see Figure 2-1)), voxel size ($1.5\,cm^3$), shimming, spectroscopy (STEAM sequence, echo time$=20\,ms$, mixing time$=30\,ms$, repetition time$=2000\,ms$, dwell time$=500\,\mu s$), pre-processing, exclusion criteria of MR spectrum, spectral fitting and metabolite quantification. Only metabolites with a group coefficient of variation ((group standard deviation / group mean) $\times$ 100%) less than 75% are reported: NAA, glutamate (Glu), glutamine (Gln), choline (Cho), total creatine (tCr), myo-inositol (Myo) in the anterior cingulate and the thalamus; taurine (Tau) and scyllo-inositol (Syl) in the thalamus only. The "total glutamatergic metabolites" (tGL) refers to a sum of Glu and Gln levels quantified individually. A complete description of MRI/MRS methods can be found in Appendix B.
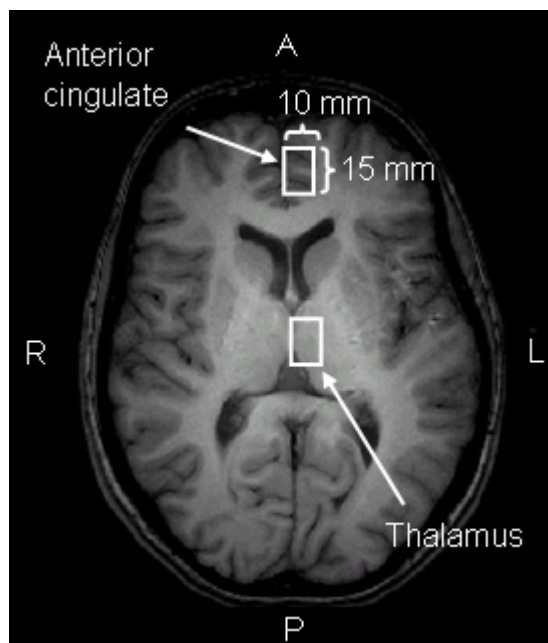
Figure 2-1: Voxel localization.

The white rectangles represent spectroscopy voxels in the left anterior cingulate and the left thalamus. Localization was performed with transverse T1-weighted images, in which the landmark of each region is seen. A, anterior; L, left; P, posterior; R, right.

2.2.3   Statistical Analysis

All statistical analysis was performed with SPSS version 17.0 for Windows. Analysis of variance (ANOVA) with a 2×2 split-plot factorial (SPF) design was conducted to investigate the data composed of two repeated measurements in two independent groups (NT and 80 months *v.* Con1 and Con2). The threshold was set at a two-tailed alpha of 0.05 for Glu, Gln, tGL and NAA, conservatively inasmuch as the *a priori* hypotheses of their decrease over 80 months were unidirectional. A similar approach was used with a separate analysis entailing the three repeated measures for the patient group; however, the SPF design was replaced with a 3-level repeated measures (within-subject only, randomized blocks) analysis (i.e. NT *v.* 10 months *v.* 80 months). An alpha of 0.05 was retained when comparing NT *v.* 80 months, as used in our previous findings while alpha

of $0.05/2 = 0.025$ (two-tailed throughout) was applied for the two remaining pair-wise comparisons (NT *v.* 10 months, 10 months *v.* 80 months). Huynh-Feldt epsilon was used to adjust error-term degrees of freedom for repeated measures sphericity violations.

Regarding the other metabolites for which we did not have *a priori* hypotheses, a region-wise multivariate analysis of variance (MANOVA) using a 2×2 SPF design was applied with an alpha of 0.05; a univariate ANOVA on each metabolite followed a significant result of the multivariate level of analysis. Commensurate with our previous procedures,[8] within-subject analyses for the patient group comprised pair-wise MANOVA's, alpha being set at $0.05/3 = 0.0167$ (to accommodate non-orthogonality of these comparisons) at both the multivariate and univariate levels, the latter analyses being contingent on multivariate-level significance.

Correlation analyses were performed between metabolite levels of the schizophrenia group and their demographic information, clinical scales (SANS/SAPS), social functioning scale (LSPRS, 80 months only), length of illness and chlorpromazine equivalent dose with the Pearson product-moment correlation coefficient. Threshold alpha was set at 0.001 with the exception of the hypothesized relationship between metabolites and LSPRS.

2.2.4   Voxel-based morphometry

Gray matter volume changes were measured with voxel-based morphometry (VBM)[16,17] on the 3D T1-weighted anatomical images using SPM2 (Wellcome Department of Imaging Neuroscience, University College London, UK) after normalization as described in the section 1.2.2.3.4 in this thesis or elsewhere.[8] The general linear model with *t*-statistics was applied for statistical comparisons; unpaired *t*-tests were used for between-subject comparisons (Con1 *v.* NT, Con2 *v.* 80 months), and paired *t*-tests were used for repeated measures, within-subject comparisons (NT *v.* 10 months *v.* 80 months, three-level; Con1 *v.* Con2). The threshold for each test within each set of tests was established according to a multiple-comparison False Discovery Rate (FDR) corrected alpha of 0.001

with the extent threshold (cluster size $k=5$). Correlation analysis between gray matter changes and two of the metabolites, glutamine and NAA, was performed with a test-wise alpha of 0.001.[8]

2.3 Results

No significant change in the signal-to-noise ratio was detected in the weekly quality control throughout the entire study. A total of 168 MRS data (2 regions × (17 patients × 3 time points + 17 controls × 2 time points) - 2 missing data at 10 months assessment) were collected for this study. Nine of these spectra were excluded due to voluntary or involuntary movement such as excessive movement or breathing-related movement during the data acquisition. Glutamate and glutamine levels in the anterior cingulate from one schizophrenia patient were excluded because the raw data for this participant at 80 months did not fit a glutamate and glutamine peak in this instance. Because of the non-physical values for glutamate and glutamine for this case, they were excluded. However, for this individual the other metabolites were well resolved, therefore it was decided to include them in the statistical analysis. MRS results are shown in the Figure 2-2 with the error bar representing the standard deviation of each group. As indicated in Figures 2-2, we were not able to follow-up all subjects for technical and/or clinical reasons. Voxel-based morphometry data were analyzed from 83 anatomical volumes (17 patients × 3 time points - 2 missing time points + 17 controls × 2 time points) as shown in Table 2-1.

Left anterior cingulate
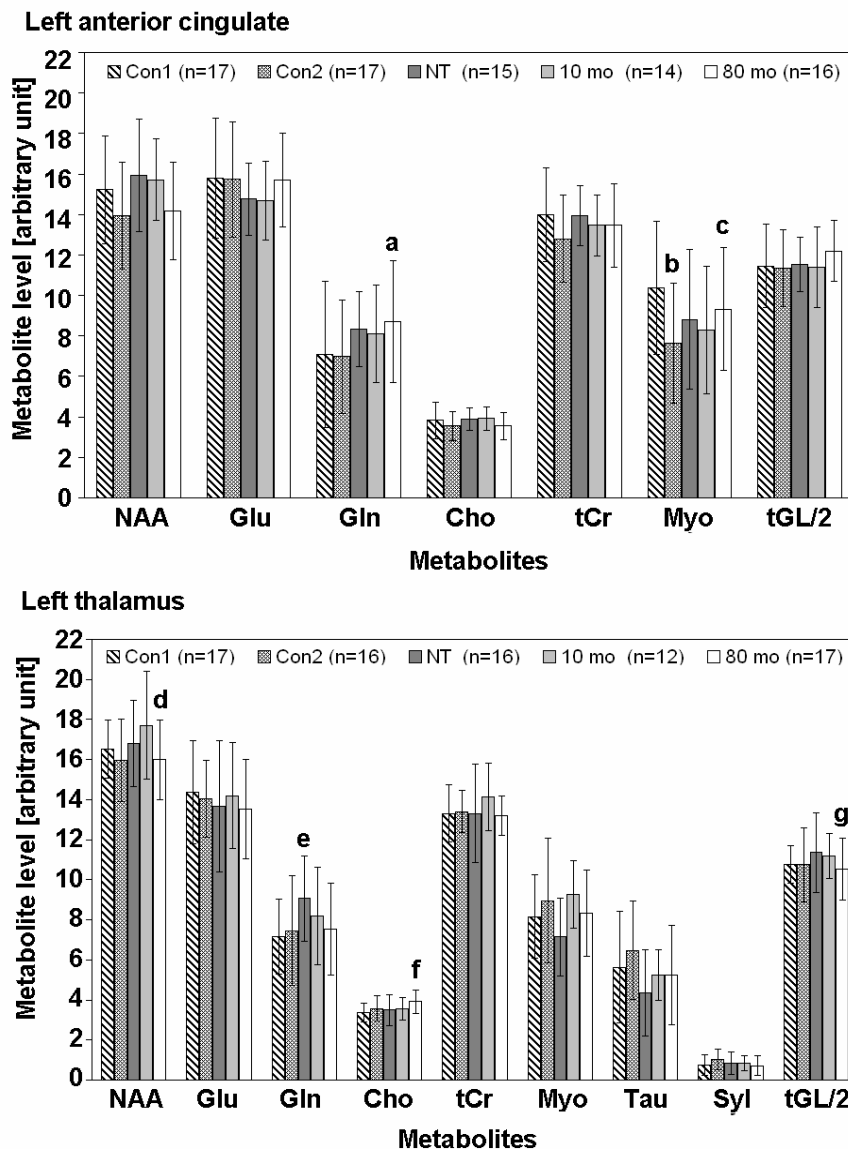
Left thalamus

Figure 2-2: Metabolite levels.

Metabolite levels measured in the left anterior cingulate and the left thalamus from healthy volunteers (Con1, Con2) and schizophrenia patients (NT, 10 mo and 80 mo). a, NT & 80 mo higher than Con1 & Con2, 2×2 SPF analysis in group effect; b, Significant reduction from Con1 to Con2 in two-tailed paired t-test; c, 2×2 SPF analysis in group×time interaction; d, Significant reduction from 10 mo to 80 mo in two-tailed paired t-test; e, Significantly higher level in NT than in Con1 in two-tailed unpaired t-test; f, Con2 & 80 mo higher than Con1 & NT, 2×2 SPF analysis in time effect; g, Significant reduction from 10 mo to 80 mo in two-tailed paired t-test. Cho, choline; Con1, healthy volunteers at the initial assessment; Con2, follow-up examination for the healthy volunteers; Gln, glutamine; Glu, glutamate; NAA, N-acetylaspartate; NT, never-treated; Myo, myo-inositol; Syl, scyllo-inositol; Tau, taurine; tCr, total creatine; tGL, sum of glutamate and glutamine; 10 mo, 10 months assessment; 80 mo, 80 months assessment.

2.3.1   Between-subject comparison

A 2×2 univariate SPF ANOVA on anterior cingulate glutamine yielded a significant group effect only ($F=5.04$, d.f.$=1,28$, $P=0.033$). Note that this analysis was applied to 30 data sets (13 patients and 17 controls) for which glutamate and glutamine were available at both time points. Analyses of NAA, glutamate and tGL levels yielded no statistically significant results. Multivariate and univariate tests did not evince significant effects for any other metabolite. In the thalamus, the univariate 2×2 SPF analysis did not reveal any group effect for NAA, glutamate, glutamine and tGL. For comparisons at the individual time points, the glutamine level of the NT group was significantly higher than that of Con1 group ($t=2.72$, d.f.$=1,31$, $P=0.011$) as presented in Figure 2-2. Neither multivariate nor univariate tests revealed significant group effects in the other metabolites.

No significant gray matter difference between groups was observed at each time point at the FDR alpha of 0.001. Gray matter differences were only seen at an uncorrected alpha of 0.001; Con1 gray matter volume was greater than in the NT group in the left thalamus (x y z, -20 -24 10, pulvinar, $t=3.71$, d.f.$=1,32$), Con2 gray matter volume was greater than the 80 month group in the left sub-lobar (x y z, -16 28 0, caudate body, $t=4.02$, d.f.$=1,32$) and left superior temporal gyrus (x y z, -66 -8 2, BA 22, $t=3.87$, d.f.$=1,32$).

2.3.2   Within-subject comparison (three-level)

Region-wise univariate three-level repeated measures analyses yielded no significant findings for NAA, glutamate, glutamine and tGL. Multivariate repeated measures in the other metabolites did not yield statistical significance in either the anterior cingulate ($P=0.083$) or the thalamus ($P=0.034>0.0167$).

Among the schizophrenia patients, gray matter in the left anterior cingulate (x y z, -1 53 2, BA 24 and 32, $t=6.08$, d.f.$=1,28$) and the left thalamus (x y z, -12 -2 -2, $t=4.52$, d.f.$=1,28$) significantly diminished from the never-treated to 80 months assessment. Figure 2-3 represents gray matter loss over 80 months. Significant decrease occurred with

respect to the cross-sectional images of the T1-weighted template, centred at the left thalamus. Significant loss was also observed in the frontal (BA 4, 10, 45 and 46), temporal (BA 21), parietal (BA 7), occipital (BA 18 and 30), limbic lobes (BA 24 and 30) and sub-lobar (putamen) regions. Significant gray matter loss from 10 months to 80 months assessment was seen in the frontal lobe (BA 4, 6 and 9). All coordinates are listed in Table 2-3. No gray matter loss was observed in 10 months as compared to NT.
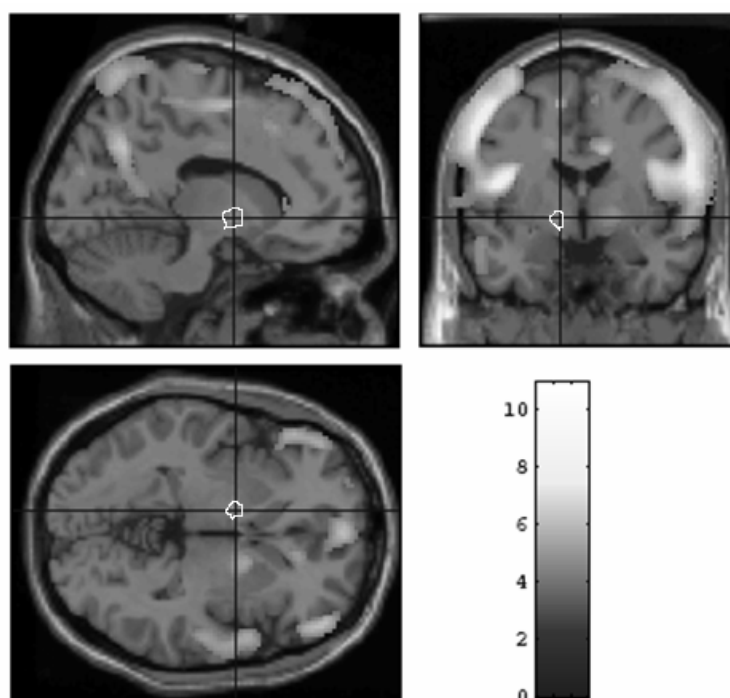
Figure 2-3: Gray matter loss in schizophrenia over 80 months.

Gray matter loss from never-treated state to 80 months assessment in schizophrenia patients with 3-level repeated measures (false discovery rate corrected $P<0.001$). Significant reductions represented as shaded region are super imposed on to the cross-sectional T1-weighted template images. The bar at the bottom right represents the *t*-value. The cursor in the images was placed in the left thalamus (x y z, -12 -2 -2, MNI coordinate). This area showing the significant gray matter loss was indicated in the white line.

Table 2-3: Voxel-based morphometry: significant gray matter loss with the 3-level repeated measures in schizophrenia patients

x	y	z	R / L	Lobe	Gyrus	BA/sub-structure	Cluster k^a	Voxel t
			NT	**> 80 mo**	**(k=5, corrected p**	**<0.001, d.f.**	**=1,28)**	
58	26	24	R	Frontal	Inferior frontal	45	61942	10.86
54	30	32	R	Frontal	Middle frontal	46	61942	10.78
-26	62	4	L	Frontal	Superior frontal	10	61	4.69
-50	-14	60	L	Frontal	Precentral	4	61942	10.86
-56	-4	-24	L	Temporal	Middle temporal	21	146	4.79
-12	-62	36	L	Parietal	Precuneus	7	991	6.11
18	-62	30	R	Occipital	Precuneus	30	873	5.65
-12	-86	22	L	Occipital	Cuneus	18	32	4.74
14	-2	34	R	Limbic	Cingulate	24	1281	6.14
16	10	32	R	Limbic	Cingulate	24	1281	5.40
-18	-60	16	L	Limbic	Posterior cingulate	30	991	5.43
22	-56	14	R	Limbic	Posterior cingulate	30	873	5.35
-1	53	2	L	Limbic	Anterior cingulate	24, 32	61492	6.08
12	54	10	R	Limbic	Anterior cingulate	24, 32	64492	6.89
18	6	2	R	Sub-lobar	Lentiform	Putamen	275	5.42
-12	-2	-2	L	Sub-lobar	Thalamus	Ventral anterior	49	4.52
		10	**mo**	**> 80 mo**	**(k=5, corrected p**	**<0.001, d.f.**	**=1,28)**	
28	50	40	R	Frontal	Superior frontal	9	17	6.27
-46	6	58	L	Frontal	Middle frontal	6	5	6.10
50	-14	62	R	Frontal	Precentral	4	14	5.94

(k=5, FDR corrected *P*<0.001, d.f.=1,28)
NT, Never-treated; 10 mo, 10 months assessment; 80 mo, 80 months assessment; BA, Brodmann area; FDR, False discovery rate; L, left; R, right.
a. Cluster size (voxels).

2.3.3   Within-subject comparison (two-level)

Within the univariate 2×2 SPF layout, no significant time effect or group $\times$ time interaction was found in NAA, glutamate, glutamine and tGL in the anterior cingulate. In a paired comparison, a trend toward decreased in NAA level from 10 months to 80

months was found ($t=2.44$, d.f.$=1,12$, $P=0.031>0.025$). The MANOVA on the remaining metabolites yielded no statistically significant results. A significant univariate group$\times$time interaction was found for myo-inositol ($F=5.01$, d.f.$=1,29$, $P=0.033$), resulting from a significant decrease over time in controls ($t=2.51$, d.f.$=1,16$, $P=0.023$). In the absence of statistical significance at the multivariate level of analysis, like the non-significant univariate-analysis trend, above, this local result should be considered with caution. It nevertheless is reported for possible future consideration.

Thalamic NAA, glutamate, glutamine and tGL did not show significant effects with respect to either time or group $\times$time sources in the univariate 2×2 SPF analysis. There was a trend toward a decreased glutamine level at 80 months compared to the NT measure ($t=1.82$, d.f.$=1,15$, $P=0.089$) while tGL significantly decreased from NT to 80 months ($t=2.20$, d.f.$=1,15$, $P=0.044$). An example of glutamate and glutamine components as well as the fit spectra is presented in Appendix C. Thalamic NAA of the schizophrenia group at 80 months significantly decreased from measured levels at 10 months ($t=2.97$, d.f.$=1,11$, $P=0.013$). The 2×2 SPF MANOVA revealed a significant time effect in the remaining metabolites ($F=2.84$, d.f.$=5,26$, $P=0.035$). The significant multivariate effect was paralleled by a significant univariate time effect for choline ($F=4.19$, d.f.$=1,30$, $P=0.049$). There was a trend to increasing choline level at 80 months compared to NT ($t=1.87$, d.f.$=1,15$, $P=0.080$) but no significant change was observed between Con1 and Con2. No significant gray matter loss was found in controls between their two scans (Con1 v. Con2).

2.3.4   Correlations

Correlation between gray matter reduction and loss of thalamic glutamine over 80 months was found in the ventral regions such as the right temporal pole (x y z, 16 14 -34, BA 38, $r=0.884$, $P<0.001$), presented in Figure 2-4. The detailed area is listed in Table 2-4. NAA reduction over 80 months in the left anterior cingulate correlated with the gray matter loss in the posterior regions, listed in Table 2-5.[18] Figure 2-5 represents the correlation between NAA loss and gray matter reduction in the right inferior parietal

lobule (x y z, 62 40 28, BA 40, $r=0.841$, $P<0.001$). The correlation between the losses of gray matter and either glutamine in the anterior cingulate, NAA in the thalamus, or tGL in both regions did not reach the $P<0.001$ level. Among the changes in metabolites, the losses in NAA and tGL levels from 10 months to 80 months tended to be positively correlated in the anterior cingulate ($r=0.625$, $P=0.025$, N=13).
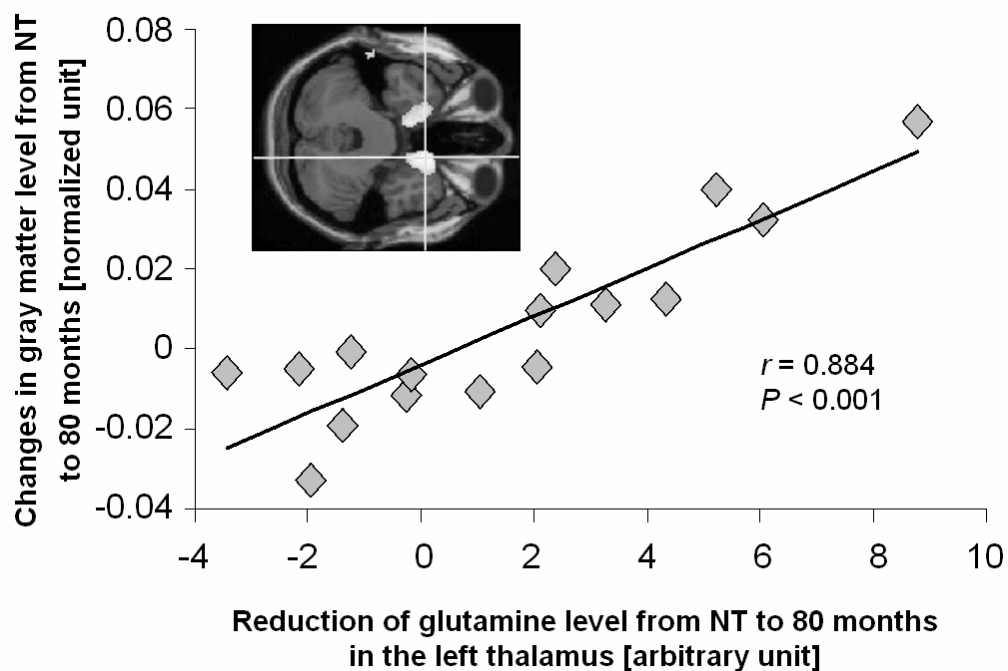
Figure 2-4: Correlation between gray matter loss and glutamine reduction.

Gray matter loss in the right temporal pole (x y z, 16 14 -34, BA 38) was significantly correlated with the reduction of thalamic glutamine from never-treated to 80 months assessment in schizophrenia.

Table 2-4: Voxel-based morphometry: positive correlation between gray matter loss and glutamine loss in the left thalamus from NT to 80 months

x	y	z	R / L	Lobe	Gyrus	BA/sub-structure	Voxel k[a]	Voxel t
-10	66	-12	L	Frontal	Superior frontal	11	493	5.96
6	68	-14	R	Frontal	Superior frontal	11	493	5.11
42	34	-4	R	Frontal	Middle frontal	47	199	5.35
-44	34	-4	L	Frontal	Middle frontal	47	11	4.26
30	32	-2	R	Frontal	Inferior frontal	47	199	5.06
-14	16	-14	L	Frontal	Subcallosal	47	51	4.62
16	14	-34	R	Temporal	Superior temporal	38	529	7.09
-70	-34	-18	L	Temporal	Middle temporal	21	676	4.97
40	-34	0	R	Temporal	Sub gyral	-	5	4.01
-30	-64	34	R	Parietal	Angular	39	13	4.08
-12	6	-34	L	Limbic	Uncus	28	370	5.07

(k=5, uncorrected $P<0.001$, d.f.=1,14)

NT, Never-treated patients; BA, Brodmann area; L, left; R, right.

a. Cluster size (number of voxels).
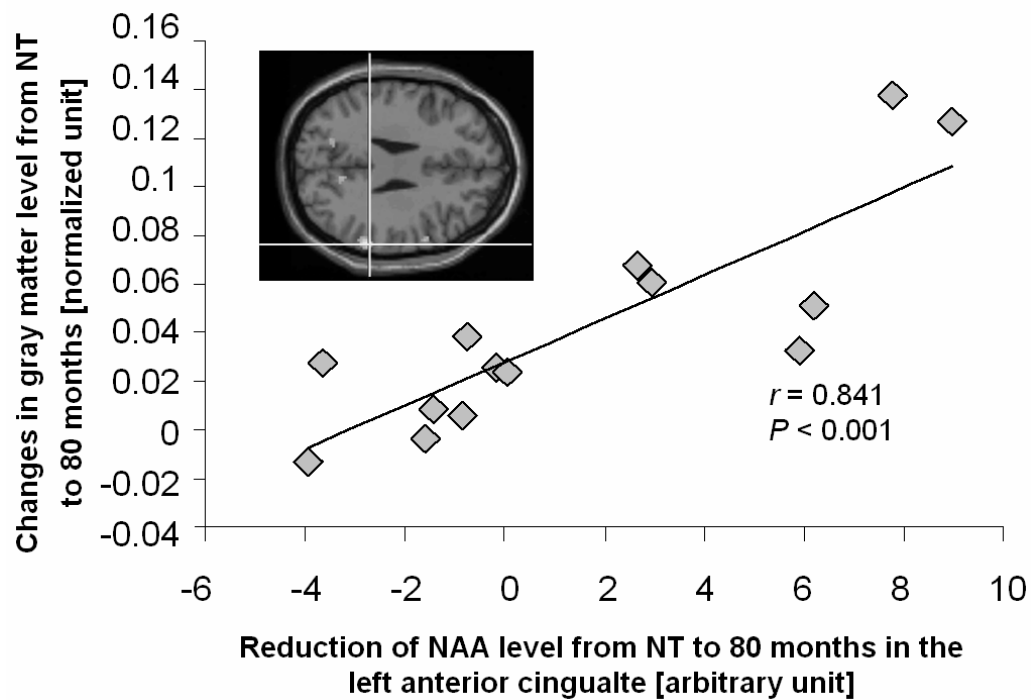
Figure 2-5: Correlation between gray matter loss and NAA.

Gray matter loss in the right inferior parietal lobule (x y z, 62 40 28, BA 40) was significantly correlated with the reduction of NAA in the left anterior cingulate from never-treated to 80 months assessment in schizophrenia.

Table 2-5: Voxel-based morphometry: positive correlation between gray matter loss and NAA loss in the left anterior cingulate from NT to 80 months

x	y	z	R / L	Lobe	Gyrus	BA/sub-structure	Voxel k[a]	Voxel t
-32	22	58	L	Frontal	Superior frontal	8	7	4.52
56	8	34	R	Frontal	Inferior frontal	9	287	7.15
56	42	4	R	Frontal	Inferior frontal	46	148	6.14
62	52	2	R	Frontal	Inferior frontal	46	148	4.56
36	16	60	R	Frontal	Middle frontal	6	27	4.55
56	-8	46	R	Frontal	Precentral	4	287	5.58
-44	-64	54	L	Parietal	Superior parietal	7	1720	8.48
-30	-56	68	L	Parietal	Superior parietal	7	1720	7.87
16	-74	62	R	Parietal	Superior parietal	7	752	5.65
54	-40	52	R	Parietal	Inferior parietal	40	142	6.86
62	-40	28	R	Parietal	Inferior parietal	40	122	5.39
54	-48	50	R	Parietal	Inferior parietal	40	142	4.95
66	-36	38	R	Parietal	Inferior parietal	40	122	4.33
46	-68	46	R	Parietal	Inferior parietal	40	5	4.13
-50	-74	-34	L	Parietal	Angular	39	1720	7.24
16	-58	74	R	Parietal	Postcentral	7	752	7.47
56	-16	48	R	Parietal	Postcentral	3	287	5.09
-10	-68	40	L	Parietal	Precuneus	7	30	5.05
-18	-66	26	L	Parietal	Precuneus	7	30	4.57
-10	-74	48	L	Parietal	Precuneus	7	30	4.31
-12	-62	22	L	Parietal	Precuneus	31	30	3.96
22	-62	22	R	Occipital	Precuneus	31	285	6.55
12	-62	26	R	Occipital	Precuneus	31	285	4395
-18	84	-2	L	Occipital	Lingual	17	230	6.04
28	-66	0	R	Occipital	Lingual	19	285	5.47
20	-96	14	R	Occipital	Cuneus	18	14	4.76

(k=5, uncorrected $P<0.001$, d.f.=1,12)
NT, Never-treated patients; BA, Brodmann area; L, left; R, right.
a. Cluster size (number of voxels).

No correlation between loss of thalamic glutamine level and gray matter reduction was found between two measurements in controls. The only significant correlation between anterior cingulate NAA reduction with gray matter loss in controls was found in a small

cluster (voxel k=5) in the middle frontal gyrus (x y z, 28 -14 64, BA 6, *r*=0.736, *P*<0.001).

LSPRS evaluated at 80 months was negatively correlated with the loss of thalamic tGL from NT to 80 months (*r*=0.694, *P*=0.003) (Figure 2-6). Significant correlation between chlorpromazine equivalent dose at 80 months assessment and gray matter loss from never-treated to 80 months was found in bilateral sub-gyral (x y z, -50 -44 -12, BA 37, *r*=0.710; x y z, 48 -42 -8, BA 37, *r*=0.704) in the temporal lobe at *P*<0.001 level. No other correlations were found in the other metabolite levels with SANS/SAPS scores, length of illness, the LSPRS and chlorpromazine equivalent dosage.
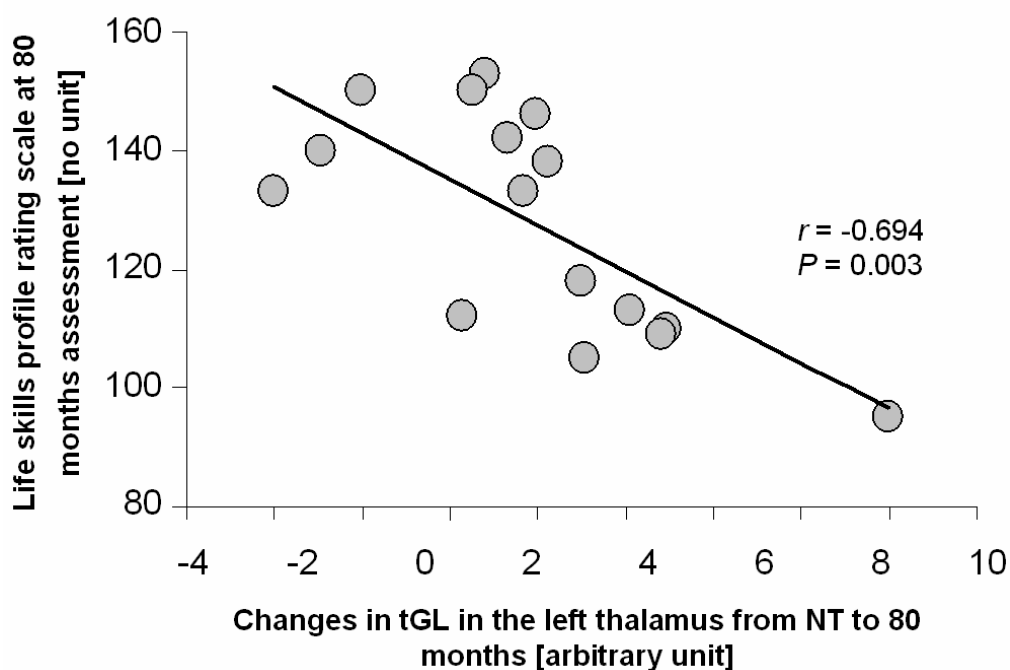
Figure 2-6: Negative correlation between LSP and tGL loss

Life skills profile rating scale at 80 months assessment was negatively correlated with the total glutamatergic metabolites (tGL) in the thalamus from never-treated to 80 months assessment in schizophrenia

2.4   Discussion

2.4.1   Neurochemical Alterations

Glutamine levels in never-treated patients were significantly higher than controls in the left thalamus in keeping with the previous reports[5,8] while levels in the anterior cingulate were not significantly different between groups possibly due to higher standard deviations in the control samples. No differences were seen between never-treated patients and patients stabilized on medications suggesting that neuroleptic medication did not affect glutamatergic metabolite levels.

Although we did not see a significant reduction in thalamic glutamine level over 80 months in schizophrenia, there was a significant decrease in the total glutamatergic metabolites (tGL), suggesting glutamatergic metabolism continues to decline with disease progression. This glutamatergic loss in the thalamus could also suggest a loss of neuropil in schizophrenia. This observation is consistent with the suggestion that excitotoxicity occurs primarily in the early stages of illness.[19] However it is also possible that glutamatergic findings could be accounted for by alterations in the activity and density of glutamate dehydrogenase and glutamine synthetase which have been reported to be anomalous in post-mortem schizophrenic brain extracts.[20] The thalamic tGL reduction was inversely correlated with the LSPRS, suggesting a connection between glutamatergic neurophysiological changes and the impairment of social behavior. It is of note that this correlation was found despite treatment with antipsychotic medications. Therefore, this finding indicates that the change in glutamatergic metabolites may be a potential indicator of severity in schizophrenia in terms of social functioning.

Indeed, Tibbo et al.[21] reported a correlation between Glu/Gln ratio in the frontal cortex in adolescents at high-risk for schizophrenia and Global Assessment of Functioning Scale, suggesting the glutamatergic changes are a candidate marker in the early stage of schizophrenia. Wood et al.[22] reported a strong correlation between NAA/Cr ratio in the middle frontal gyrus in the patients with psychosis and the Social Functional Assessment Scale at 18 months follow-up. Although there are several differences such as the

metabolite and its region compared to this study, they also suggest a connection between metabolites and functional outcome.

In addition to the glutamatergic findings, a trend in the reduction in the levels of NAA was found in the left anterior cingulate ($P=0.031>0.025$) and a reduction was found the left thalamus ($P=0.013$) between the 10 months stabilized on medication and the 80 months assessment. These NAA deficits were not found to differ in a 30 month study.[8] As NAA levels are generally thought to reflect neuronal integrity, this decline would be consistent with decreasing glutamatergic metabolite levels and possibly a loss of neuropil or limited apoptosis. Indeed, NAA and tGL reductions from 10 months to 80 months assessment tended to be positively correlated in the anterior cingulate suggesting that both metabolites may be related to neuropil loss. However, medication effects are also a possibility as NAA levels in never-treated patients were not statistically different from the same patients at 80 months follow-up.

No differences in glutamate, glutamine, tGL and NAA were seen in controls between baseline and follow-up scans. Those findings were consistent with the measurement at 30 months.[8] However, controls in this study were not followed as long as patients due to decommissioning of the MRI system. This study had been running over 12 years on the same MRI scanner. Compared at the latest assessment, glutamate and glutamine levels in schizophrenia were not significantly different from those in controls. Decreased levels of both metabolites have been reported in the anterior cingulate in chronic patients who had been ill in excess of 20 years.[6] The lack of differences at 80 months between controls and patients implies that metabolite levels change more slowly over a considerable length of time.

2.4.2　Volumetric Alterations

There was no significant difference between never-treated schizophrenia patients and controls with FDR corrected $P<0.001$ level while some gray matter losses were observed with the uncorrected $P<0.001$ level in the thalamus, where significantly higher glutamine

level was found in schizophrenia. However, these differences were not to the extent expected if schizophrenic symptoms were due to a programmed loss of neuropil.[3]

Significant gray matter loss in schizophrenia patients over 80 months was observed in many brain regions including the anterior cingulate and the thalamus. This result suggests that it takes 7 years until gray matter losses are observable in many regions. Indeed, no reduction in the anterior cingulate and the thalamus was found during the 30 months assessment in our previous report.[8] A gray matter reduction was also found in the frontal lobe in the 80 months compared to never-treated assessment and to the 10 months assessment, highlighting the importance of the frontal lobe in schizophrenia. There was no significant gray matter loss from never-treated to 10 months assessment, suggesting that the acute effects of medication are minimal. Significant correlations between gray matter loss over 80 months and chlorpromazine equivalent dose were found only in the sub-gyral in temporal lobe bilaterally suggesting that medication is not likely the explanation for the widespread gray matter losses seen in these patients.

There was no significant gray matter loss in controls between the two assessments, implying aging effects are minimal. However, the mean scan period of controls was around 3.5 years, shorter than the patients' scan period. No significant gray matter difference (FDR corrected $P < 0.001$) was found in Con2 compared to 80 months. There were differences in the left superior temporal gyrus and caudate nucleus, albeit by more liberal criteria (uncorrected $P < 0.001$), but which nevertheless are consistent with both our earlier study[8] and with another study.[23]

2.4.3 Correlations between Gray Matter and Metabolite Losses at 80 months

The amount of thalamic glutamine in schizophrenia patients was significantly correlated with gray matter volume in the middle and inferior frontal gyrus as well as in the temporal pole. A similar correlation between thalamic glutamate and gray matter loss in these regions was reported in subjects at risk of developing schizophrenia.[24] Several prefrontal regions and temporal pole are associated with social and emotional processing

which may be deficient in schizophrenia patients.[25,26] As discussed in the previous section, social functioning on the LSPRS was negatively correlated with tGL loss in the thalamus in patients, suggesting this correlation is mediated in part by these widespread structural changes. No correlations were found between losses of thalamic glutamine and gray matter in controls, suggesting that aging did not play a significant role.

The reduction of NAA in the anterior cingulate was significantly correlated with the gray matter loss over 80 months in posterior-parietal areas. This area is associated with attention which many investigators have found to be altered in schizophrenia.[27] These regions are also interconnected and form part of the default network associated with self-monitoring. Aberrant connectivity between the anterior portions of this network and other regions in schizophrenia patients has been reported by our group and others.[28-30] Localized changes in these networks reflected by metabolic measures could lead to difficulties in self-monitoring which may underlie many symptoms of schizophrenia.[29] In contrast to multiple locations in schizophrenia, reduction in the anterior cingulate NAA levels in controls was only correlated with gray matter loss in the motor area. This cluster size was equal to the extent threshold, suggesting minimal correlation between neuronal integrity and neuropil in normal aging.

2.4.4   Excitotoxicity or Plasticity

Although metabolite reductions, gray matter loss and their correlations over 80 months may suggest a neurodegenerative process in schizophrenia, there has been a debate about whether these anomalies are caused by excitotoxicity or plasticity. In contrast to our previous report,[8] here, a loss of glutamatergic metabolites was observed in the thalamus concurrently to gray matter loss within the spectroscopic voxels (i.e. the anterior cingulate and the thalamus). If there is an excitotoxic process in schizophrenia, significant loss of gray matter in the thalamus might be expected in patients compared to controls at their initial assessment. However, there was no significant difference between these groups, suggesting the glutamatergic metabolite changes may be more sensitive to early changes not associated with gray matter loss.

Thalamic glutamatergic neurons are interconnected to all the cortical regions which were associated with gray matter loss in the schizophrenia patients. They also form part of the basal ganglia-thalamocortical neuronal circuit implicated in the pathophysiology of schizophrenia.[31] Thus glutamatergic changes in the thalamus could be associated with glutamatergic changes throughout the cortex. Cortical gray matter losses could be accounted for by excitotoxicity into these regions. Increased membrane breakdown has been reported in first episode schizophrenia patients in a phosphorus MRS study.[32] The decrease in NAA and decrease in gray matter over time in the anterior cingulate in this study would be compatible with this explanation. The trend to increased thalamic choline levels in patients at 80 months may also suggest excitotoxicity as these levels reflect mostly membrane metabolites. A positive correlation between choline and the duration of untreated psychosis has been found in first episode patients.[33] However, it is possible that these circuits are simply being down-regulated leading to plastic changes in gray matter and the metabolic changes.

2.4.5   Limitations

Although the absence of differences in metabolites and gray matter between the never-treated and 10 month assessments in patients argues against medication effects, the effects of exposure to medication can never completely be eliminated due to ethical considerations. Another limitation may be the stability of the MR scanner associated with the inevitable hardware replacements and/or upgrades that occur during such a long-term period but the stability of our MR system was carefully monitored through routine weekly quality control. We did not regularly calibrate the metabolite quantification. However, the metabolite levels were quantified with the internal water reference which minimizes short- and long-term scanner drift. Due to scanner replacement, we were unable to follow controls as long as patients. Consequently we cannot exclude the possibility that controls may have had further NAA losses had we followed them longer. The lack of obvious changes in tGL between the two assessments in controls suggest that aging alone would be unlikely to account for changes seen in patients at the 80 month assessment.

2.5   Acknowledgement

2.6   References

1. DeLisi LE. The concept of progressive brain change in schizophrenia: implications for understanding schizophrenia. *Schizophr Bull* 2008; **34**: 312-21.

2. McClure RK, Phillips I, Jazayerli R, Barnett A, Coppola R, Weinberger DR. Regional change in brain morphometry in schizophrenia associated with antipsychotic treatment. *Psychiatry Res* 2006; **148**: 121-32.

3. Selemon LD, Goldman-Rakic PS. The reduced neuropil hypothesis: a circuit based model of schizophrenia. *Biol Psychiatry* 1999; **45**: 17-25.

4. Olney JW, Farber NB. Glutamate receptor dysfunction and schizophrenia. *Arch Gen Psychiatry* 1995; **52**: 998-1007.

5. Théberge J, Bartha R, Drost DJ, Menon RS, Malla A, Takhar J et al. Glutamate and glutamine measured with 4.0 T proton MRS in never-treated patients with schizophrenia and healthy volunteers. *Am J Psychiatry* 2002; **159**: 1944-6.

6. Théberge J, Al-Semaan, Williamson PC, Menon RS, Neufeld RWJ, Schaefer B et al. Glutamate and glutamine in the anterior cingulate and thalamus of medicated patients with chronic schizophrenia and healthy comparison subjects measured with 4.0-T proton MRS. *Am J Psychiatry* 2003; **160**: 2231-3.

7. Tayoshi S, Sumitani S, Taniguchi K, Shibuya-Tayoshi S, Numata S, Iga J et al. Metabolite changes and gender differences in schizophrenia using 3-Tesla proton magnetic resonance spectroscopy (1H-MRS). *Schizophr Res* 2009; **108**: 69-77.

8. Théberge J, Williamson KE, Aoyama N, Drost DJ, Manchanda R, Malla AK et al. Longitudinal grey-matter and glutamatergic losses in first-episode schizophrenia. *Br J Psychiatry* 2007; **191**: 325-34.

9. Clark JB. N-acetyl aspartate: A marker for neuronal loss or mitochondrial dysfunction. *Dev Neurosci* 1998; **20**: 271-6.

10. Rothman DL, Behar KL, Hyder F, Shulman RG. In vivo NMR studies of the glutamate neurotransmitter flux and neuroenergetics: implications for brain function. *Annu Rev Physiol* 2003; **65**: 401-27.

11. Rowland LM, Bustillo JR, Mullins PG, Jung RE, Lenroot R, Landgraf E et al. Effects of ketamine on anterior cingulate glutamate metabolism in healthy humans: a 4-T proton MRS study. *Am J Psychiatry* 2005; **162**: 394-6.

12. First MB, Spitzer RL, Gibbon M, Williams JBW. *Structured Clinical Interview for DSM-IV Axis I Disorders (SCID).* New York: New York State Psychiatric Institute, Biometrics Research, 1997.

13. Andreasen NC. *Scale for the Assessment of Negative Symptoms (SANS).* Iowa City: University of Iowa, 1983.

14. Andreasen NC: *Scale for the Assessment of Positive Symptoms (SAPS).* Iowa City: University of Iowa, 1983.

15. Rosen A, Hadzi-Pavlovic D, Parker G. The life skills profile: a measure assessing function and disability in schizophrenia. *Schizophr Bull* 1989; **15**: 325-37.

16. Ashburner J, Friston KJ. Voxel-based morphometry--the methods. *Neuroimage* 2000; **11** (6 Pt 1): 805-21.

17. Ashburner J, Friston KJ. Why voxel-based morphometry should be used. *Neuroimage* 2001; **14**: 1238-43.

18. Gardner RC, Neufeld RWJ. Use of the simple change score in correlational analyses. *Educ Psychol Meas* 1987; **47**: 849-64.

19. Jarskog LF, Glantz LA, Gilmore JH, Lieberman JA. Apoptotic mechanisms in the pathophysiology of schizophrenia. *Prog Neuropsychopharmacol Biol Psychiatry* 2005; **29**: 846-58.

20. Burbaeva GS, Boksha IS, Turishcheva MS, Vorobyeva EA, Savushkina OK, Tereshkina EB. Glutamine synthetase and glutamate dehydrogenase in the prefrontal cortex of patients with schizophrenia. *Prog Neuropsychopharmacol Biol Psychiatry* 2003; **27**: 675-80.

21. Tibbo P, Hanstock C, Valiakalayil A, Allen P. 3-T proton MRS investigation of glutamate and glutamine in adolescents at high genetic risk for schizophrenia. *Am J Psychiatry* 2004; **161**: 1116-8.

22. Wood SJ, Berger GE, Lambert M, Conus P, Velakoulis D, Stuart GW et al. Prediction of functional outcome 18 months after a first psychotic episode: a proton magnetic resonance spectroscopy study. *Arch Gen Psychiatry* 2006; **63**: 969-76.

23. Takahashi T, Wood SJ, Yung AR, Soulsby B, McGorry PD, Suzuki M et al. Progressive gray matter reduction of the superior temporal gyrus during transition to psychosis. *Arch Gen Psychiatry* 2009; **66**: 366-76.

24. Stone JM, Day F, Tsagaraki H, Valli I, McLean MA, Lythgoe DJ,et al. Glutamate dysfunction in people with prodromal symptoms of psychosis: relationship to gray matter volume. *Biol Psychiatry* 2009; **66**: 533-9.

25. Bertrand MC, Sutton H, Achim AM, Malla AK, LePage M. Social cognitive impairments in first episode psychosis. *Schizophr Res* 2007; **95**: 124-33.

26. Olson IR, Plotzker A, Ezzyat Y. The enigmatic temporal pole: A review of findings on social and emotional processing. *Brain* 2007; **130** (Pt 7): 1718-31.

27. Cornblatt BA, Keilp JG. Impaired attention, genetics, and the pathophysiology of schizophrenia. *Schizophr Bull* 1994; **20**: 31-46.

28. Bluhm RL, Miller J, Lanius RA, Osuch EA, Boksman K, Neufeld RW et al. Spontaneous low-frequency fluctuations in the BOLD signal in schizophrenic patients: anomalies in the default network. *Schizophr Bull* 2007; **33**: 1004-12.

29. Williamson P. Are anticorrelated networks in the brain relevant to schizophrenia? *Schizophr Bull* 2007; **33**: 994-1003.

30. Neufeld RWJ, Boksman K, Vollick D, George L, Carter JR. Stochastic dynamics of stimulus encoding in schizophrenia: theory, testing and application. *J Math Psychol* 2010; **54**: 90-108.

31. Alexander GE, Crutcher MD, DeLong MR. Basal ganglia-thalamocortical circuits: parallel substrates for motor, oculomotor, "prefrontal" and "limbic" functions. *Prog Brain Res* 1990; **85**: 119-46.

32. Miller J, Williamson P, Jensen JE, Manchanda R, Menon R, Neufeld R, et al. Longitudinal 4.0 Tesla (31)P magnetic resonance spectroscopy changes in the anterior cingulate and left thalamus in first episode schizophrenia. *Psychiatr Res Neuroimaging* 2009; **173**: 155-7.

33. Théberge J, Al-Semaan Y, Drost DJ, Malla AK, Neufeld RW, Bartha R, et al. Duration of untreated psychosis vs. N-acetylaspartate and choline in first episode schizophrenia: a 1H magnetic resonance spectroscopy study at 4.0 Tesla. *Psychiatr Res Neuroimaging* 2004; **131**: 107-14.

Chapter 3

3 Gray matter vs. metabolite signal to noise ratio

3.1 Introduction

Advances in neurochemical and structural imaging have contributed much to the understanding of neuropsychiatric diseases such as Alzheimer's disease and schizophrenia.[1] Since these illnesses are progressive, they are possibly neurodegenerative disorders.[2,3] Decreases in N-acetylaspartate (NAA) level, an indicator of neuronal integrity and neuropil volume, have been reported in longitudinal studies of both conditions.[4,5] Glutamate is another possible marker of neurodegeneration because of excitotoxicity associated with the excessive release of this neurotransmitter in conditions like schizophrenia.[6] However, findings are inconsistent in terms of the pattern of brain changes. Therefore, it has been suggested that volumetric measurements should be combined with metabolite changes.[7]

Magnetic resonance imaging (MRI) and proton magnetic resonance spectroscopy (1H MRS) are used to measure volumetric and neurochemical abnormalities in the human brain, respectively. In the past three decades, anomalies in brain tissue and in metabolite levels in schizophrenia have been reported with these techniques. Our group found increased levels of glutamine in the anterior cingulate and the thalamus in schizophrenia patients before treatment compared to a control group using MRS.[8] Théberge et al.[8] also reported correlated losses of thalamic glutamine and gray matter in those patients over a 30 month period.[9] We recently found longitudinal decreases in the levels of NAA and total glutamatergic metabolites in the thalamus in the same schizophrenia patients after 80 months.[10]

It was unclear if our findings represented actual or apparent decreases in metabolite levels due to the gray matter loss in the spectroscopy voxel. These quantified metabolite levels were normalized with an arbitrary correction factor, composed of gray matter, white matter and cerebrospinal fluid (CSF) percentage in the spectroscopy voxel. However, we did not correlate the raw metabolite MR signal with the actual amount of

gray matter in the voxel to determine if they were related. If gray matter changes correlate highly with glutamatergic metabolite changes then glutamatergic changes may reflect a loss of neuropil rather than physiologically-relevant concentration changes in this neurotransmitter. We also did not examine the effects of losses in gray matter in the voxel on signal-to-noise ratio (SNR) which may have affected the precision of the metabolite determination.

Long term longitudinal studies of neuropsychiatric disorders are becoming increasingly common. However, to our knowledge no studies have examined the effects of gray matter loss on the precision of measurements of relevant brain metabolites over time. The purpose of this study was to examine the effects of gray matter loss on the measurement of NAA and glutamatergic metabolites over 80 months in a group of schizophrenic patients and controls. We hypothesize that gray matter losses alone would not account for longitudinal changes in glutamatergic metabolites but that losses of gray matter may affect SNR making it more difficult to detect changes over time.

3.2   Methods

3.2.1   MR imaging and spectroscopy

Data were collected from seventeen schizophrenic patients and seventeen comparable controls using *in vivo* proton magnetic resonance spectroscopy. Participant's demographic information, details of the medication, imaging sequence, spectroscopy sequence, spectrum fitting, preprocessing and quantification are described in our previous studies[9,10] and in Chapter 2 of this thesis. Briefly; patients were scanned three times: at their first assessment in a never-treated state (NT), at 10 months, and at 80 months after their initial examination. Healthy volunteers were scanned twice (Con1, Con2); the mean interval between the two assessments was approximately 43 months. In order to observe the influence of the gray matter segments in the spectroscopy voxel, a correction factor composed of the tissue percentage was excluded in the quantification procedure. Voxel segmentation is described in the following section. Metabolite levels in this study were uncorrected values. Only neuron relevant metabolite levels, N-acetylaspartate (NAA) and

total glutamatergic metabolites (tGL) are included in the statistical analysis. The SNR of water and the metabolites are calculated in the time domain. For the SNR calculation, the signal was taken as the water or metabolite signal at time $= 0$ (which is proportional to peak area in the frequency domain). The noise level was defined as the standard deviation of the last 32 complex pairs in the time domain.

3.2.2   Voxel segmentation

Segmentation analyses for the spectroscopy voxel were performed with ANALYZE and an in-house software Xstatpack, developed by J Davis. The T1 weighted transverse images were reoriented based on the anterior-posterior cingulate plane and reformatted to the isotropic resolution ($0.78 \times 0.78 \times 0.78$ mm^3) using ANALYZE software. After the localized spectroscopy voxel was positioned, a quantitative histogram of the signal intensity was created in each slice with Xstatpack. Thresholds of tissue types were determined with the histogram. Voxel bins that were registered into gray matter, white matter or CSF were summed throughout all slices within the spectroscopy voxel ($15 \times 10 \times 10$ mm^3). The gray matter fraction was calculated as the volume of gray matter divided by the total volume of the spectroscopy voxel, 1500 mm^3.

3.2.3   Statistics

To probe the interplay between gray matter percentage in the spectroscopy voxel and the quantified metabolite levels, analyses of variance were performed with a varying continuous independent variable (i.e. gray matter) in each 3-level repeated measures (NT vs. 10 months vs. 80 months) and 2×2 split plot factorial designs (NT & 80 months vs. Con1 & Con2). Predictive Analysis of Software (PASW) only handles a constant covariate throughout the measurement periods per subject with analysis of covariance (ANCOVA) or Multiple ANCOVA. According to procedures described by Dr. Robert C. Gardner,[11] in ANOVA a varying continuous variable is taken into account using multiple regression analysis. Metabolite levels, SNRs, peak areas and gray matter are all

dependent variables in this study. To perform this multiple regression analysis, gray matter was selected as a varying independent variable (i.e. covariate). Either metabolite level, SNR or peak area was set as a dependent variable. The covariate, gray matter, was "centered" (individual value minus the grand mean of gray matter) in each data analysis. Centering the gray matter allows the comparison of the intercept, which represents an expected dependent variable if gray matter was consistent in a comparison (e.g. NT vs. 80 months). The use of a covariate allows all subjects to be normalized with respect to a confounding variable. Thus, it is statistically possible to control for gray matter values.

The statistical comparison using the adjusted gray matter values was performed in the left thalamus for: NAA level, tGL level, NAA SNR, tGL SNR, NAA peak area and tGL peak area. Thresholds for the statistical analyses, 3-level repeated measures and 2×2 SPF analysis, were described in our previous study (Chapter 2).[10]

3.3 Results

Significant findings in the regression analyses described above and the significance from our previous study[10] are summarized in Table 3-1. The NAA peak area was found to be significant with the three-level repeated measures in the original 80 months data ($F = 5.55$, d.f. $= 2,22$, $P = 0.011$). However, there was no significance in the NAA peak area following the gray matter adjustment ($F = 3.65$, d.f. $= 2,20$, $P = 0.045 > 0.0167$). No significance in the three-level repeated measures was found in any other variables in either the original data sets or those with the gray matter adjustment.

Table 3-1: Statistical significance in the thalamic (a) NAA and (b) tGL levels before and after the gray matter adjustment.

(a)

NAA	Metabolite levels		SNR		Peak area	
	Original	ANCOVA	Original	ANCOVA	Original	ANCOVA
3-level RM						
Time	0.071	0.185	0.039	0.125	**0.011***	0.045
NT vs. 10mo	0.776	0.761	0.835	0.746	0.058	0.165
NT vs. 80mo	0.153	0.262	0.277	0.494	0.980	0.439
10movs. 80mo	**0.013***	0.031	0.028	0.065	**0.011***	0.027
2x2 SPF						
Group	0.878	0.861	0.323	0.294	0.897	0.429
Time	0.075	0.129	0.128	0.242	0.371	0.823
Group × Time	0.745	0.546	0.668	0.722	0.352	0.174
NT vs. Con1	0.692		0.322		0.442	
80mo vs. Con2	0.971		0.473		0.826	

(b)

tGL	Metabolite levels		SNR		Peak area	
	Original	ANCOVA	Original	ANCOVA	Original	ANCOVA
3-level RM						
Time	0.442	0.585	0.074	0.190	0.104	0.136
NT vs. 10mo	0.638	0.864	0.835	0.756	0.188	0.230
NT vs. 80mo	**0.044***	0.970	0.190	0.569	0.733	0.793
10movs. 80mo	0.267	0.317	0.075	0.136	0.066	0.098
2x2 SPF						
Group	0.677	0.656	0.300	0.498	0.875	0.844
Time	0.206	0.865	0.127	0.383	0.148	0.376
Group × Time	0.132	0.970	0.483	0.939	0.069	0.195
NT vs. Con1	0.273		0.233		0.228	
80mo vs. Con2	0.724		0.604		0.370	

Original, original 80 months study; ANCOVA, analysis of covariance (gray matter as a covariate). *$P < 0.0167$ (Time, 3-level), *$P < 0.025$ (NT vs. 10mo, 10mo vs. 80mo), *$P < 0.050$ (NT vs. 80mo, comparisons in 2x2 SPF).

Schizophrenia: 10mo, 10months assessment; 80mo, 80 months assessment. NT, never-treated. Control: Con1, initial scan in healthy volunteers; Con2, follow-up scan in the healthy volunteers. 3-level RM, three-level repeated measures; 2×2 SPF, two-by-two split plot factorial design (NT & 80 mo vs. Con1 & Con2).
NAA, N-acetylaspartate; SNR, signal-to-noise ratio; tGL, total glutamatergic metabolite levels (glutamate + glutamine)

There was a trend toward decreasing thalamic NAA metabolite levels following the gray matter adjustment between the 10 months and 80 months assessments ($F=6.28$, d.f. $= 1,10$, $P=0.031$) while a significant decrease was found in this comparison in the original study using a two-tailed paired t-test ($t=2.97$, d.f. $= 1,11$, $P=0.013$). Regression plots at 10 months and 80 months assessment are presented in Figure 3-1. No significant change was found in gray matter adjusted thalamic tGL levels from NT to 80 months ($F<0.01$, d.f. $= 1,14$, $P=0.970$) while those tGL levels were significantly decreased in the original 80 months study ($t=2.20$, d.f. $= 1,15$, $P=0.044$). Figure 3-2 shows their correlation plots at NT and 80 months.

No significant change in NAA SNR from 10 months to 80 months was found using the ANCOVA analysis ($F=4.28$, d.f. $= 1,10$, $P=0.065$) while there was a decreased trend in the original 80 months study ($t=2.54$, d.f. $= 1,11$, $P=0.028$). There were no significant changes in tGL SNR from the NT to the 80 months assessment in either the original data or those with the gray matter adjustment (Table 3-1).

The NAA peak area at 80 months was significantly decreased compared to 10 months in the original data sets ($t=3.07$, d.f. $= 1,11$, $P=0.011$) while there was a trend toward a decreasing NAA peak area after the adjustment using the ANCOVA ($F=6.67$, d.f. $= 1,10$, $P=0.027>0.025$). No significant changes were observed in the tGL peak area in any comparisons in either the original or the data with the gray matter adjustment.

There was no significant effect in the 2×2 SPF analyses in either the original or the gray matter adjusted variables (Table 3-1).

Figure 3-1: Thalamic NAA level adjusted by gray matter in the voxel.

Average NAA level indicates the mean value in the individual measurement period. Intercept in a regression equation indicates the NAA level if gray matter does not change between (a) 10 months and (b) 80 months. NAA, N-acetylaspartate
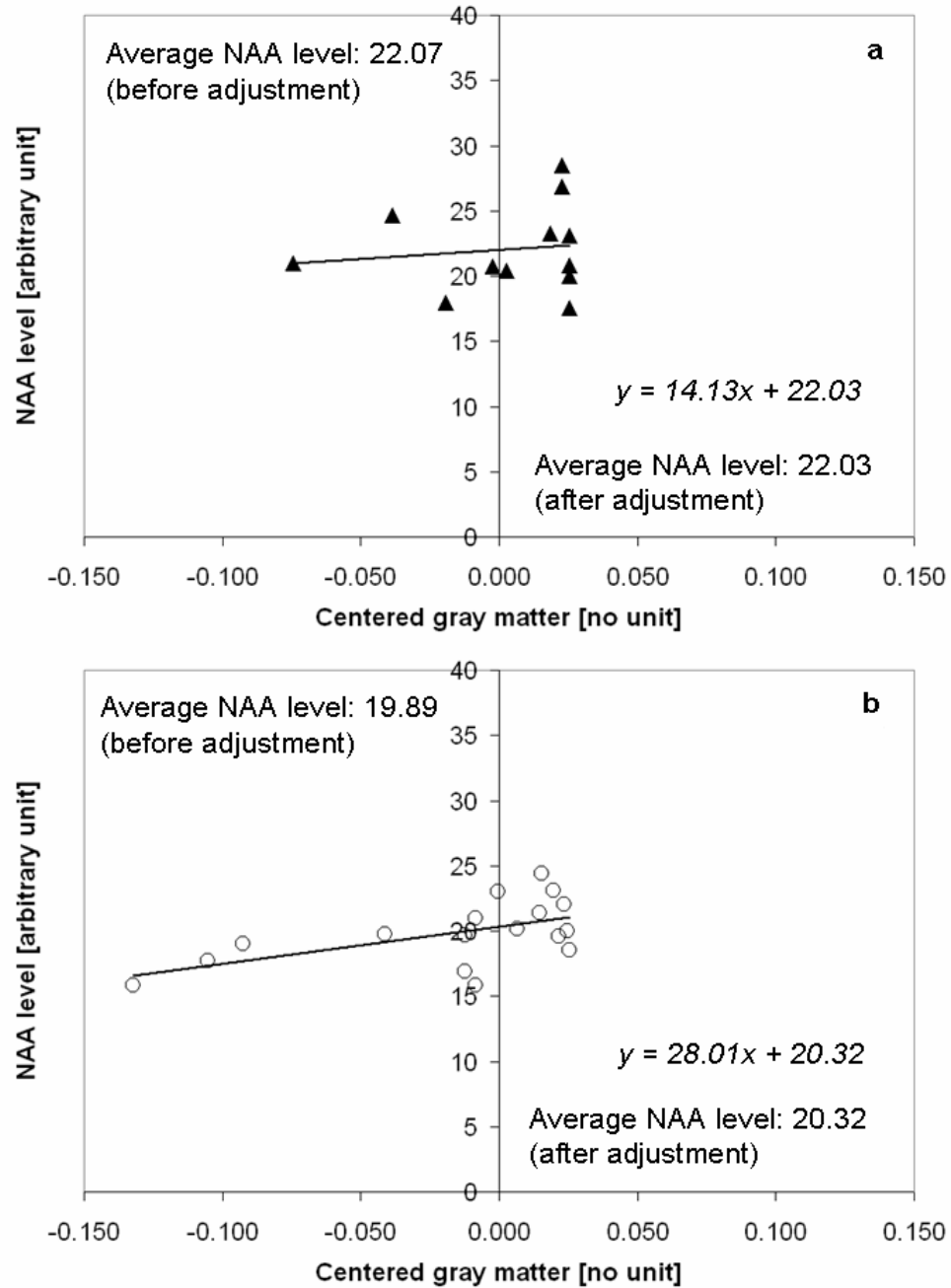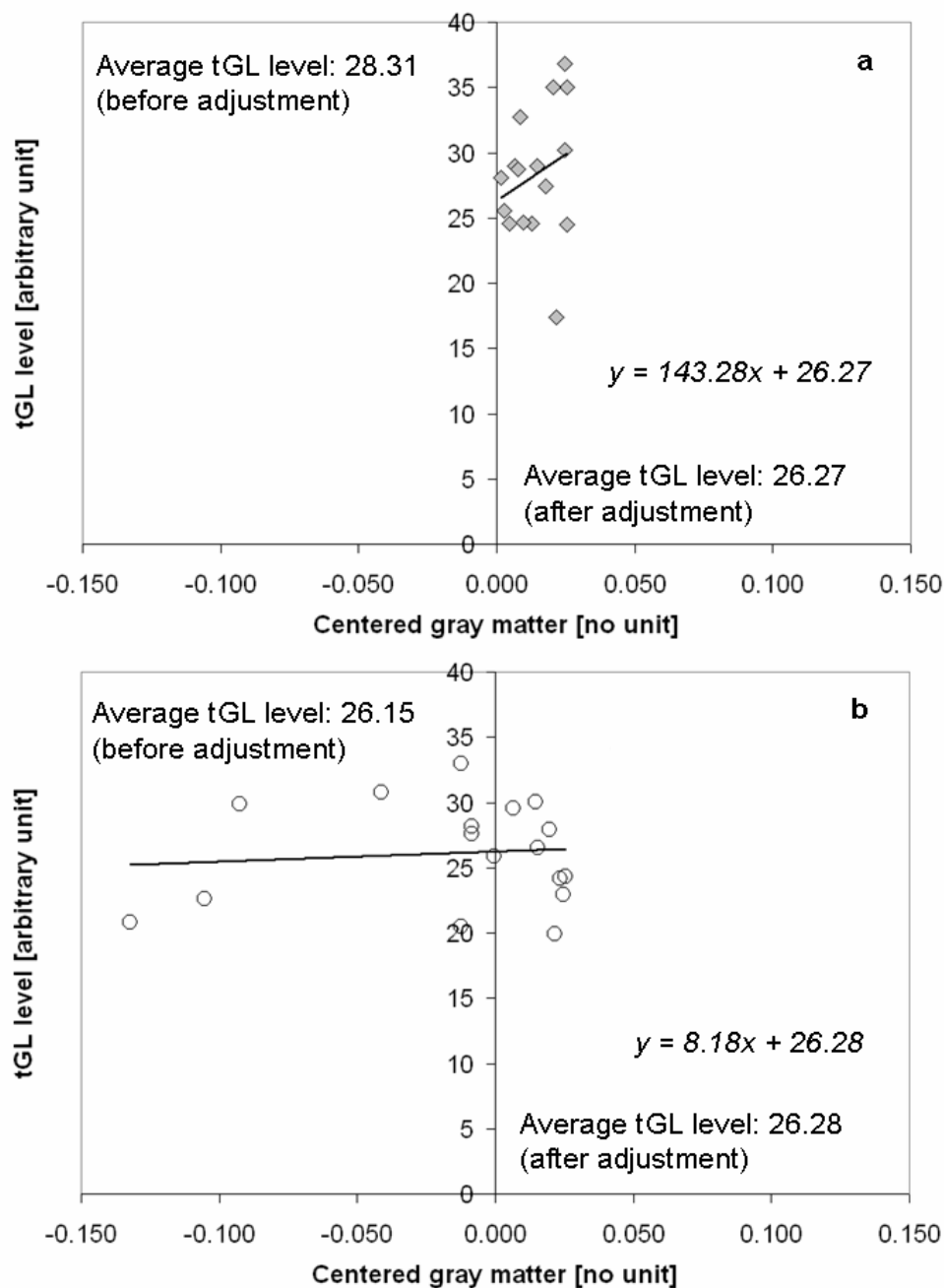
Figure 3-2: Thalamic tGL level adjusted by gray matter in the voxel.

Average tGL level indicates the mean value in the individual measurement period. Intercept in a regression equation indicates the tGL level if gray matter does not change between (a) NT and (b) 80 months. NT, never-treated schizophrenia patient; tGL, total glutamatergic metabolites (glutamate + glutamine)

3.4   Discussion

3.4.1   Gray matter effect against NAA and tGL

While the thalamic NAA level in schizophrenia patients was significantly decreased from the 10 months to the 80 months assessment in the original study ($P=0.013$), only a trend toward a decreasing level was observed in the gray matter adjusted NAA level ($P=0.031>0.025$). This result suggests that gray matter in the spectroscopy voxel affects the NAA level but that the influence is minimal because there was only a trend to lower levels in this comparison.

NAA SNR and peak area at 80 months were both lower than those at the 10 months assessment, but the significance of those differences became less prominent following the gray matter adjustment. The significance of the NAA SNR between 10 and 80 months moved from a trend ($P=0.028$) to non-significant ($P=0.065$), while the significance difference in the NAA peak area between 10 and 80 months ($P=0.011$) was reduced to the level of a trend following the gray matter adjustment ($P=0.027$). These results imply that gray matter in the spectroscopy voxel might be associated with NAA SNR and peak area as well as NAA metabolite level. However, the statistical p-value in ANCOVA hovers around the threshold, suggesting the effect of gray matter is subtle because the SNR and peak area depend more upon the hardware performance rather than tissue composition in the voxel of interest.

Thalamic tGL level adjusted by gray matter did not significantly decrease from NT to 80 months ($P=0.970$) while in the original study, it was found to be significantly decreased ($P=0.044$). Unlike NAA level in the thalamus, the statistical significance in the adjusted tGL level completely disappeared, suggesting that gray matter loss may be responsible for the decreased tGL level from NT to 80 months.

No significant change in tGL SNR or peak area was found in either the original study or the analysis with the gray matter adjustment. The statistical p-value in tGL SNR (NT vs. 80 months) with the gray matter adjustment ($P=0.569$) varied from the tGL level without adjustment ($P=0.190$), whereas the p-values in the adjusted and non-adjusted tGL peak area were quite similar. Consistent statistical significance suggests the tGL peak area was

not affected by gray matter. It indicates that noise from the data without water suppression was possibly increased due to the gray matter loss in the spectroscopy voxel from NT to the 80 months assessment. In fact, different statistical p-values in the tGL SNR with and without adjustment suggest that metabolite SNR was affected by gray matter loss. This reduction in gray matter might lead to increased magnetic susceptibility artifacts, suggesting a structural change.

3.4.2   Physiological or structural change?

Although both NAA and tGL are neuron relevant metabolites, gray matter changes may affect each of these metabolites differently. While NAA levels tended to be reduced after the gray matter adjustment ($P = 0.031$, 10 months vs. 80 months), no significance in the adjusted tGL level was found ($P = 0.970$, NT vs. 80 months). NAA level measured with MR spectroscopy is considered to be a marker of neuronal integrity.[12] Significantly lower NAA levels in schizophrenia patients are often found in the studies of MR spectroscopy but this does not necessarily imply that there is a loss of neurons.[13] In fact, NAA can be affected by medications without apparent loss of neurons.[14] Thus NAA is likely a marker of neuronal integrity which may be somewhat independent of structural changes providing some explanation for the minimal effects of gray matter loss on NAA changes over time in this study.

While NAA level is considered to be associated with neuronal integrity, tGL levels composed of glutamate and glutamine may be a reflection of synaptic integrity. Glutamate is stored in the vesicle in the axon terminal and is physiologically activated as a neurotransmitter in the synaptic cleft, the gap between two neurons.[15] Glutamine is synthesized after glutamate is taken up from the synapse into glial cells. It then diffuses back to the neuron to be used again as a neurotransmitter. Decreased levels of glutamate and glutamine measured by MR spectroscopy over time can be related to a physiological down-regulation of glutamate signaling or a loss of gray matter due to excitotoxicity, loss of neurotrophic factors or a number of other factors.[7] In postmortem studies, Selemon et al.[16] found significantly increased neuronal density in the prefrontal cortex in

schizophrenia compared to controls which was interpreted as a loss of neuropil or synaptic connections. Our observation of tGL differences over 80 months[10] could be explained either by a physiological down-regulation or a loss of synaptic gray matter in the regions studied. Glutamatergic metabolite levels were normalized to some extent by a correction factor in this study. However, the findings in the present study suggest that tGL level differences over time in schizophrenic patients disappear when the effects of gray matter are more carefully controlled. Thus the present results suggest that differences over time in tGL level in schizophrenic patients are more likely to be related to loss of neuropil and gray matter than a physiological down-regulation of neurotransmitter activity.

The significance in the metabolite SNRs and peak areas with the gray matter adjustment was similar to the analyses without the adjustment. Although statistical p-values in tGL SNR were changed, both differences in tGL SNR with and without adjustment were non-significant. This observation suggests that gray matter loss did not affect the magnetic susceptibility making it more difficult to detect metabolite changes. However, the metabolite SNR defined in this study depended on the hardware performance on the date of the scan.

3.4.3 Implications for excitotoxicity

It is still unclear whether both tGL level and gray matter were decreased at a similar rate or whether the reduction in tGL level was led by gray matter loss. ANOVA with a varying continuous variable takes gray matter into account when the statistical comparisons in the metabolites are conducted. This method only indicates whether gray matter amount is associated with the metabolite level but does not indicate how metabolite level might have changed without gray matter loss in our previous 80 months study.[10] It is possible that there might have been an early physiological increase in glutamatergic metabolites leading to excitotoxicity and loss of synapses and gray matter which then led to the loss of glutamatergic metabolites. Consequently an early

physiological increase in glutamatergic activity followed by structural changes in neuropil cannot be ruled out.

3.4.4   Limitations

Decreased gray matter fraction is possibly caused by a misplacement of the spectroscopy voxel due to an involuntary movement of the subject before and after the voxel localization. Subjects were monitored from the superior part of their head during the experiment. However, it is difficult to detect a head movement along the Z axis, paralleled to the B_0 direction and the head rotation in the anterior-posterior direction. For instance, if the subject slightly moved to the superior direction before the spectroscopy acquisition, the localized voxel would be inferior to what was selected using the T1 weight images. Therefore, this spectrum would be composed of the MR signals from the voxel of interest and from signal outside of the voxel.

Voxel localization might not be identical between the first and follow-up scans. Although the spectroscopy voxel was localized using landmarks in the brain, the localized voxel may not be exactly the same as that in the other follow-up scans. Furthermore, the data was collected by three operators, which might result in a misplacement of the spectroscopy voxel.

The scan interval in the healthy volunteers was not comparable to that in the schizophrenia patients. Gray matter loss in controls might be missed due to the shorter follow-up period. Small gray matter changes make it difficult to detect the correlation to with the metabolite levels, SNRs and peak areas.

Gray matter in this study may include white matter. Although the thalamus is mostly composed of the gray matter, it also contains some white matter. Since gray matter is abundant compared to the white matter, most image pixels are recognized as gray matter in terms of the contrast. Metabolite levels are different between gray matter and white matter, even though gray matter and white matter are indistinguishable in this image

analysis. It may be that the influence of white matter is negligible due to the small amount of white matter compared to the amount of gray matter.

3.5   Acknowledgements

3.6   References

1.   Gogtay N, Thompson PM. Mapping gray matter development: implications for typical development and vulnerability to psychopathology. *Brain Cogn* 2010;**72**(1):6-15

2.   Rund BR. Is schizophrenia a neurodegenerative disorder? *Nord.J Psychiatry* 2009;**63**(3):196-201

3.   Maccioni RB, Munoz JP, Barbeito L. The molecular bases of Alzheimer's disease and other neurodegenerative disorders. *Arch Med Res* 2001:**32**(5):367-381

4.   Bustillo JR, Lauriello J, Rowland LM, Thomson LM, Petropoulos H, Hammond R, Hart B, Brooks WM. Longitudinal follow-up of neurochemical changes during the first year of antipsychotic treatment in schizophrenia patients with minimal previous medication exposure. *Schizophr Res* 2002;**58**(2-3):313-321

5.   Pilatus U, Lais C, Rochmont Adu M, Kratzsch T, Frolich L, Maurer K, Zanella FE, Lanfermann H, Pantel J. Conversion to dementia in mild cognitive impairment is associated with decline of N-actylaspartate and creatine as revealed by magnetic resonance spectroscopy. *Psychiatry Res* 2009;**173**(1):1-7

6.   Olney JW, Farber NB. Glutamate receptor dysfunction and schizophrenia. *Arch Gen Psychiatry* 1995;**52**(12):998-1007.

7.   DeLisi LE. The concept of progressive brain change in schizophrenia: implications for understanding schizophrenia. *Schizophr Bull* 2008;**34**(2):312-321

8.   Théberge J, Bartha R, Drost DJ, Menon RS, Malla A, Takhar J, Neufeld RW, Rogers J, Pavlosky W, Schaefer B, Densmore M, Al Semaan Y, Williamson PC. Glutamate and glutamine measured with 4.0 T proton MRS in never-treated patients with schizophrenia and healthy volunteers. *Am J Psychiatry* 2002;**159**(11):1944-1946.

9. Théberge J, Williamson KE, Aoyama N, Drost DJ, Manchanda R, Malla AK, Northcott S, Menon RS, Neufeld RW, Rajakumar N, Pavlosky W, Densmore M, Schaefer B, Williamson PC. Longitudinal grey-matter and glutamatergic losses in first-episode schizophrenia. *Br J Psychiatry* 2007;**191**:325-334.

10. Aoyama N, Théberge J, Drost DJ, Manchanda R, Northcott S, Neufeld RWJ, Menon RS, Rajakumar N, Pavlosky WF, Densmore M, Schaefer B, Williamson PC. Grey matter and social functioning correlates of glutamatergic metabolite loss in schizophrenia *Br J Psychiatry.* accepted

11. Gardner RC. *Analysis of Variance with a Continuous Independent Variable: Model I: The Unique Approach.* London, Canada: University of Western Ontario; 2003. Unpublished monograph

12. Clark JB. N-acetyl aspartate: A marker for neuronal loss or mitochondrial dysfunction. *Dev Neurosci* 1998; **20**: 271-6.

13. Cendes F, Andermann F, Dubeau F, Matthews PM, Arnold DL. Normalization of neuronal metabolic dysfunction after surgery for temporal lobe epilepsy. Evidence from proton MR spectroscopic imaging. *Neurology.* 1997;**49**(6):1525-33.

14. Vion-Dury J, Nicoli F, Salvan AM, Confort-Gouny S, Dhiver C, Cozzone PJ. Reversal of brain metabolic alterations with zidovudine detected by proton localised magnetic resonance spectroscopy. *Lancet.* 1995;**345**(8941):60-1.

15. Rothman DL, Behar KL, Hyder F, Shulman RG. In vivo NMR studies of the glutamate neurotransmitter flux and neuroenergetics: implications for brain function. *Annu Rev Physiol.* 2003;**65**:401-27.

16. Selemon LD, Rajkowska G, Goldman-Rakic PS. Elevated neuronal density in prefrontal area 46 in brains from schizophrenic patients: application of a three-dimensional, stereologic counting method. *J Comp Neurol.* 1998;**392**(3):402-12.

Chapter 4

4   The perils of long-term proton magnetic resonance spectroscopy studies

4.1   Introduction

Neuroimaging techniques are useful in the cross-sectional investigation of abnormalities in psychiatric disorders.[1] However, long-term observation is essential for the understanding of neurodegenerative disorders such as Alzheimer's disease and schizophrenia.[2] Magnetic resonance imaging and spectroscopy allow the examination of long term structural and neurochemical changes. In a previous study, we examined first episode schizophrenia patients before treatment, followed by 10 months and 30 months after the medication, using magnetic resonance spectroscopy at 4 Tesla.[3]

For a long term study however, the reliability of the data is strongly dependent upon the stability of the hardware during the course of the project. Ideally the Signal to Noise Ratio (SNR) should be maintained at the same level throughout the project. Despite that, because MRI systems are complex clinical systems, there will inevitably be hardware upgrades and/or replacements required to maintain the system. The longer the project duration, the more likely such difficulties will arise. Our group recently conducted an 80 month follow-up study using magnetic resonance spectroscopy at 4 Tesla. Data was collected from schizophrenia patients over 7 years and anomalies were found in NAA and glutamatergic metabolites in schizophrenia patients.[4] During the 7 year duration of this project, there were several upgrades in the MR system. Consequently, a critical part of internal quality control is to ensure that these measured metabolite concentration levels are not artificially modified by the changes in the hardware.

SNR is a good measure to track the hardware stability in a long term project.[5] In this present study, SNR was measured in the time domain rather than in the frequency domain. The advantage of measuring SNR in the time domain is that signal amplitude is independent of the linewidth while peak intensity in the frequency domain is significantly dependent on the linewidth. Under the same metabolite concentration level, peak area

underneath the metabolite spectrum is constant while peak intensity varies with respect to the linewidth, determined by T2*. If SNR is measured in the frequency domain, peak intensity should be corrected by linewidth before comparing the SNR. Linewidth is another good standard to gauge the quality of the spectrum; however it is more affected by differences in the head structure of the participants and voxel positioning in the brain, and location with respect to isocentre, rather than hardware changes.

The purposes of this study were: (i) to determine if the SNRs of the MR signals for water, NAA and tGL in both the schizophrenia and the control groups were significantly correlated with magnet age; (ii) if there are any significant differences in these SNR levels throughout the duration of the study, to determine if any hardware modifications may be responsible, and if so to simulate comparable SNR levels throughout the 10 year period; and (iii) to evaluate the NAA and tGL concentration levels after replacing the original data with this simulated data, using the same statistical comparison conducted in the 80 month study.[4] We hypothesize that the significant differences or changes observed in the metabolite levels in an 80 month study would persist when the original data were replaced with the SNR adjusted (addition of random noise) data.

4.2 Methods

4.2.1 Participants, imaging and spectroscopy

Data were acquired from 17 schizophrenia patients and 17 healthy volunteers, those who participated in our previous study.[4] Demographic information was exactly the same as our previous study (see Chapter 2). Schizophrenia patients were scanned before treatment (NT, never-treated) as well as at 10 months and 80 months after their initial assessment. Controls were scanned twice (Con1, Con2), and the time period between the two assessments was approximately 43 months. All experiments were performed with a 4 Tesla whole body scanner located at the Functional and Metabolic Mapping Centre at the Robarts Research Institute, London, Ontario Canada. All procedures including shimming, imaging sequence, voxel localization, spectroscopy sequence (STEAM, echo

time $=20$ ms, mixing time $=30$ ms, repetition time $=2$ s, dwell time $=500$ μs), pre-processing, spectral fitting and quantification have been described previously.[3,4]

4.2.2   SNR, linewidth and magnet age

Signal-to-noise ratio and raw signal were defined in the time domain. Raw signal was defined as the amplitude of the water or metabolite Free Induction Decay (FID), from which the recorded signal was decomposed through the fitting procedure introduced in this section. Noise was calculated from the standard deviation of the last 32 complex points in the time domain in each suppressed and unsuppressed dataset. Water linewidth was determined by the fitting procedure and specified as the full width at half maximum of a fitted single peak Lorentzian component. To examine the MR system stability, correlation analyses were performed versus magnet age for water linewidth, and SNR of water, NAA and tGL. The magnet age was defined with respect to the date of the earliest scan (August 27, 1997) in this study. For this discussion we are using 'magnet age' to define the age of the entire MR system as the magnet was not changed over the 7 years, whilst most of the other components were replaced and/or modified during the study (e.g. gradients, gradient amplifiers, receiver electronics, RF amplifier, MR console);

Magnet age [year] = {(Date of scan) − (August 27, 1997)} / 365 days.

This correlation analysis was performed at each measurement period in each group (e.g. NT, Con 1) as well as a correlation combining all the samples in the schizophrenia group (NT, 10 months plus 80 months) and similarly for the control group (Con1 plus Con2). The latter correlations are not meaningful statistical analyses because each sample is not truly independent in terms of subject. Nevertheless, we performed this correlation analysis only to detect a significant change in SNR at a particular time period over the entire magnet age.

4.2.3   Random noise

Presumably because of a hardware variation or other factors related to the 'sample', the SNR may vary from one time to another. The source of this hardware difference will be addressed in the discussion; however the goal here is to demonstrate that the differences in SNR were not responsible for observed changes in metabolite levels. In an attempt to make the SNR consistent throughout the study, the time point where SNR is determined to be best, we added extra noise into the raw data in the time domain using software coded using Matlab7 (Matlab, The Mathworks, Natick, MA). Noise was only added to the data collected at a particular time period, at which time the SNR of water and the metabolites were significantly higher than those collected at other time points within the study period. The time period with a reduced noise, and hence elevated SNR, was identified by the correlation analysis between SNR and magnet age. Discrete pseudo-random noise (3008 data points) was produced in the time domain. The noise amplitude was estimated from the mean noise level - the standard deviation of the last 32 complex points. The random noise amplitudes were added to each real and imaginary point utilizing the phase information obtained from the water reference of each dataset. Pre-processing, spectral fitting and quantification described in our previous study[3,4] were repeated for the simulated spectra (with extra noise). In order to reduce a bias, all procedures described in this section were repeated in triplicate. Quantified metabolite levels were averaged across the three trials.

4.2.4   Statistical analyses

Statistical analyses were completed using statistical software PASW Statistics version 18.0.0 for Windows. Correlation analyses were performed versus magnet age for the SNR, linewidth and noise level after the addition of extra noise with the Pearson product moment coefficient ($P=0.001$). As indicated above, this was performed at each measurement period in each group, including all of the samples in the patient group, and including all of the samples in the control group.

Quantified NAA and tGL levels were then compared using the same statistical method described in our previous study.[4] Correlation analyses were also conducted with respect to the subject age instead of magnet age at each measurement period. This is to identify whether there are changes within the group due to patient age.

4.2.5 SNR simulation: precision in the metabolite quantification

In this study, random noise was added to datasets in the time domain data for the time point that was identified to have a higher SNR (lower noise) than the remaining data sets in the study duration. The origin of this difference will be discussed later. In order to understand how the noise level of the data affects the fitting of the metabolites, one characteristic spectrum was selected from the entire study set. This dataset was fit to determine the metabolite levels as described above. The ideal noiseless fit was taken as an ideal spectrum and 149 different noise sets were added to this spectrum in the time domain using the same approach described in the "random noise" section of this study. Pre-processing, spectral fitting and quantification were repeated for the simulated spectra. These quantified spectra were sorted by NAA SNR, chosen to be between 1.34 and 8.49, as this is the SNR range observed the original 80 months study (as determined below). Groups (n=11) were created based on NAA SNR (group averages: 1.75, 2.19, 2.84. 3.25, 3.71, 4.22. 4.77. 5.34. 5.81, 6.25 and 7.13). Quantified metabolite peak areas were averaged in each group.

4.3 Results

4.3.1 Correlation with respect to magnet age (across measurement periods)

In the original data sets, NAA SNR decreased with magnet age in the anterior cingulate ($r=-0.460$, $P=0.002$, N=44) and the thalamus ($r=-0.460$, $P=0.001$, N=45) in schizophrenia (i.e. combining NT, 10 months and 80 months). The correlation of NAA SNR versus magnet age in the thalamus is presented in the top-left of Figure 4-1(a).
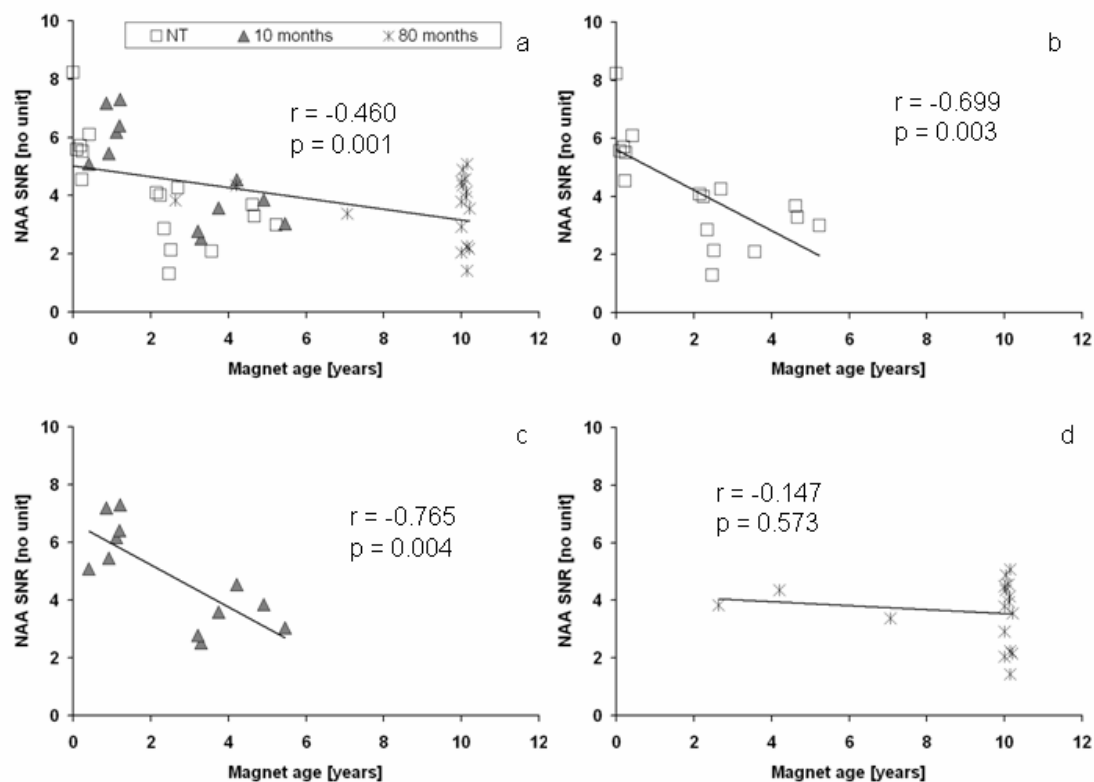
Figure 4-1: NAA signal-to-noise ratio in the left thalamus in schizophrenia versus magnet age.

Plot at the top-left (a) is a correlation across the measurement periods (n = 45). The rest of the plots are the correlations at each measurement period; NT (b), 10 months (c) and 80 months (d).

Thalamic tGL SNR in the schizophrenia group also demonstrated a trend to decrease over magnet age ($r=-0.423$, $p=0.004$). There was no significant correlation between noise levels in the water suppressed data and magnet age in the anterior cingulate ($r=0.379$, $P=0.012$) and the thalamus ($r=0.372$, $P=0.012$) in schizophrenia patients. Figure 4-2 represents the change in the metabolite noise in the left thalamus with respect to the magnet age in schizophrenia. None of the variables in the control group (Con1 plus

Con2) was significantly correlated with the magnet age in both the anterior cingulate and the thalamus.
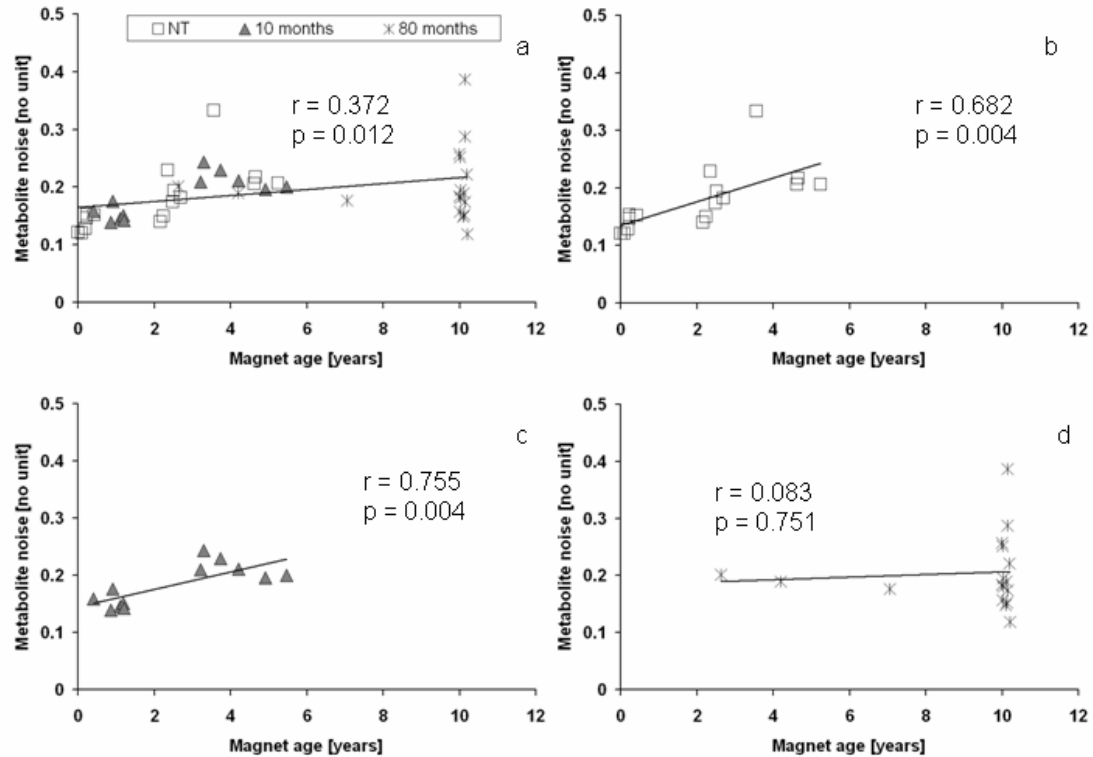
Figure 4-2: Metabolite noise in the left thalamus in schizophrenia versus magnet age.

Noise is calculated from the last 32 complex points in the time domain. Plot at the top-left (a) is a correlation across all data samples (n = 45). The rest of the plots are the correlations at each measurement period; NT (b), 10 months (c) and 80 months (d).

In these plots, there is an apparent trend toward lower noise levels during the first two years of the study (Figure 4-2). This might explain some elevated SNR, for example the water SNR, observed during that time period. This was particularly curious because of the gradient coils upgrade occurring at that specific time. One possible culprit is a change

in the digital filter that occurred at that time. Because of these hardware upgrades, a possible transition time was defined at 2 years in magnet age. The noise manipulation described in "random noise" in the method section was performed in the data collected only in the first 2 years since August 27, 1997, the oldest data set in this data analysis. Because of the timing of the measurements, extra noise was added to the six data sets at NT and 10 months assessment in the schizophrenia group and four data sets at Con1 in the control group.

4.3.2 Metabolites SNR vs. magnet age (at the individual measurement periods)

Correlations with respect to the magnet age at each measurement period are summarized in Table 4-1. In the left anterior cingulate, tGL SNR was significantly decreased over magnet age at 10 months assessment in schizophrenia ($r=-0.809$, $P=0.001$), and there was a trend toward a decrease at NT ($r=-0.741$, $P=0.002$). There was a trend toward decreasing NAA SNR at NT ($r=-0.714$, $P=0.003$) and 10 months assessment ($r=-0.750$, $P=0.005$) in schizophrenia. Metabolite noise was significantly increased at 10 months in schizophrenia ($r=-0.828$, $P=0.001$). None of the other correlations were significant in either schizophrenia or controls in the anterior cingulate.

Table 4-1: Pearson product-moment coefficients with respect to the magnet age before and after adding extra noise into the first 2 years data.

(a)

Anterior Cingualte	NT N=15		10 mo N=14		80 mo N=16	All N=44	
	Original	With noise	Original	With noise	Original	Original	With noise
Water linewidth	Ns	ns	ns	ns	ns	ns	ns
Water SNR	Ns	ns	ns	ns	ns	ns	ns
Water noise	Ns	ns	ns	ns	ns	ns	ns
Metabolite noise	Ns	ns	0.828**	ns	ns	ns	ns
NAA SNR	-0.714*	ns	-0.750*	ns	ns	-0.460*	ns
tGL SNR	-0.741*	ns	-0.809**	-0.747*	ns	ns	ns
NAA level	Ns	ns	ns	ns	ns	ns	ns
tGL level	Ns	ns	ns	ns	ns	ns	ns

(b)

Thalamus	NT N=16		10 mo N=12		80 mo N=17	All N=45	
	Original	With noise	Original	With noise	Original	Original	With noise
Water linewidth	Ns	ns	ns	ns	ns	ns	ns
Water SNR	Ns	ns	-0.810**	ns	ns	ns	0.426*
Water noise	Ns	ns	ns	ns	ns	ns	ns
Metabolite noise	0.682*	ns	0.755**	ns	ns	ns	ns
NAA SNR	-0.689*	ns	-0.765*	ns	ns	-0.460**	ns
tGL SNR	Ns	ns	-0.806**	ns	ns	-0.423*	ns
NAA level	Ns	ns	ns	ns	ns	ns	ns
tGL level	Ns	ns	ns	ns	ns	ns	ns

Significant r-values in schizophrenia in the (a) anterior cingulate and (b) thalamus are shown in this table ($**P < 0.001$, $*P < 0.005$). R-values in the original 80 months study (before adding noise) are presented in the left column (Original) in each NT, 10mo and All group section as well as 80 mo column. Statistical values after the noise manipulation are presented in the right column (With noise) with italic font in each section except 80 mo column. Extra noise were added in the data sets, collected in the first 2 years (six data sets of each NT and 10 mo).

In the left thalamus, water SNR at 10 months assessment in schizophrenia was significantly decreased over magnet age ($r=-0.810$, $P=0.001$). There is a trend toward a negative correlation with magnet age for NAA SNR at NT ($r=-0.699$, $P=0.003$) and 10 months ($r=-0.765$, $P=0.004$) and tGL SNR at the 10 months assessment ($r=-0.806$, $P=0.002$). Figure 4-1 (b, c, d) presents the correlations between NAA SNR in the thalamus and magnet age. There is a trend for metabolite noise to increase over magnet age at both NT ($r=0.682$, $P=0.004$) and 10 months ($r=0.755$, $P=0.005$) (Figure 4-2). No significant correlation was found in controls in the thalamus.

Correlations after the noise manipulation were presented in the right column in NT and 10 months in Table 4-1. Extra noise was added to the data collected in the first 2 years and replaced with the original data sets. This noise simulation was not performed in the data in the 80 months group because these data were collected beyond the transition time (i.e. first 2 years in the magnet age). An observed trend toward decreasing tGL SNR over magnet age persisted in the anterior cingulate after adding noise ($r=-0.747$, $P=0.002$). No other significant correlation was observed after the noise simulation in any other variables, measurement periods, regions and groups.

4.3.3   Metabolite levels after adding random noise

Mean metabolite levels in the original 80 months study and in these data with extra noise are presented in Figure 4-3 (anterior cingulate) and 4-4 (thalamus). There was a trend toward decreasing NAA level from 10 months to 80 months assessment in the left anterior cingulate in the original data ($P=0.031>0.025$) but no significance was observed in the same data after adding the random noise ($P=0.114$). There was no other significant difference between the original and simulated data in the left anterior cingulate. Thalamic NAA level at 80 months was significantly decreased from 10 months in the original data ($P=0.013$) (Figure 4-4). After adding the noise, this was no longer significant ($P=0.029>0.025$) but there was a trend toward a decreasing level. The tGL level at 80 months was significantly decreased from NT in schizophrenia in the original data ($P=0.044$) and the data with extra noise ($P=0.024$).
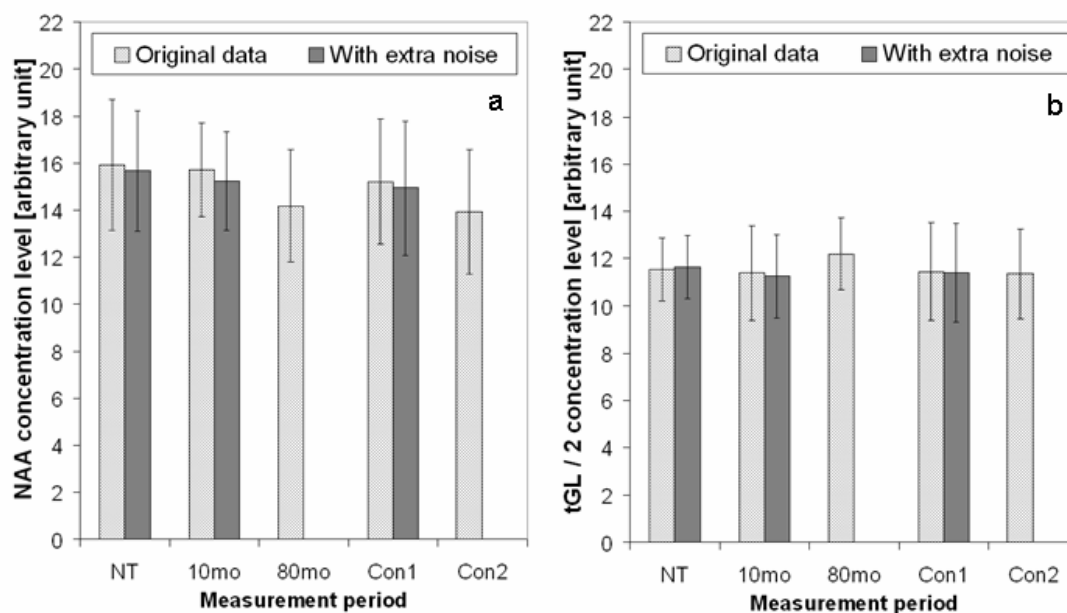
Figure 4-3: Metabolite levels in the anterior cingulated before and after data manipulation.

Anterior cingulate NAA (a) and tGL (b) concentration levels in the 80 months study (Original data) and the same data with adding random noise (With extra noise). Error bar indicates the group standard deviation in each measurement period. Extra noise were added into 6 data sets in each NT (n = 15) and 10mo measurement (n = 14), as well as 4 data sets in Con1 (n = 17).

Measurement period: NT, never-treated; 10mo, 10 months assessment; 80mo, 80 months assessment; Con1, control at scan #1; Con2, control at scan #2. Metabolites: NAA, N-acetylaspartate; tGL, sum of glutamate and glutamine.
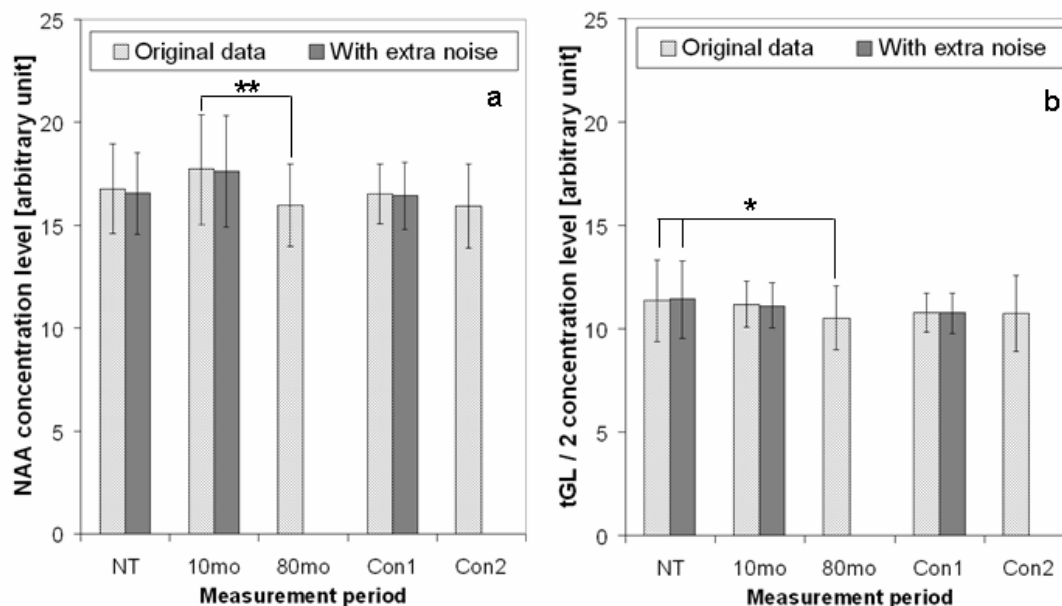
Figure 4-4: Metabolite levels in the thalamus before and after the data manipulation.

Thalamic NAA (a) and tGL (b) concentration levels in the 80 months study (Original data) and the same data with adding random noise (With extra noise). Error bar indicates the group standard deviation in each measurement period. Extra noise were added into 6 data sets in each NT (n = 16) and 10mo measurement (n = 12), as well as 4 data sets in Con1 (n = 17). **P < 0.025, *P < 0.050.

Measurement period: NT, never-treated; 10mo, 10 months assessment; 80mo, 80 months assessment; Con1, control at scan #1; Con2, control at scan #2. Metabolites: NAA, N-acetylaspartate; tGL, sum of glutamate and glutamine.

4.3.4   SNR simulation: precision in the metabolite quantification

In this study, noise was added to some time points, and the potential impact on metabolite levels was investigated. It is therefore important to know whether and to what extent modifying the noise level will alter the fitting of the metabolites. Figure 4-5 represents the variation of 7 quantified metabolite levels with respect to NAA SNR. In this study,

the addition of noise for the first 2 years of an 80 month study caused the NAA SNR in the time domain to decrease by approximately 25% (from 4.818 to 3.612). The grand mean was calculated from the data in the first 2 years of the study, including both groups (schizophrenia & control) and both regions (anterior cingulate & thalamus). These average SNR before (dashed line) and after adding the noise (solid gray line) are shown as vertical lines in Figure 4-5. The average NAA SNR drop in the anterior cingulate and the thalamus was 25.5% and 24.7%, respectively. Figure 4-6 represents the changes in quantified NAA metabolite level with respect to the simulated NAA SNR. Error bars represent the group standard deviation of the NAA level in each SNR group. The Coefficient of Variation (CV) around the mean NAA SNR before and after adding noise is approximately 10.6% and 11.9%, respectively. The CV for the glutamate level degrades from 13.3% to 21.1%, and similarly for the glutamine level, from 25.2% to 36.0%. Figure 4-7, 8 and 9 represent the quantified glutamate, glutamine and tGL levels with respect to the NAA SNR, respectively.
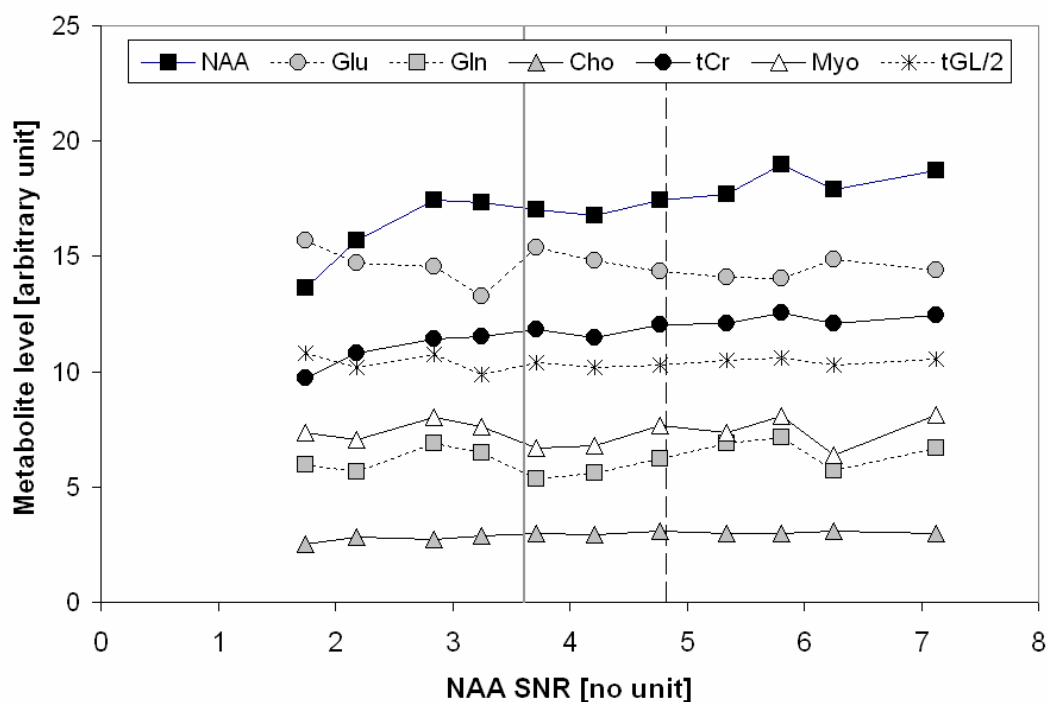
Figure 4-5: SNR simulation.

Quantified metabolite levels with respect to the NAA signal-to-noise ratio in the time domain. 149 spectra were simulated with using a noise-free spectrum. These spectra are sorted into 11 different NAA SNR. Two vertical lines show the average NAA SNR before (dashed line) and after (solid gray line) adding the extra noise in the first 2 years data in 80 months study. The averages are taken among the first 2 years data, including 6 data sets of each NT and 10 months as well as 4 data sets in Con1 in both anterior cingulate and thalamus.

Cho, choline; Gln, glutamine; Glu, glutamate; Myo, myo-inositole; NAA, N-acetylaspartate; tCr, total creatine; tGL, total glutamatergic metabolite (Glu+Gln).

Figure 4-6: SNR simulation, NAA level.

Quantified NAA levels with respect to the NAA SNR. Error bar indicates the standard deviation in each group sorted by NAA SNR. Two vertical lines show the average NAA SNR before (dashed line) and after (solid gray line) adding the extra noise in the first 2 years data in 80 months study. The averages are taken among the first 2 years data, including 6 data sets of each NT and 10 months as well as 4 data sets in Con1 in both anterior cingulate and thalamus.
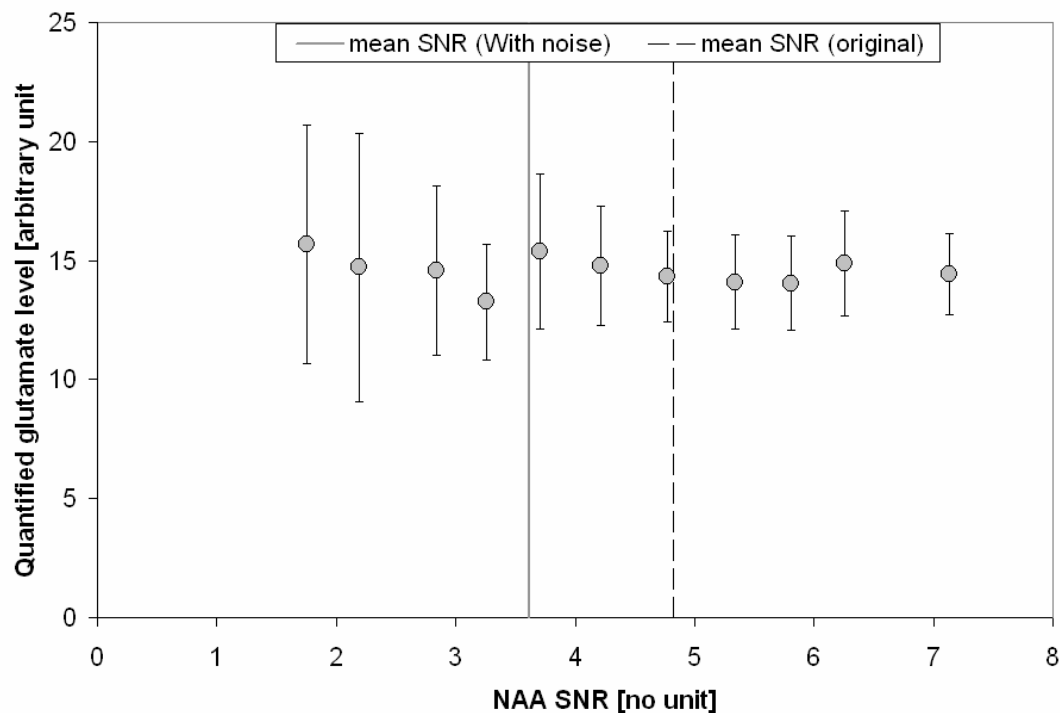
Figure 4-7: SNR simulation, glutamate level.

Quantified glutamate levels with respect to the NAA SNR. Error bar indicates the standard deviation in each group sorted by NAA SNR. Two vertical lines show the average NAA SNR before (dashed line) and after (solid gray line) adding the extra noise in the first 2 years data in 80 months study. The averages are taken among the first 2 years data, including 6 data sets of each NT and 10 months as well as 4 data sets in Con1 in both anterior cingulate and thalamus.
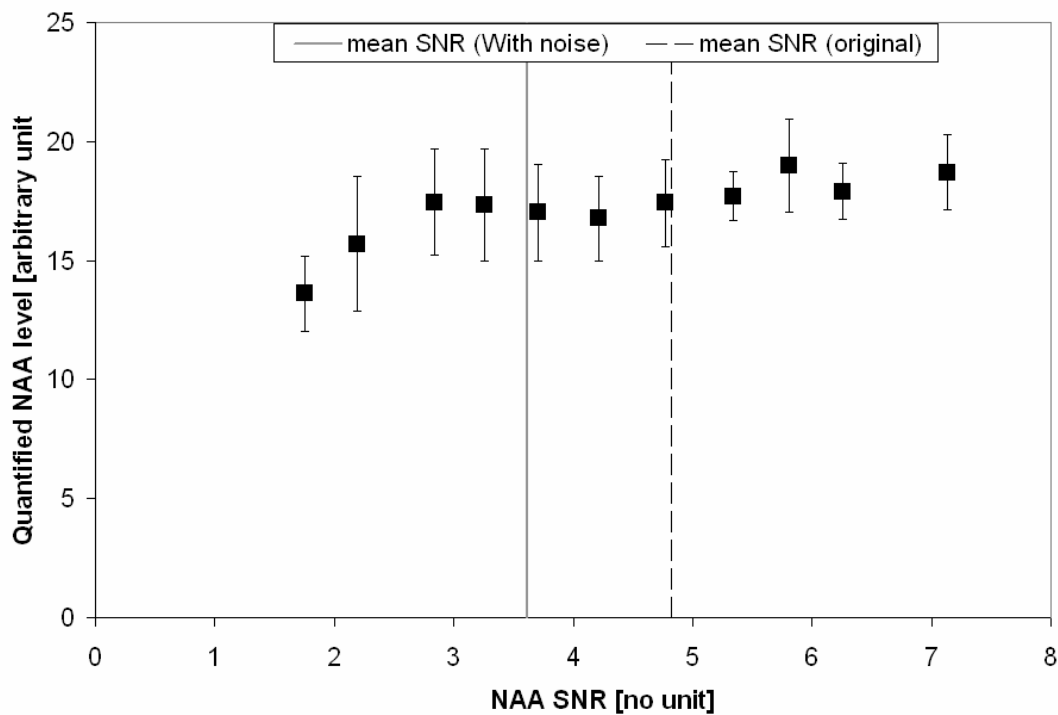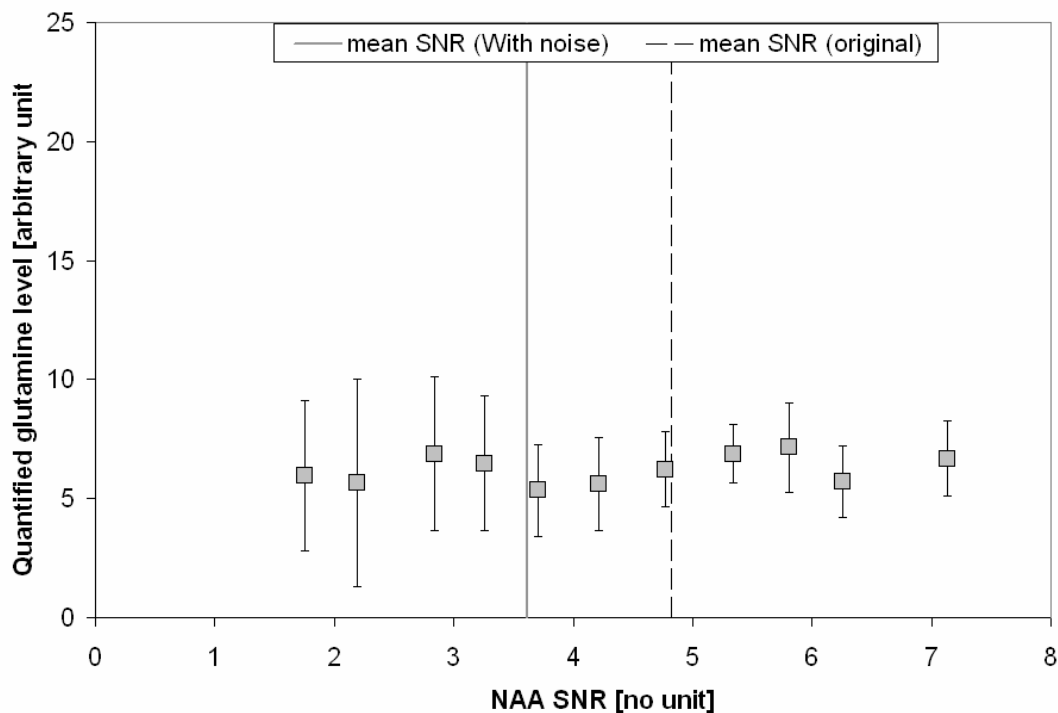
Figure 4-8: SNR simulation, glutamine level.

Quantified glutamine levels with respect to the NAA SNR. Error bar indicates the standard deviation in each group sorted by NAA SNR. Two vertical lines show the average NAA SNR before (dashed line) and after (solid gray line) adding the extra noise in the first 2 years data in 80 months study. The averages are taken among the first 2 years data, including 6 data sets of each NT and 10 months as well as 4 data sets in Con1 in both anterior cingulate and thalamus.
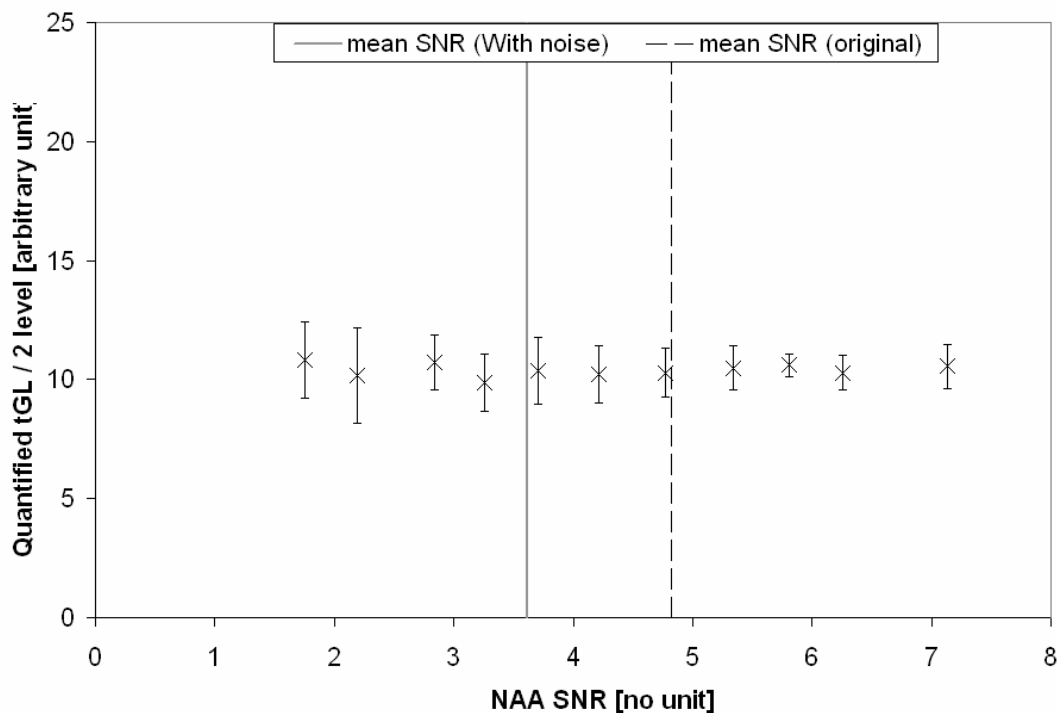
Figure 4-9: SNR simulation, tGL level.

Quantified total glutamatergic metabolites (tGL) with respect to the NAA SNR. Error bar indicates the standard deviation in each group sorted by NAA SNR. Two vertical lines show the average NAA SNR before (dashed line) and after (solid gray line) adding the extra noise in the first 2 years data in 80 months study. The averages are taken among the first 2 years data, including 6 data sets of each NT and 10 months as well as 4 data sets in Con1 in both anterior cingulate and thalamus. tGL: total glutamatergic metabolites (glutamate + glutamine)

4.3.5 NAA SNR vs. subject age

No significant correlation with respect to the subject age was found either in the anterior cingulate or the thalamus at any measurement periods, including all measurement periods in both groups. The top plot in Figure 4-10 shows the correlations between NAA SNR and the subject age in schizophrenia. The bottom plot in Figure 4-10 represents the same correlation following the addition of the pseudo-random noise. Figure 4-11 presents the

thalamic NAA SNR with respect to the subject age in controls. The original data is shown in the top plot while the bottom panel shows the data with the extra noise.
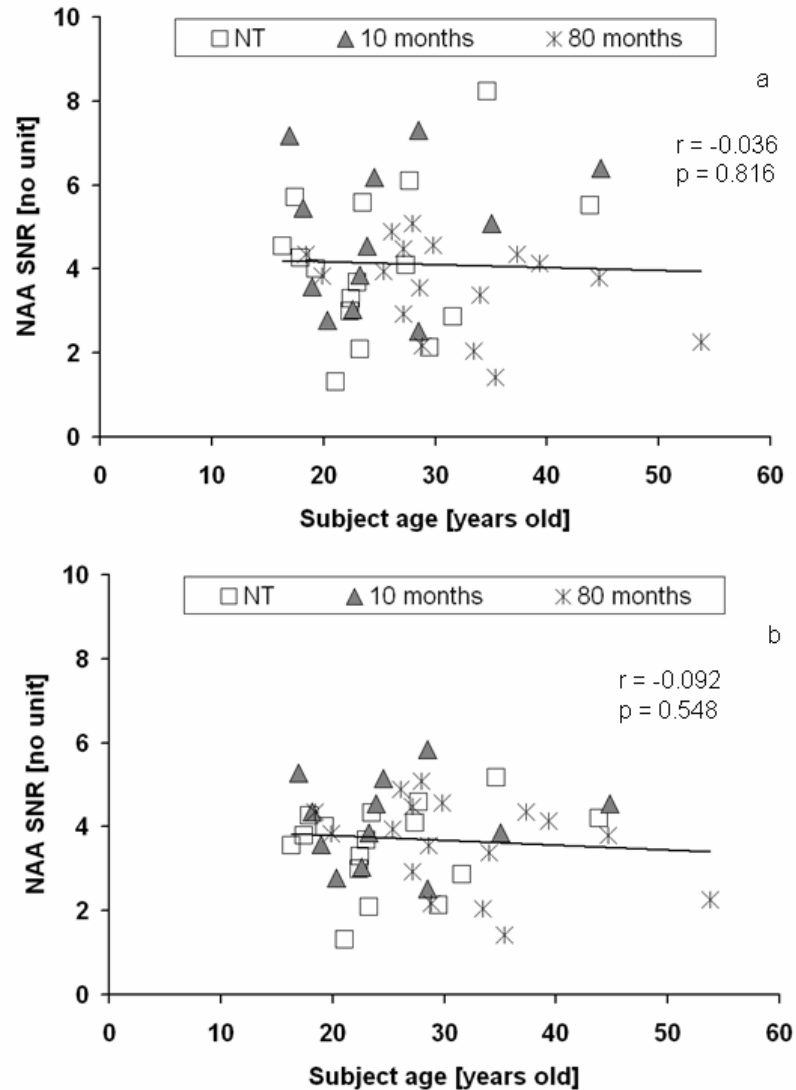
Figure 4-10: Correlations between subject age and thalamic NAA signal-to-noise ratio in schizophrenia

NAA signal-to-noise ratio at all measurement periods (N = 45) were involved in this correlation analysis. Top plot (a) indicates the original 80 months study. Bottom plot (b) indicates the data after the noise simulation, applied to the 12 data sets (6 of each NT and 10 months) collected in the first 2 years
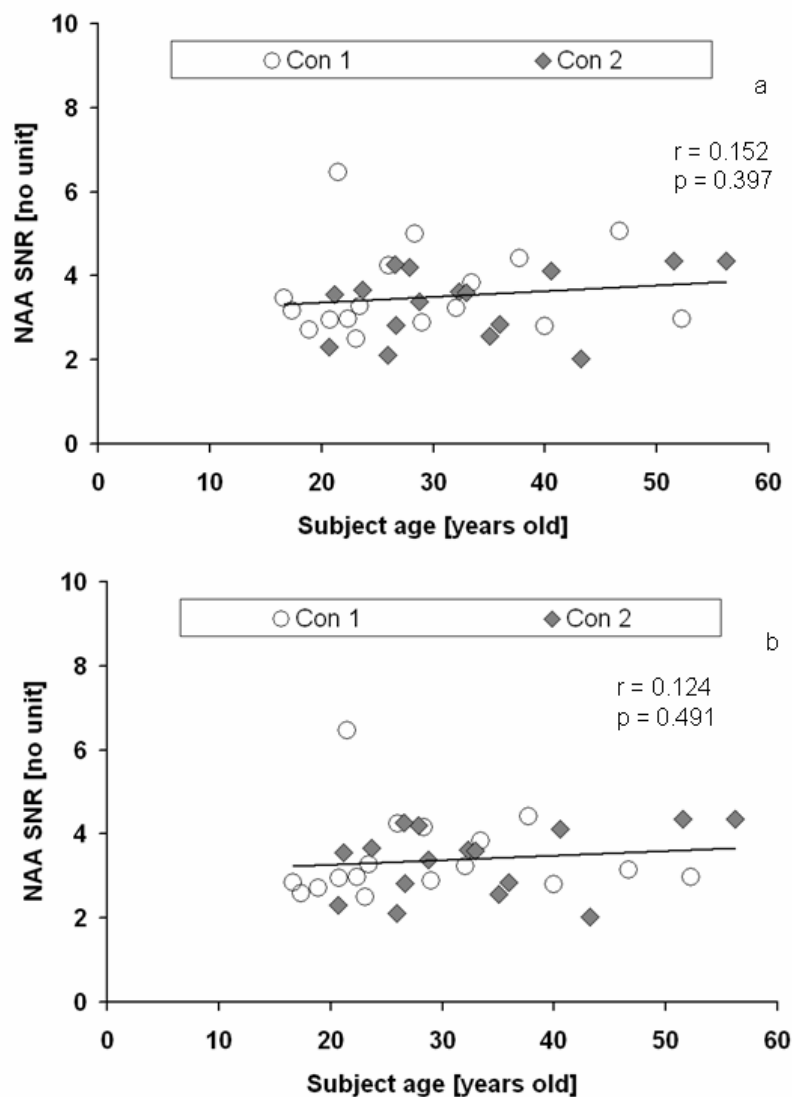
Figure 4-11: Correlations between subject age and thalamic NAA signal-to-noise ratio in controls

NAA signal-to-noise ratio at all measurement periods (N = 33) are involved in this correlation analysis. Top plot (a) indicates the original 80 months study. Bottom plot (b) indicates the data after the noise simulation, applied to the 4 data sets in Con 1 group collected in the first 2 years. Con 1, initial scan for the controls; Con 2, follow-up scan for the same controls.

4.4 Discussion

4.4.1 Correlations in SNRs with magnet age

Metabolite SNRs in both the anterior cingulate and the thalamus in schizophrenia were significantly or demonstrated a trend to be decreased over magnet age while there was no correlation in those SNRs in the control group. These decreases in SNRs may be a result of or enhanced by the hardware changes. Several hardware components in our MR system were upgraded or replaced in the first two years. This partially explains why no significant correlation against magnet age was found in controls, who were scanned much later than schizophrenia patients. In addition, only four control scans were performed in the first two years while twelve scans (six scans in each NT and 10 months) were completed in the schizophrenia group.

Despite the significant drop in metabolite SNRs, no SNR change was confirmed in the routine QA, which was performed by a system manager every week. Quality control in our 4T MR system was conducted by taking a magnitude image with the echo planar imaging (EPI) sequence using an identical phantom each week. It is possible that SNRs measured by a spectroscopy sequence are more sensitive compared to SNRs determined using an imaging sequence. Indeed, water SNR in this study was not significantly correlated with the entire magnet age in any regions or groups.

Another possible explanation is the digital filter. In our protocol, the digital filter was manually turned on during the MRS acquisition to reduce the noise in the first two years of the study. At this point in time, the hardware upgrade removed the need for the digital filter, and the operating protocol was adjusted as such. Therefore, metabolite SNRs in the first two years might be higher than SNRs in the remaining years. Water SNRs were not as high as metabolite SNRs in the first two years. This suggests noise reduction by the digital filter might be insufficient to improve the water SNR because water signal was too high to be affected by the noise reduction. Since metabolite SNRs were influenced by the hardware replacement and/or the digital filter, we were concerned whether the observed differences in metabolite levels in our 80 months study[4] could be attributed to this artifact. It will be discussed in the next section whether the differences in metabolite

levels observed in the 80 months study are affected by the changes in SNRs caused by the addition of the random noise.

4.4.2 Metabolite concentration levels: influence of random noise

Thalamic tGL level was still significantly decreased at 80 months from NT in schizophrenia patients even though some of the data sets in NT were replaced with the manipulated data. The differences were more significant ($P=0.024$) compared to the original data sets ($P=0.044$). Thalamic NAA level in schizophrenia, however, only showed a trend toward decreasing from 10 months to 80 months after the data manipulation ($P=0.029$) while significant decrease was observed before adding extra noise ($P=0.013$). The significance in the anterior cingulate NAA level ($P=0.031$) worsened after extra noise was added ($P=0.114$). This data is artificial in the sense that noise has been added in the first two years of data to make the SNR comparable across the study duration. However this still demonstrates that a hardware modification such as this may be responsible for a trend or a significant finding in the data that is not physiological in nature. Thus particularly in a long-term study, significantly different SNRs may skew statistical comparisons.

The influence of the noise is inconsistent between NAA and tGL levels. This most likely originates because the NAA level is due to a single metabolite while tGL level is composed of two different metabolites. tGL level was found to be higher than the NAA level, and the standard deviation of the tGL level is lower than that of NAA. Therefore, tGL is more stable than NAA in terms of the quantified metabolite level in the spectroscopic study. A possible explanation for the differential improvement in the significance in the thalamus and anterior cingulate would be the metabolite SNR in the original in-vivo data. Overall, SNR measured in the anterior cingulate spectra is lower than those in the thalamus spectra. Lower SNR in the anterior cingulate is caused by the decreased sensitivity due to the sinus cavity. Lower SNR spectrum often leads to misfit and inconsistent spectral fitting compared to the higher SNR spectra. Therefore, spectra in the anterior cingulate are vulnerable to increasing noise level compared with the

spectra in the thalamus. The effect of the SNR changes on metabolite quantification will be discussed with an SNR simulation in the next section.

4.4.3   SNR simulation: SNR and precision of the metabolite quantification

Metabolite quantification is sensitive to the SNR. In this SNR simulation, all quantified metabolite levels vary within the actual range of the NAA SNR in the 80 months study (Figure 4-5). The standard deviation of quantified metabolite levels are observed to worsen as the SNR of NAA decreases. In particular, glutamate and glutamine levels show a large standard deviation at NAA SNR less than 3 (Figure 4-7 and 4-8). Insufficient SNR leads to inconsistent quantification because fitting of the lower SNR spectra is dependent on the noise signal at the data collection.

At the higher NAA SNR, group standard deviations are more consistent compared to those at lower SNR but metabolite levels still vary. This simulation suggests that it is very important to maintain the SNR at a constant level, especially in longitudinal studies. Significant SNR changes between or within subjects may lead to errors in statistical comparisons.

One key finding of these simulations is that noise level may impact the fitting of the metabolite spectra. In fact, Figure 4-5 suggests that changing the SNR to below 3 would result in a very different fit of the metabolites. However over the change in SNR in this study, Figures 4-5 to 4-9 suggest that a significant change in the metabolite level is not expected. Thus the change in noise level of this simulation is not expected to impact the fit of the metabolite level.

4.4.4   Limitations

Either metabolite levels or SNRs were not corrected for subject age. Neuronal metabolites such as NAA are expected to decrease as the subjects age.[6] High metabolite

SNR at the first two years might be influenced by subject age as the data were collected at an earlier age compared to their 80 months assessment. However, since there is no correlation between metabolite SNR and subject age (Figure 4-10 and 4-11), an age effect for the metabolite SNR is less likely in this study.

4.5   References

1. Crespo-Facorro B, Roiz-Santiáñez R, Pérez-Iglesias R, Tordesillas-Gutiérrez D, Mata I, Rodríguez-Sánchez JM, de Lucas EM, Vázquez-Barquero JL. Specific brain structural abnormalities in first-episode schizophrenia. A comparative study with patients with schizophreniform disorder, non-schizophrenic non-affective psychoses and healthy volunteers. *Schizophr Res*. 2009;**115**:191-201

2. Mané A, Falcon C, Mateos JJ, Fernandez-Egea E, Horga G, Lomeña F, Bargalló N, Prats-Galino A, Bernardo M, Parellada E. Progressive gray matter changes in first episode schizophrenia: a 4-year longitudinal magnetic resonance study using VBM. *Schizophr Res.* 2009;**114**:136-43.

3. Théberge J, Williamson KE, Aoyama N, Drost DJ, Manchanda R, Malla AK, Northcott S, Menon RS, Neufeld RW, Rajakumar N, Pavlosky W, Densmore M, Schaefer B, Williamson PC. Longitudinal grey-matter and glutamatergic losses in first-episode schizophrenia. *Br J Psychiatry* 2007;**191**:325-34

4. Aoyama N, Théberge J, Drost DJ, Manchanda R, Northcott S, Neufeld RWJ, Menon RS, Rajakumar N, Pavlosky WF, Densmore M, Schaefer B, Williamson PC. Grey matter and social functioning correlates of glutamatergic metabolite loss in schizophrenia *Br J Psychiatry*, accepted

5. van der Graaf M, Julià-Sapé M, Howe FA, Ziegler A, Majós C, Moreno-Torres A, Rijpkema M, Acosta D, Opstad KS, van der Meulen YM, Arús C, Heerschap A. MRS quality assessment in a multicentre study on MRS-based classification of brain tumours. *NMR Biomed* 2008;**21**(2):148-58.

6. Lim KO, Spielman DM. Estimating NAA in cortical gray matter with applications for measuring changes due to aging. *Magn Reson Med.* 1997;**37**(3):372-7.

Chapter 5

5   Thesis summary

5.1   Results summary and implications

This thesis presents the results of a long-term study of schizophrenia, which is an extension of a previous longitudinal study.[1] In the initial study, it was reported that the initially elevated glutamine level in schizophrenia patients decreased over the 30 month assessment period. Chapter 2 of this thesis presents a longitudinal study to investigate whether or not these findings persist out to 80 months in the same population. The driving hypothesis of this study was as follows:

Hypothesis 1: Significantly higher glutamatergic metabolites during the first episode will decrease in schizophrenia over the 80 months. Glutamatergic metabolite decreases will correlate with widespread gray matter losses and social functioning at a 7 year follow-up.

In Chapter 2, we found that glutamatergic metabolites and NAA levels as well as gray matter volume were significantly decreased in schizophrenia over 80 months. Reductions in those metabolite levels were significantly correlated with gray matter loss in the regions associated with schizophrenic symptoms. These results suggest that physiological and structural deterioration persist in schizophrenia for at least 7 years. Significant correlations suggest that an excitotoxic process may lead to a neuronal dysfunction, which is eventually observable as widespread gray matter loss.

Loss of glutamatergic metabolite levels were inversely correlated with the Life Skills Profile (LSP) rating scale, a standardized social functioning, in schizophrenia at 80 months assessment. Glutamatergic reduction over 80 months was larger in a patient with lower LSP score, which indicates impaired social functioning. This negative correlation suggests that glutamatergic metabolite levels may reflect deteriorating social functioning in schizophrenia.

These results confirm our first hypothesis that glutamatergic metabolites and gray matter decreased over time. The loss of metabolite was significantly correlated with the gray matter losses, and social functioning was negatively correlated with the loss of glutamatergic metabolite levels. This long-term study demonstrates evidence of neurodegenerative processes in schizophrenia correlating metabolite levels with the physiological and structural changes, as well as social functioning. This is the first study to demonstrate these findings.

However coincident reductions in neuronal metabolite levels and gray matter volume raise a further question. Is it possible that structural changes in the brain resulting in change in gray matter volume are affecting metabolite levels such as glutamatergic metabolites and NAA? The purpose of Chapter 3 of this thesis was therefore to probe whether or not changes in the gray matter in the spectroscopy voxel could be responsible for observed changes in metabolite levels. To answer this question, the following hypothesis was derived:

Hypothesis 2: Loss of glutamatergic metabolites in first episode patients over time will be related to gray matter loss in the voxel of interest but will not be significantly affected by signal-to-noise changes associated with gray matter loss. NAA levels will be less likely to be affected by gray matter loss in the voxel of interest or signal-to-noise changes.

In Chapter 3, we examined whether decreased metabolite levels were significantly associated with the loss of gray matter in the long-term study (Chapter 2). Comparing the metabolite levels adjusted by the gray matter in the voxel of interest, significance in NAA levels hovered around the threshold while significance in the glutamatergic metabolite levels turned out to be non-significant. This suggests that gray matter in the spectroscopy voxel may not be responsible for the NAA levels but possibly for the glutamatergic metabolite levels. This therefore suggests that significantly decreased glutamatergic metabolite levels in the long-term study may be explained through the loss of neuropil, which is observed as gray matter loss. The subtle association between gray matter and

NAA level may be partially explained by the connection between 1H MRS measured NAA levels and neuronal integrity.

Significances in metabolite signal-to-noise ratio were unchanged by the gray matter adjustment. Despite the significant loss of gray matter in the voxel of interest, the influence of the gray matter on the metabolite signal-to-noise ratios was likely minimal. It suggests that signal-to-noise ratio defined in this study is more affected by the hardware performance and the data acquisition than the anatomical structure and location in the head.

These results confirm the hypothesis that gray matter may be associated with the glutamatergic metabolite levels but not with the NAA levels. This line of inquiry led to a significant amount of discussion surrounding hardware performance, and factors that may impact the signal-to-noise ratio. It is important for example that the metabolite levels and gray matter volumes were measured under the same experimental condition in the MR system. That way observed differences were due to biological changes and not a result of the hardware. This is an even more important consideration when undertaking a long term study such as ours that spanned 7 years.

It was noted from our long term study that due to a hardware modification, there was a change in the noise level of the system. Hardware replacements and/or upgrades are inevitable, particularly as the duration of a study becomes longer. Although our MR technician carefully maintained the MR system, with rigorous quality control, this change in the system noise may have affected the metabolite signal-to-noise ratio in our study. It then became crucial to understand whether or not the signal-to-noise ratio changed due to this hardware modification, and if so, whether or not the metabolite quantification was affected. In Chapter 4, a series of data manipulations and simulations were presented to answer these questions. It was hypothesized that:

Hypothesis 3: Significant differences in brain metabolites observed in our long-term study would persist after data manipulation to simulate a constant signal-to-noise ratio

throughout this study. Thus, Signal-to-noise ratio changes during our long-term study were not a major issue if the changes are modest.

Chapter 4 demonstrated the influence of signal-to-noise ratio on the metabolite quantification. Data manipulation, adding extra noise into the corresponding data, in the long-term study (Chapter 2) showed that the impact of signal-to-noise ratio is different for each of the individual metabolites. Significance in the NAA levels reported in the long-term study turned out to be a trend while the significance in tGL levels was improved after the data manipulation. This implies a risk in long term studies that an errant or inconsistent signal-to-noise ratio may skew the statistical significance of the quantified metabolite levels.

A signal-to-noise simulation was conducted to examine how metabolite signal-to-noise ratios affect the quantified metabolite levels. Differing amounts of noise were added into a noise-free spectrum generated from a data set in the long-term study. Lower signal-to-noise leads to an increased standard deviation in each metabolite level in groups of measurements having similar signal-to-noise ratios in this study. Quantification precision is decreased in those spectra with lower signal-to-noise. This simulation showed a potential risk that larger distributions of signal-to-noise ratio within a subject group may lead to difficulties in observing statistically significant differences or changes.

Thus these results confirm hypothesis 3, that these simulations in Chapter 4 demonstrate that significance in metabolite levels in the long-term study (Chapter 2) persisted with the addition of extra noise. Metabolite signal-to-noise ratios in the long-term study were maintained within a reasonable range, holding a similar precision in the metabolite quantification throughout the study. A broad range of signal-to-noise ratios however may lead to inconsistent metabolite quantification and a distorted statistical significance. This is crucial when differences or changes are reported using the statistical significance. To our knowledge, this is the first study to examine the role of hardware and signal-to-noise over long periods of time in this type of clinical study.

In summary, this thesis demonstrated the following using in vivo 1H MRS: (1) evidence that glutamatergic and NAA metabolite levels decline in schizophrenia for at least 7 years, (2) decreases in glutamatergic metabolite levels are associated with widespread gray matter losses and decreases in social functioning in schizophrenic patients, (3) decreases in glutamatergic metabolites may be accounted for at least in part by a loss of neuropil within the voxel of interest although an earlier degenerative process resulting in both the loss of neuropil and decreased glutamatergic metabolites cannot be ruled out, and (4) although hardware changes over time can influence signal-to-noise, differences in metabolite level persisted demonstrating that it is possible to carry out a long-term MRS study in a clinical population.

These findings have a number of implications for the understanding of the pathophysiology of schizophrenia as well as the feasibility of long-term MRS studies of clinical disorders. On the whole, findings would be consistent with degeneration related to glutamatergic excitotoxicity.[2] However, they do not rule out an early neurodevelopmental lesion related to genetic or environmental factors which might have been uncovered by cortical pruning which occurs during adolescence. The findings could also be accounted for in part by a genetically programmed loss of neuropil caused by a loss of nerve growth or other factors but the finding of increased glutamatergic metabolites without a change in gray matter in the first assessment would not be consistent with this explanation. If a loss of nerve growth factors caused the loss of gray matter, loss of gray matter would be expected at the first assessment. The effect of medication cannot be ruled out as well but it appears unlikely as there were few differences in gray matter and no differences in glutamatergic metabolites between the initial assessment before medication and the follow-up 10 months later on medication. It is possible that chronic medication effects may have influenced metabolite levels and gray matter but there appeared to be few significant correlations between the dose of medication and gray matter loss and no significant correlation between the dose of medication and metabolite levels.

Findings in the present studies are consistent with a parallel series of 31P MRS studies which demonstrated increased membrane breakdown products in first episode schizophrenic patients in regions associated with increased glutamatergic metabolites.[3] A follow-up of these patients showed diminished membrane breakdown products over time in these regions in keeping with the loss of glutamatergic metabolites.[4] An increase in membrane breakdown products was also demonstrated in a subsequent study[5] in regions showing later loss of gray matter suggesting that a degenerative process may precede the loss of gray matter. The findings of this thesis combined with the 31P MRS studies implicates glutamate as a possible target of therapeutic intervention in this disorder. Current treatments do not prevent social deterioration. The association between the loss of glutamatergic metabolites and social functioning in this study suggests that it might be possible to arrest this process with pharmaceuticals that target glutamate.

One recommendation arising from this study would be that researchers engaged in long term spectroscopy studies not only track the daily quality assurance using the SNR of a uniform phantom, but also that the metabolite signal and noise be monitored on a regular basis, in particular, before and after major hardware upgrades. In this way the potential risk of hardware signal/noise changes impacting the metabolite quantification can be mitigated.

5.2 Future work

This thesis is composed of data acquired at 4 Tesla, which provided a good separation between glutamate and glutamine spectra. As described in Chapter 2 and 3, glutamine levels measured with 1H MRS are better indicators for the glutamate neurotransmission, which might cause an excitotoxicity in schizophrenia. In Chapter 2, these two metabolite levels were quantified separately. Using a higher magnetic field strength such as 7 Tesla would be the logical next step to improve the spectral resolution. Improved signal-to-noise ratio is expected at 7 Tesla compared to at 4 Tesla as the signal-to-noise ratio is

proportional to the magnetic field strength. High signal-to-noise ratios may improve a measurement of low concentration metabolites in the human brain such as GABA, which is synthesized from glutamate with an enzyme glutamic acid decarboxylase.

High signal-to-noise ratio also supports better spectral fitting and the precision of the metabolite quantification. Using a phased array coil also improves the signal-to-noise ratio when compared to a head coil. 32 channel phased array coils are available. Using a phased array coil at 7 Tesla, our laboratory conducts functional magnetic resonance spectroscopy (fMRS), which allows the measurement of dynamic metabolite changes from a functionally activated area determined by fMRI. It would be interesting for example whether external stimuli might impact observed metabolite changes, helping to understand the disease mechanism, or perhaps hinting at other approaches to disease management. We are also utilizing two dimensional chemical shift imaging, which measures the metabolite levels within the entire slice. Two dimensional CSI will enable the evaluation of metabolite changes simultaneously over a wider area. Perhaps metabolite changes in one region may reflect similar changes in other regions of the brain not presently under consideration, further enhancing our understanding of the disease mechanism.

Updating a priori knowledge is necessary to improve the spectral fitting. If a metabolite or macromolecule component is missing in the a priori information, the fitting algorithm attempts to compensate the missing peak with the existing components, resulting in a quantification error. An automated fitting procedure minimizes a user-dependent factors such as setting the seeding values, which are required to run the Fitman program and are manually chosen in each spectrum. The Fitman program uses the Levenberg-Marquardt minimization algorithm that seeks the global minima, the best compromise between raw data and fitting. If the seeding value is not properly set, the fitting algorithm may find the local minima and not the best fit global minimum.

Some difficulties associated with longitudinal studies were discussed in Chapter 4. A longitudinal study is a powerful way to investigate progressive disorders such as schizophrenia and Alzheimer's disease. The longer the follow-up period is, however, the

more likely hardware upgrades or replacements are required. Thus, the signal-to-noise ratio might be different before and after the hardware changes. We demonstrated that a wide range of signal-to-noise ratio might distort the metabolite quantification and statistical comparison in Chapter 4. Measuring the water signal-to-noise ratio in vivo as well as the regular quality control with a phantom would help to maintain the quality of the spectra in a longitudinal study.

To maintain a reasonable range for the signal-to-noise ratio, the same head coil could be utilized with similar MR systems. If the signal-to-noise ratio was significantly elevated due to a hardware upgrade during a project, a possible solution to maintain a certain signal-to-noise ratio would be to transfer the head coil to another MR system, in which a similar signal-to-noise ratio is expected.

5.3   References

1. Théberge J, Williamson KE, Aoyama N, Drost DJ, Manchanda R, Malla AK, Northcott S, Menon RS, Neufeld RW, Rajakumar N, Pavlosky W, Densmore M, Schaefer B, Williamson PC. Longitudinal grey-matter and glutamatergic losses in first-episode schizophrenia. *Br J Psychiatry.* 2007;**191**:325-34.

2. Olney JW, Farber NB. Glutamate receptor dysfunction and schizophrenia. *Arch Gen Psychiatry.* 1995;**52**(12):998-1007.

3. Jensen JE, Miller J, Williamson PC, Neufeld RW, Menon RS, Malla A, Manchanda R, Schaefer B, Densmore M, Drost DJ. Focal changes in brain energy and phospholipid metabolism in first-episode schizophrenia: 31P-MRS chemical shift imaging study at 4 Tesla. *Br J Psychiatry* 2004;**184**:409-15.

4. Miller J, Williamson P, Jensen JE, Manchanda R, Menon R, Neufeld R, Rajakumar N, Pavlosky W, Densmore M, Schaefer B, Drost DJ. Longitudinal 4.0 Tesla (31)P magnetic resonance spectroscopy changes in the anterior cingulate and left thalamus in first episode schizophrenia. *Psychiatry Res: Neuroimag*. 2009;**173**(2):155-7.

5. Miller J, Drost D, Neufeldd RWJ, Jensen JE, Manchanda R, Northcott S, Rajakumar N, Pavlosky W, Densmore M, Schaefer B, Williamson PC. Progressive membrane phospholipid changes in first episode schizophrenia with high field magnetic resonance spectroscopy. *Psychiatry Res: Neuroimag.* submitted

Appendices

Appendix A: No differences in metabolite levels in mood disorder patients compared to healthy volunteers

Nery et al.[1] reported no statistical differences in the metabolite levels between 37 unmedicated participants with major depressive disorder (MDD) and 40 matched healthy controls. They measured the metabolites N-acetyl aspartate (NAA), glutamate (Glu), phosphocreatine plus creatine (PCr + Cr), choline-containing compounds (GPC + PC), myo-inositol (Myo) and Glu plus glutamine (Glu + Gln) in a $2.0 \times 2.0 \times 2.0$ cm voxel in the left dorsolateral prefrontal cortex using *in-vivo* proton magnetic resonance spectroscopy (1H MRS) at 1.5 T. Nery et al.[1] also found that NAA levels negatively correlated to the length of illness in MDD patients ($r = $ -0.460, $P = 0.003$) and they found gender differences in PCr + Cr concentrations.

Our group measured metabolite levels in a $1.5 \times 1.0 \times 1.0$ cm voxel in the left anterior cingulate using 1H MRS at 4 Tesla.[2] In contrast to Nery et al.,[1] our methods allowed the measurement of Glu and Gln separately. The data shown in Figure A-1, was taken from 6 depressed patients with psychotic symptoms and 3 likely bipolar patients with a mixed state with psychotic symptoms. Sixteen first episode schizophrenia patients and 16 controls matched to the schizophrenic group on which we have previously reported were included for comparison.[2] All patients were drug naïve. Three of 16 data sets from schizophrenia patients were excluded. These 3 spectra were unusable because of the subjects involuntary movements and/or excessive breathing during the scan.
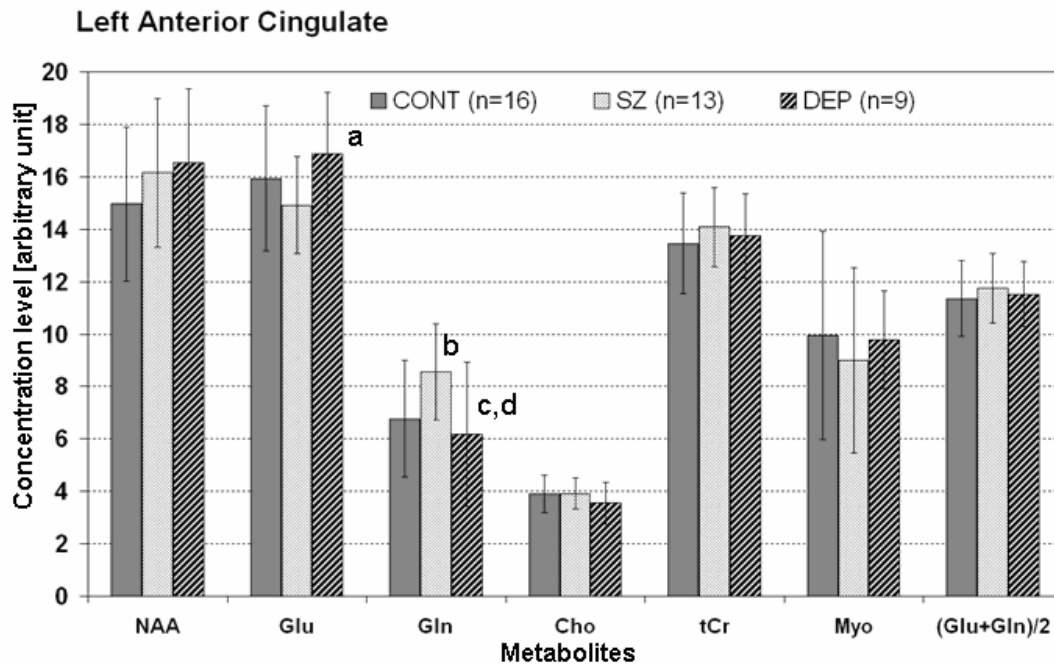
Figure A-1: Metabolite levels in schizophrenia, control, and mood disorder.

Metabolite levels measured by proton magnetic resonance spectroscopy from 1.5cm³ in the left anterior cingulate. Error bar represents the group standard deviation. a, SZ vs. DEP (unpaired two-tailed t-test, $t = 2.084$, $P = 0.055$); b, CONT vs. SZ ($t = 2.373$, $P = 0.025$); c, SZ vs. DEP ($t = 2.267$, $P = 0.041$); d, group effect in multivariate test ($F = 3.619$, $P = 0.037$).

Group: CONT, normal control; DEP, depressed patients with psychotic symptoms; SZ, schizophrenia. Metabolites: Cho, choline; Gln, glutamine; Glu, glutamate; Myo, myo-inositol; NAA, N-acetylaspartate; tCr, total creatine.

The three-group univariate F, 2/35, corresponding to these differences in Gln levels was 3.619 ($P = 0.037$). LSD post-hoc test was performed in each pair of the groups (two-tailed, $\alpha = 0.05$). 1H MRS metabolite levels in 9 mood disordered patients before treatment were not significantly different from controls. Although the sample was small, our result and those of the MDD study[1] suggest there may be no significant differences in

1H MRS metabolites in frontal areas between depressed patients and healthy controls. However, there may be differences between depressed patients with psychotic symptoms and schizophrenic patients. We observed significantly decreased Gln levels ($t = 2.494$, $P = 0.019$, d.f. $= 1,35$) and a trend toward elevated Glu ($t = 1.914$, $P = 0.068$, d.f. $= 1,35$) in mood disordered compared to schizophrenic patients in the left anterior cingulate. Moreover, Gln levels in schizophrenia patients were significantly lower than controls ($t = 2.150$, $P = 0.040$, d.f. $= 1,35$). These results suggest that the mechanisms of mood disorders and schizophrenia are different in spite of some overlap in clinical symptoms.

Glutamatergic metabolites have been found to be generally decreased in depressed patients compared to controls and increased compared to controls in studies of bipolar patients.[3,4] Nery et al.[1] point to a number of reasons for differences between studies including sample characteristics, acquisition and post-processing parameters. The Nery et al. study[1] also points out the need for publication of negative findings which are too often not reported. We observed that mood disordered patients differ from schizophrenia, but not from controls.   If the comparison had only been made between mood disordered patients and controls, then this negative result may not have been reported. This illustrates the need for comparative psychiatric groups to parse out findings related to psychosis from those unique to MDD.

References

1. Nery FG, Stanley JA, Chen HH, Hatch JP, Nicoletti MA, Monkul ES, Matsuo K, Caetano SC, Peluso MA, Najt P, Soares JC. Normal metabolite levels in the left dorsolateral prefrontal cortex of unmedicated major depressive disorder patients: a single voxel (1)H spectroscopy study. *Psychi Res: Neuroimaging.* 2009;**74**: 177-83.

2. Théberge J, Williamson KE, Aoyama N, Drost DJ, Manchanda R, Malla AK, Northcott S, Menon RS, Neufeld RW, Rajakumar N, Pavlosky W, Densmore M, Schaefer B, Williamson PC. Longitudinal grey-matter and glutamatergic losses in first-episode schizophrenia. *Br J Psychiatry.* 2007;**191**:325-34.

3. Yildiz-Yesiloglu A, Ankerst DP. Neurochemical alterations of the brain in bipolar disorder and their implications for pathophysiology: a systematic review of the in

vivo proton magnetic resonance spectroscopy findings. Progress *in Neuro-Psychopharmacology & Biological Psychiatry.* 2006;**30**:969-95.

4.   Yildiz-Yesiloglu A, Ankerst DP. Review of 1H magnetic resonance spectroscopy findings in major depressive disorder: a meta-analysis. *Psychiatry Research* 2006;**147**;1-25.

Appendix B: Description of imaging, spectroscopy, pre-processing, fitting and quantification

Data were acquired with a 4.0 Tesla Varian (Palo Alto, California, USA)/Siemens (Erlangen, Germany) whole body scanner with a Varian Unity Inova console, located at the Centre for Functional and Metabolic Mapping of the Robarts Research Institute, London, Ontario, Canada. A circularly polarized transmit and receive head coil was used. Global shimming was manually performed with linear and 2nd order shim coils and followed by T1-weighted transverse anatomical images (three-dimensional magnetization prepared fast low angle shot (MP-FLASH) sequence, repetition time (TR) = 11 ms, echo time (TE) = 6.4 ms, inversion time (TI) = 500 ms, flip angle = 30 degrees, 64 slices, matrix 256×256, 0.78×0.78 mm resolution, field of view = 20 cm, slice thickness = 2.75 mm). Using those T1-weighted images, the $10 \times 15 \times 10$ mm (right-left, anterior-posterior, inferior-superior direction) 1H spectroscopy volumes were positioned at the left anterior cingulate gyrus (Brodmann Area (BA) 32) and the left thalamus.

Magnetic resonance spectroscopy data were obtained with a single voxel stimulated echo acquisition mode (STEAM) sequence (TE = 20 ms, mixing time (TM) = 30 ms, TR = 2000 ms, dwell time = 500 µs, 8 step phase-cycling). The power of the 90-degree radio frequency pulses and the CHESS water suppression pulses were optimized for each voxel. After local shimming, water suppressed data (256 averages) followed by water unsuppressed data (16 averages) were collected. Data post processing included zero order eddy current correction (ECC) and line shape correction with the QUECC technique.[1] The remnant water resonances in the water suppressed spectra were subtracted with the Hankel-Lanczos singular value decomposition algorithm.[2] Water suppressed spectra were fit through an in-house software Fitman program[2,3] to the first 1024 data points (512 ms) in the time domain using a priori knowledge. Our model is based on *in vitro* measurements from twelve metabolites plus literature values for eleven macromolecules added to the a priori knowledge.[4,5] Metabolite concentration levels were quantified with equations[6] that included the ratio to water concentration in each spectroscopy voxel. The voxel water concentration depends on the voxel fraction of gray matter, white matter, and

CSF along with the water content of each of these tissues. The measured water signal was therefore corrected by the voxel's fractional tissue content and assumed literature values for the water content of each tissue type (gray matter 81%, white matter 71%, CSF 100%). Fractional tissue content was measured from semi-automated segmentation of the voxel location within the 3D T1-weighted image set as in our previous study.[6]

Quality of each MR spectrum was evaluated with using Visual Appreciation Scale (from 1 to 5) as well as Baseline and Artefact Scale (from A to E), introduced by Théberge et al.[6] We excluded the spectra in which the gamma-glutamate peak (2.35 ppm) was not identified and/or severe hashing was seen in a part of the spectra (i.e. rating lower than 5B). Only metabolites with a group coefficient of variation (group $CV = (\text{group standard deviation} / \text{group mean}) \times 100\%$) less than 75% are reported. Group CV less than 75% in the normally distributed samples means that 10% of the samples have a chance to be negative values, which never emerge in our fitting procedure. This criterion protects the statistical analysis from the metabolites which reach the lower detection threshold. We elected not to use a criteria based on percent Cramér–Rao lower bound (CRLB) since CRLB are only a portion of the total inter-individual variability of the data. It is the total inter-individual variability (group standard deviation) that determines the final ability to distinguish between two groups (a.k.a, SDD = smallest detectable difference). Metabolites survived from the criterion are NAA, glutamate (Glu), glutamine (Gln), choline (Cho), total creatine (tCr), myo-inositol (Myo) in the anterior cingulate and the thalamus, taurine (Tau) and scyllo-inositol (Syl) in the thalamus only. The "total glutamatergic metabolites" (tGL) refers to a sum of Glu and Gln levels measured individually. It should be noted that tGL is different from Glx, which is commonly used in the spectroscopy literature. Glx has an investigator-dependent definition which can refer to a variety of quantities. Often, it refers to the integrated spectral area encompassing the peaks from the 3C and 4C multiplets of Glu, Gln, GABA (gamma-aminobutyric acid), the aspartyl moiety of NAA and NAAG, the glutamate moiety of NAAG as well as signals from macromolecules. The concept of Glx was useful in the context of overlapping peaks at lower field strengths (1.5 T) and was used by many of the earlier studies where separate quantification of these metabolites may have been more difficult.

References

1. Bartha R, Drost DJ, Menon RS, Williamson PC. Spectroscopic lineshape correction by QUECC: combined QUALITY deconvolution and eddy current correction. *Magn Reson Med.* 2000;**44**(4):641-5.

2. Bartha R, Drost DJ, Williamson PC. Factors affecting the quantification of short echo in-vivo 1H MR spectra: prior knowledge, peak elimination, and filtering. *NMR Biomed.* 1999;**12**(4):205-16.

3. Bartha R, Drost DJ, Menon RS, Williamson PC. Comparison of the quantification precision of human short echo time (1)H spectroscopy at 1.5 and 4.0 Tesla. *Magn Reson Med*. 2000;**44**(2):185-92.

4. Kauppinen RA, Kokko H, Williams SR. Detection of mobile proteins by proton nuclear magnetic resonance spectroscopy in the guinea pig brain ex vivo and their partial purification. *J Neurochem.* 1992;**58**(3):967-74.

5. Behar KL, Ogino T. Characterization of macromolecule resonances in the 1H NMR spectrum of rat brain. *Magn Reson Med.* 1993;**30**(1):38-44.

6. Théberge J, Williamson KE, Aoyama N, Drost DJ, Manchanda R, Malla AK, Northcott S, Menon RS, Neufeld RW, Rajakumar N, Pavlosky W, Densmore M, Schaefer B, Williamson PC. Longitudinal grey-matter and glutamatergic losses in first-episode schizophrenia. *British Journal of Psychiatry.* 2007;**191**:325-34.

Appendix C: Sample spectra
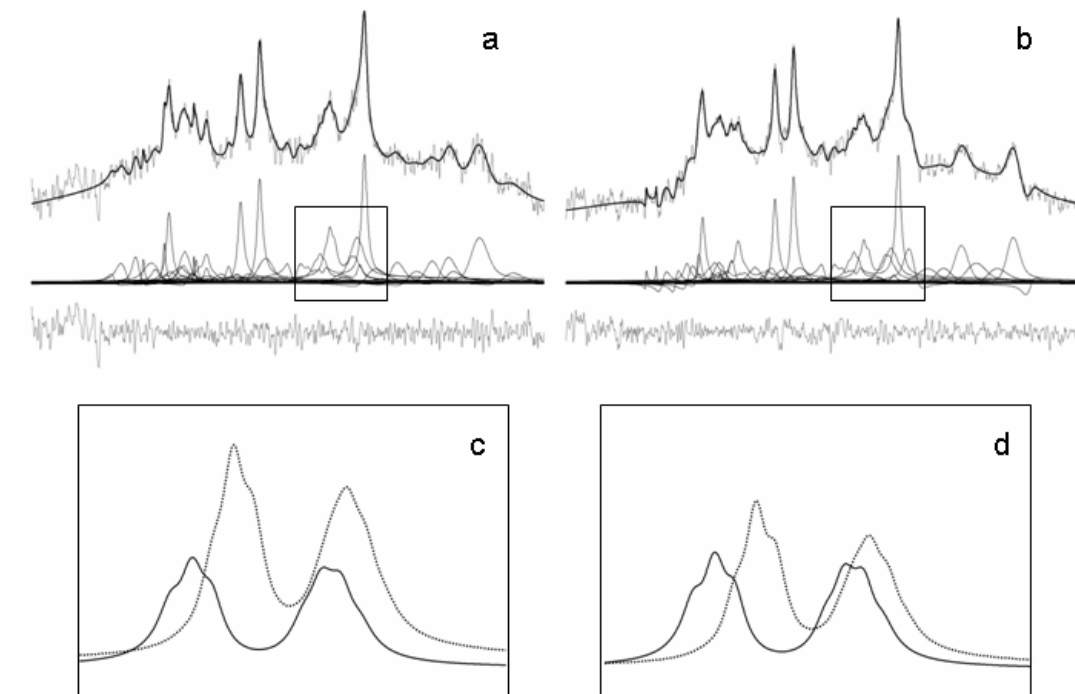
Figure C-1: Fitted *in vivo* MR spectra

Fitted spectra with 2Hz line broadening collected from the left thalamus in a schizophrenia patient at NT (a) and at 80 month assessment (b). Preprocessed spectrum (gray line) with fit (solid line) on the top, corresponding metabolite components in the middle, and the residual shown below. The boxed regions indicated in (a) and (b) are magnified in (c) and (d) showing the glutamate (dotted line) and glutamine (solid line) components.

Appendix D: Ethics approval
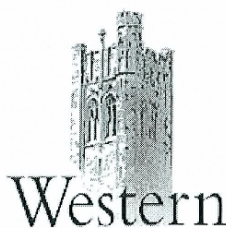
Office of Research Ethics

The University of Western Ontario
Room 00045 Dental Sciences Building, London, ON, Canada N6A 5C1
Telephone: (519) 661-3036 Fax: (519) 850-2466 Email: ethics@uwo.ca
Website: www.uwo.ca/research/ethics

Western

Use of Human Subjects - Ethics Approval Notice

Principal Investigator: Dr. P.C. Williamson	
Review Number: 13209	**Review Level:** Full Board
Review Date: April 03, 2007	

Protocol Title: Candidate Neuronal Circuits in Mental Illness

Department and Institution: Psychiatry, London Health Sciences Centre

Sponsor:

Ethics Approval Date: July 05, 2007   **Expiry Date:** September 30, 2012

Documents Reviewed and Approved: Letter of Information and Consent for Healthy Volunteers and Letter of Information and Consent for Patients.

Documents Received for Information:

This is to notify you that The University of Western Ontario Research Ethics Board for Health Sciences Research Involving Human Subjects (HSREB) which is organized and operates according to the Tri-Council Policy Statement: Ethical Conduct of Research Involving Humans and the Health Canada/ICH Good Clinical Practice Practices: Consolidated Guidelines; and the applicable laws and regulations of Ontario has reviewed and granted approval to the above referenced study on the approval date noted above. The membership of this REB also complies with the membership requirements for REB's as defined in Division 5 of the Food and Drug Regulations.

The ethics approval for this study shall remain valid until the expiry date noted above assuming timely and acceptable responses to the HSREB's periodic requests for surveillance and monitoring information. If you require an updated approval notice prior to that time you must request it using the UWO Updated Approval Request Form.

During the course of the research, no deviations from, or changes to, the protocol or consent form may be initiated without prior written approval from the HSREB except when necessary to eliminate immediate hazards to the subject or when the change(s) involve only logistical or administrative aspects of the study (e.g. change of monitor, telephone number). Expedited review of minor change(s) in ongoing studies will be considered. Subjects must receive a copy of the signed information/consent documentation.

Investigators must promptly also report to the HSREB:
    a) changes increasing the risk to the participant(s) and/or affecting significantly the conduct of the study;
    b) all adverse and unexpected experiences or events that are both serious and unexpected;
    c) new information that may adversely affect the safety of the subjects or the conduct of the study.

If these changes/adverse events require a change to the information/consent documentation, and/or recruitment advertisement, the newly revised information/consent documentation, and/or advertisement, must be submitted to this office for approval.

Members of the HSREB who are named as investigators in research studies, or declare a conflict of interest, do not participate in discussion related to, nor vote on, such studies when they are presented to the HSREB.

Chair of HSREB: Dr. John W. McDonald
Deputy Chair: Susan Hoddinott

Ethics Officer to Contact for Further Information		
☑ Jennifer McEwen (jmcewen4@uwo.ca)	☐ Denise Grafton (dgrafton@uwo.ca)	☐ Ethics Officer (ethics@uwo.ca)

cc: ORE File
LHRI

This is an official document. Please retain the original in your files.

Curriculum Vitae

Name: Naoko Aoyama

Post-secondary   The University of Tokai
Education and   Hiratsuka, Kanagawa, Japan
Degrees: 1996-2000 B.Sc. Physics

                             The University of Tokai
                             Hiratsuka, Kanagawa, Japan
                             2000-2002 M.Sc. Physics

                             The University of Western Ontario
                             London, Ontario, Canada
                             2003-present Ph.D., Medical Biophysics

Honours and   University Scholarship (which covered half of the tuition fee)
Awards: The University of Tokai
                             1996-2002

                             International Graduate Student Scholarship
                             The University of Western Ontario
                             2003-2005

                             Special University Scholarship
                             The University of Western Ontario
                             2003-2005

                             New Entrant Stipend Award
                             International Society for Magnetic Resonance
                             in Medicine (ISMRM) 12th Scientific Meeting, Kyoto, JAPAN
                             2004

                             Western Graduate Research Scholarship
                             The University of Western Ontario
                             2005-2008

Publications:
Peer reviewed publications:

Théberge J, Williamson KE, <u>Aoyama N</u>, Drost DJ, Manchanda R, Malla AK, Northcott S, Menon RS, Neufeld RW, Rajakumar N, Pavlosky W, Densmore M, Schaefer B, Williamson PC. Longitudinal grey-matter and glutamatergic losses in first-episode schizophrenia. *British Journal of Psychiatry* 2007;**191**:325-334.

Manuscript accepted to peer reviewed journal:

<u>Aoyama N</u>, Théberge J, Drost DJ, Manchanda R, Northcott S, Neufeld RWJ, Menon RS, Rajakumar N, Pavlosky WF, Densmore M, Schaefer B, Williamson PC. Grey matter and social functioning correlates of glutamatergic metabolite loss in schizophrenia *British Journal of Psychiatry.* January 2011

Manuscript in preparation:

<u>Aoyama N</u>, Thompson RT, Moran GR, Théberge J, Neufeld RWJ, Gardner RC, Densmore M, Schaefer B, Williamson PC. Gray matter vs. metabolite signal-to-noise ratio. *Psychiatry Research: Neuroimaging.*

<u>Aoyama N</u>, Moran GR, Williamson PC, Théberge J, Neufeld RWJ, Densmore M, Schaefer B, Thompson RT. The perils of long-term proton magnetic resonance spectroscopy studies *Magnetic Resonance in Medicine*

Abstracts:

<u>Aoyama N</u>, Théberge J, Williamson KE, Drost DJ, Manchanda R, Malla AK, Northcott S, Menon RS, Neufeld RWJ, Rajakumar N, Densmore M, Schaefer B, Williamson PC. "Longitudinal Study of Schizophrenia: Gray Matter Loss and Glutamtaregic Activity in the Limbic Basal Ganglia Thalamo-Cortial Circuit (BGTC)". **Department Psychiatry Annual Research Day**, University of Western Ontario, London, Ontario CANADA, 2005

<u>Aoyama N</u>, Drost DJ, Williamson PC. "Schizophrenia vs. Bipolar Disorder: Comparison Study with 1H Magnetic Resonance Spectroscopy (1H MRS)". **Lawson Health Research Institute Research Day**, London, Ontario, CANADA, 2007

<u>Aoyama N</u>, Théberge J, Drost DJ, Neufeld RWJ, Manchanda R, Densmore M, Schaefer B, Williamson PC. "Glutamtergic Activity in Bipolar Disorder and Schizophrenia: Proton Magnetic Resonance Spectroscopy (^{1}H MRS) Study". **Department of Psychiatry**

Annual Research Day, University of Western Ontario, London, Ontario CANADA, 2007

Aoyama N, Théberge J, Drost DJ, Neufeld RWJ, Manchanda R, Densmore M, Schaefer B, Williamson PC. "Glutamatergic and Gray Matter Losses in Schizophrenia after Long Term Assessment". **International Society for Magnetic Resonance in Medicine (ISMRM) 16th Scientific Meeting**, Toronto, Ontario, CANADA, 2008 (poster presentation)

Aoyama N, Théberge J, Drost DJ, Neufeld RWJ, Manchanda R, Densmore M, Schaefer B, Williamson PC. "Glutamatergic and Gray Matter Losses in Schizophrenia after Long Term Assessment". **Department of Psychiatry Annual Research Day**, University of Western Ontario, London, Ontario CANADA, 2008